Title

Photoelectric Control of Daylight-Following Lighting Systems

Authors

Rubinstein, F
Verderber, R
Ward, G

Publication Date

1989-02-01

LBL-24872

Lawrence Berkeley Laboratory
UNIVERSITY OF CALIFORNIA

APPLIED SCIENCE
DIVISION

Photoelectric Control of Daylight-Following Lighting Systems

F. Rubinstein, R. Verderber, and G. Ward

February 1989

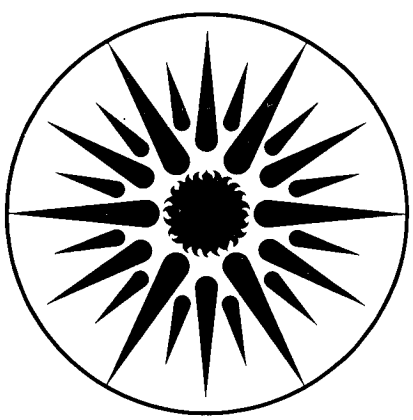

APPLIED SCIENCE DIVISION

Prepared for the U.S. Department of Energy under Contract Number DE-AC03-76SF00098.

DISCLAIMER

LBL-24872
L-130

PHOTOELECTRIC CONTROL OF DAYLIGHT-FOLLOWING LIGHTING SYSTEMS
(Daylight-Sensing Photocell Placement)

Research Project 2285-03

Initial Report, July 1987
Final Report, February 1989

Prepared by:

Applied Science Division
Lawrence Berkeley Laboratory
1 Cyclotron Road
Berkeley, California 94720

Principal Investigator: R.R. Verderber
Chief Researcher: F.M. Rubinstein
Researcher: G. Ward

Prepared for:

Electric Power Research Institute
3412 Hillview Avenue
Palo Alto, California 94304

EPRI Project Manager: K.F. Johnson
Residential and Commercial Program
Energy Management and Utilization Division

ABSTRACT

The ability of daylight-following lighting systems to provide a minimum specified light level at the task surface is influenced by 1) the control algorithm used, 2) the spatial response of the ceiling-mounted control photosensor and 3) the location of the photosensor relative to task and window. Best performance was obtained with a closed-loop proportional control system controlled by a photosensor, with a large field of view but shielded from direct light from the window. A minimum specified illuminance level could be maintained at specific points on the task surface regardless of daylight condition or room geometry provided that the system gain was properly calibrated to account for the local luminous environment.

Open-loop proportional control also performed adequately but offered less precise control than closed-loop systems due to the necessity of using a photosensor that was not shielded from direct window light. Integral-reset systems that were tested performed poorly, but performance could be improved slightly by completely shielding the photocell from direct window light.

ACKNOWLEDGMENTS

We wish to acknowledge and thank the Electric Power Research Institute for their support of this work, especially the contributions of Mr. Gary Purcell, Mr. Karl Johnson, Dr. Arvo Lannus, Mr. Stephen Pertusiello, and Mr. James Jewell. We also thank Mr. Larry Carmichael of EPRI for his constructive comments on the final report.

This work was partially supported by the Assistant Secretary for Conservation and Renewable Energy, Office of Buildings and Community Systems, Buildings Equipment Division of the U.S. Department of Energy under Contract No. DE-AC03-76SF00098.

CONTENTS

ILLUSTRATIONS

TABLES

Section 1

INTRODUCTION

Many utilities in the United States have begun to look at daylighting as a means to reduce daytime peak lighting energy demand. Since daylight availability coincides with peak demand times for many utilities, it is logical to shift part of the lighting requirement from electricity to daylighting. For daylight to efficiently contribute to the design light level at the task, the electric lighting system should be "daylight following," that is, photo-electrically controlled to respond (dim) in proportion to the amount of available daylight. The location and spatial sensitivity of the photosensor, which controls the electric lighting system, must be chosen so that the photosensor's output is a simple function of the illumination at the task surfaces in the building space. Furthermore, the control system's algorithm, which relates the photosensor signal to the output of the electric lights, should properly account for the location of the control photosensor relative to the task and the sources of illumination within the controlled space. If these criteria are not met, the illumination at the task will deviate significantly from the design level and the occupants may respond negatively, especially if the light level provided is lower than the design level.

This report presents an analysis of how the control algorithm and the photosensor's location and spatial response affect the ability of a daylight-following lighting system to maintain a minimum specified light level at the task by responding to changes in daylight levels. We discuss our objectives for the control system in Section 2 and design considerations for daylight-following systems in Section 3. In Section 4 we describe the scale model developed at Lawrence Berkeley Laboratory (LBL) to measure, under real skies, the relationship between daylight on the task and daylight falling on various ceiling-mounted control photosensors. In section 5 we discuss data collection and analysis. We present and then discuss the experimental results from the scale model in Section 6 and 7, respectively. We present preliminary design guidelines in Section 8 and our recommendations and conclusions in Section 9.

BACKGROUND

Although the technology for daylight-following lighting systems has been available for over two decades, there are very few installations in buildings that have been instrumented and monitored well enough for an unbiased evaluation of the performance of the dimming systems.

A study conducted by V.H.C. Crisp at the British Research Station Reference 1 concluded that more research was required to identify a photosensor configuration that would maintain a constant relationship between workplane illuminance and the illuminance on the

photosensor. Crisp did not examine how well existing systems maintain design light levels, but did note that most energy analysis calculations are based on the assumption that the lighting control system actually does provide the design light level under different daylighting conditions.

Unpublished results from lighting controls demonstrations at the Pacific Gas and Electric Company building in San Francisco and the P.S.E.G. building in New Jersey suggested that total light levels (i.e., daylight plus supplied electric light) at workplane level were generally below the design light level under most daylight conditions. Furthermore, a follow-on study at the Pacific Gas and Electric building Reference 2 indicated that a lighting control system designed to maintain a constant amount of light on a ceiling-mounted photocell will generally supply less than the target light level in most daylighting applications.

Section 2

DESIGN OBJECTIVES FOR DAYLIGHT-FOLLOWING LIGHTING SYSTEMS

To analyze the performance of daylight-following systems, it is first necessary to identify the objectives for the control system. In *nondaylighted* spaces, one important objective for the electric lighting system is to provide and maintain a task illuminance level appropriate to the work being performed. Task illuminance is a measure of how much light falls perpendicular to the task surface; it is expressed in SI units as lux (lumens/m^2) or as footcandles (lumens/ft^2) in English units. In typical office environments, for example, the Illuminating Engineering Society of North America (IESNA) recommends task illuminance levels of 500 to 750 lux, or 50 to 75 footcandles (fc) depending on the age of the workers and the difficulty of the task Reference 3.

Maintaining a prescribed illuminance level at the task is a more difficult objective to achieve for a space that is illuminated by daylight as well as electric light because daylight varies continually both in time and across the space. Furthermore, maintaining a light level exactly *equal* to the design level may be a physical impossibility since, in some spaces, daylight alone may be sufficient to significantly exceed the design light level at certain times. These saturating daylight conditions will exceed the control range of even an "ideal" daylight-following system and the lighting system would simply provide some minimum light output (possibly zero). Rigorously stated, the objective of a daylight-following system should be to provide a total light level at specified points on the task surface equal to or exceeding the target design level while minimizing electric lighting use. If the system supplies insufficient electric light, productivity may suffer. On the other hand, if too much electric light is supplied, more energy is used for electric lighting than is necessary to achieve the control objective.

Section 3

DESIGN CONSIDERATIONS FOR DAYLIGHT-FOLLOWING LIGHTING SYSTEMS

A lighting control system that is designed to follow changes in daylight consists of three basic components:

1) A control photosensor that generates an electrical signal proportional to the amount of light impinging on its surface.
2) A controller that incorporates an algorithm to process the signal from the photosensor and convert it to a signal that controls the dimming unit.
3) A dimming unit that smoothly varies the light output of the electric lights by altering the amount of power flowing to the lamps.

Although the dimmer actually modulates light output, its influence on the control system objectives is insignificant compared to the photosensor and the controller, and we focus on the design characteristics of the photosensor and controller.

CONTROL PHOTOSENSOR

The control photosensor typically consists of a silicon photodiode in a housing that selectively shields the photodiode from light from one or more different directions. A color-correcting photopic filter makes the control photosensor evaluate the spectral content of the measured light as the human eye would. To ensure that the signal generated by the sensor is proportional to the light impinging on its surface, the photodiode is connected to a transimpedance operational amplifier, which produces an output voltage, S(t), that is proportional over a large range to the light falling on the photodiode.

CONSTRAINTS ON PHOTOSENSOR PLACEMENT

Since the control objective is to provide an illuminance level at the task equal to the target design level, it would seem that the best location for the control photosensor is on the task surface. There are two serious drawbacks to such a solution. First, a control photosensor located near the task surface will be affected by shadows of objects (and people) at the workplane. Second, it is difficult to electrically integrate a workplane photosensor with the lighting control system. For these reasons, manufacturers design control photosensors for placement in the ceiling of the controlled space; inside the window wall pointing outward horizontally; or outside the building envelope (usually aimed horizontally).

Most photosensors incorporate some diffusing material in front of the light-sensitive element that causes the photocell to be sensitive to incoming light within a fairly large solid angle. This reduces the possibility of the photocell overreacting to a very localized brightness such as might occur with a specular reflection from a shiny surface.

DESIGN AND APPLICATION CONSTRAINTS

There are a number of factors that further constrain the design and application of photoelectric control systems. The most important of these are:

1. To keep wiring and materials cost to a minimum, a minimal number of photocells should be used per control zone.
2. The system should be simple to use, calibrate and adjust after installation.

The first constraint is essentially an economic one. Dimming photoelectric control systems are relatively expensive (typically $0.50 - $1.50/sq. ft.) even if only one photocell is used for each control zone. Each additional photocell adds considerably to the wiring costs and should therefore be avoided unless significant performance improvements can be demonstrated. The second constraint is primarily operational. Dimming photoelectric controls are generally perceived by building managers as being complex to operate, at least compared to conventional (i.e., nondimming) systems. Since the perceived complexity of photoelectric controls may reduce their appeal for end-users, the calibration procedure (which must be done for any photoelectric control system during building commissioning) should be designed to be performed by relatively untrained personnel and should not require frequent recalibration and adjustment.

Because of the above considerations, we restricted our investigation to systems that use only one control photosensor per control zone (constraint 1). Furthermore, we only examined systems that have a linear relationship between photosensor input and electric light output as discussed below. Since two points make a line, a linearly responding control system requires no more than two calibrations to completely determine its operation. As shown in the following section, some linearly responding systems require only one calibration depending on the circuit design parameters; others require two.

CONTROLLER AND CONTROL ALGORITHMS

The controller adjusts the output of the dimmer and thus the electric light level using an algorithm formulated to process the photosensor signal in a particular manner. The control algorithm determines the specific form of the transfer function that relates the controller input (i.e., photosensor signal) to its output (i.e., electric light level). This algorithm is thus critical to achieving the control system objectives discussed in the previous section.

This report discusses photoelectric control systems that dim linearly with respect to a change in measured photosensor signal. Although it is quite possible to design systems that do not dim linearly (for example, a logarithmic or quadratic response can, in principle, be implemented), they are far more difficult to characterize and are beyond the scope of this report. Linearly-responding systems can use three types of control algorithms: 1) integral reset (I); 2) closed-loop proportional (P); and 3) open-loop proportional (OL). Integral reset and closed-loop proportional control are classified as closed-loop systems because the output (electric light) is *fed back* to the controller via the photosensor Reference 4. Closed-loop systems, therefore, use a control photosensor that, by virtue of its location and spatial response, is susceptible to the electric light that it controls. With open-loop control, the output is not intended to be fed back to the controller, and the control photosensor is located either entirely outside the controlled space or shielded from the controlled electric light.

Closed-loop and open-loop systems are used for many control applications. Open-loop systems are generally not as accurate as closed-loop systems because they do not contain error-detecting circuitry that actuates the system when the output does not equal the input. However, the analysis and operation of the open-loop system is simpler than closed-loop control. Furthermore, because the output of an open-loop system is not used as input for the controller, open-loop systems are not susceptible to oscillations that can mar the performance of improperly designed closed-loop systems.

Below, we derive equations for each control algorithm that express the total light level at the task as a function of the daylight component of the photosensor signal and daylight on the task. These equations are used in the three simulation programs discussed in Section 5 for computing the total illuminance at the workplane for the different control algorithms. Figures 3-2, 3-3, and 3-4 are generic circuit diagrams for the algorithms.

NOMENCLATURE

The nomenclature is defined as follows:

$S_T(t) \equiv$ signal produced by photosensor (time-dependent).

$S_D(t) \equiv$ daylight component of $S_T(t)$.

$S_E(t) \equiv$ electric light component of $S_T(t)$.

$\delta \equiv$ fractional output of electric lights ($\delta_{min} \leq \delta \leq 1$). Full light output $\delta = 1$, minimum light output $\delta = \delta_{min}$.

$I_{Em} \equiv$ task illuminance level for $\delta = 1$ without daylight.

$S_{Em} \equiv$ signal produced by photosensor for $\delta = 1$ without daylight.

$I_T(t) \equiv$ total light at task (time-dependent).

$I_D(t) \equiv$ daylight at task (time-dependent).

$I_E(t) \equiv$ electric light at task.

$I_T(t)$, $I_D(t)$, and $I_E(t)$ as defined above refer to the particular point or points on the workplane where the design objective is to be satisfied.

Since the illumination at the task and at the photosensor at any time t is simply the sum of the respective daylight and electric light components, we can write:

$$S_T(t) = S_D(t) + S_E(t) \qquad \text{(Eq. 1)}$$

and

$$I_T(t) = I_D(t) + I_E(t) \qquad \text{(Eq. 2)}$$

If we assume that the electric lighting is controlled so that all the lights within the controlled space dim uniformly then we can make two important simplifications:

$$S_E(t) = \delta(t) S_{Em} \qquad \text{(Eq. 3)}$$

$$I_E(t) = \delta(t) I_{Em} \qquad \text{(Eq. 4)}$$

The above equations may be interpreted to mean that the luminance distribution from electric light remains constant regardless of the actual dimming level $\delta(t)$. Note that these equations would *not* be true in a room where the electric lights nearer the window could, for example, dim more than the lights at the back of the room. Such lighting systems require a more sophisticated mathematical treatment than that presented here.

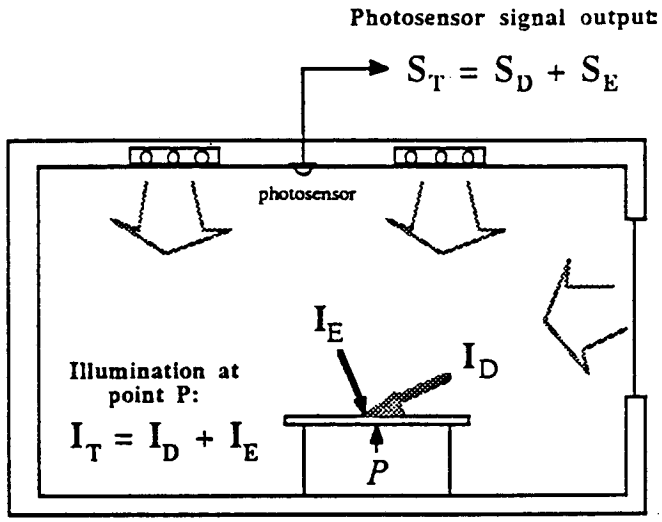

Figure 3-1. Cross section of daylit room showing window and photosensor

If the photosensor is located inside the controlled space, as shown in Figure 3-1, and is to be susceptible to the electric light that it controls, then the integral-reset or closed-loop proportional control algorithms would be used. If, on the other hand, the photosensor is outside the controlled space (or inside but shielded from electric light) so that it can detect only daylight, then the system would use the open-loop proportional control algorithm.

The three following sections contain derivations of the governing equations for the three algorithms. First, the algorithm is defined in terms of its corresponding control circuit. This is equivalent to specifying an output-level function. This function is then used to obtain equations for the workplane illuminance in terms of time-dependent daylight conditions.These equations are the mathematical basis of simulation programs we use to predict control system response based on the daylight information collected from the scale model.

Integral-Reset Systems

An integral-reset system continually adjusts the light output, δ, to keep the photosensor signal, $S_T(t)$, at a preset reference level. Figure 3-2 shows a simplified integral-reset control circuit. The control photosensor output is fed into the summing node of a simple operational amplifier integrator circuit Reference 5. If the lighting system is to provide full light output at night, which is usually the case, the control circuit is calibrated at night with the electric lights at full power and the setpoint adjusted until the photosensor input generated under these conditions (S_{Em}) is appropriately nulled. Increasing daylight in the space (and on the photosensor) will drive the inverting input high, causing the op-amp output to drop

at a rate determined by the circuit capacitances and resistances. This in turn causes the electric lights to dim, reducing the photosensor output and the potential at the inverting input until it once again matches the setpoint level. The circuit shown has effectively infinite DC gain.

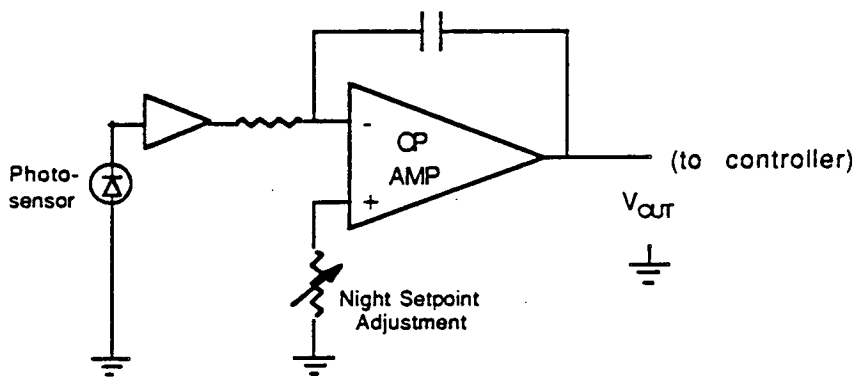

Figure 3-2. Generic circuit diagram of integral reset control

Assuming it is calibrated at night as described above, an integral-reset system operating in its dynamic range is defined by the following expression:

$$S_T(t) = S_{Em} \qquad \text{(Eq. 5)}$$

Applying Eqs. 1 and 3 to Eq. 5, one can solve for δ in terms of the independent variable $S_D(t)$:

$$\delta = 1 - \frac{S_D(t)}{S_{Em}} \qquad 0 \le S_D(t) \le (1 - \delta_{min})\, S_{Em} \qquad \text{(Eq. 6)}$$

Eq. 6 describes the dependence of δ on $S_D(t)$ for an integral-reset system operating in its dynamic range. For $S_D(t)$ larger than $(1-\delta_{min})S_{Em}$, the system will provide minimum light output:

$$\delta = \delta_{min} \qquad S_D(t) > (1 - \delta_{min})\, S_{Em} \qquad \text{(Eq. 7)}$$

If $S_D(t)$ is in the range covered by Eq. 7, then the system is no longer in its operating range. Substituting Eqs. 2 and 4 into Eqs. 6 and 7, one can solve for the total illuminance at the workplane in terms of $I_D(t)$ and $S_D(t)$:

$$I_T(t) = I_D(t) + I_{Em}\left(1 - \frac{S_D(t)}{S_{Em}}\right) \qquad 0 \le S_D(t) \le (1 - \delta_{min})\, S_{Em} \qquad \text{(Eq. 8)}$$

$$I_T(t) = I_D(t) + \delta_{min} I_{Em} \qquad S_D(t) > (1 - \delta_{min}) S_{Em} \qquad \text{(Eq. 9)}$$

Open-Loop Proportional Control

Open-loop proportional control is defined as a system for which the light output is a linear function of the photosensor signal:

$$\delta = M\, S_T(t) + 1 \qquad \text{(Eq. 10)}$$

A simplified circuit diagram for the open-loop system is shown in Figure 3-3. The control photosensor output is fed into the summing node of a negative-feedback, variable-gain operational amplifier. This circuit is designed assuming that a zero signal on the inverting input corresponds to full light output. Using a photosensor that is insensitive to electric light ensures that $S_{Em} \approx 0$ as required. The gain of the amplifier is adjusted by varying the value of the feedback resistor (equivalent to changing M in Eq. 3-10) under appropriate daylight conditions. Calibrating the system during the day allows the user to tailor the system's gain to prevailing daylight and room conditions.

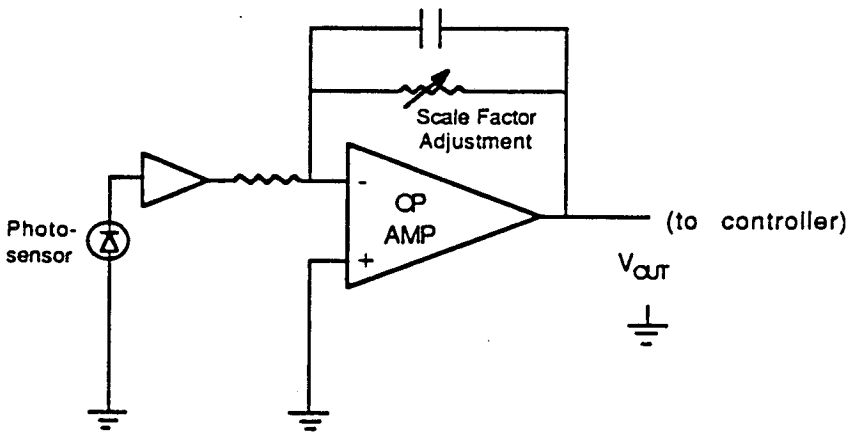

Figure 3-3. Generic circuit of open-loop proportional control

Applying Eqs. 1 and 3 to Eq. 10 and solving for δ, one obtains:

$$\delta = \frac{M\,S_D(t) + 1}{1 - M\,S_{Em}} \qquad 0 \le S_D(t) \le \frac{\delta_{min}(1 - M\,S_{Em}) - 1}{M} \qquad \text{(Eq. 11)}$$

and

$$\delta = \delta_{min} \qquad S_D(t) > \frac{\delta_{min}(1 - M\,S_{Em}) - 1}{M} \qquad \text{(Eq. 12)}$$

Assuming that the system is calibrated so that the total light level provided at the task matches the design level at the time of calibration, t_c, we can solve for the system gain M in terms of the prevailing daylight conditions. Substituting Eq. 3 into:

$$L_T(t_c) \equiv I_{Em} = I_D(t_c) + I_E(t_c)$$

and using Eq.11 yields:

$$M = \frac{I_D(t_c)}{I_D(t_c)\,S_{Em} - I_{Em}\,S_{Em} - I_{Em}\,S_D(t_c)} \qquad \text{(Eq. 13)}$$

The photosensor for an open-loop system must be much more sensitive to daylight than electric light. Consequently, the first two terms in the denominator in Eq.13 are much smaller than the third term and, to first order, the system gain M is proportional to the ratio $I_D(t_c)/S_D(t_c)$.

To obtain expressions for total illuminance at the workplane for open-loop systems, Eqs. 11 and 12 are used with Eqs. 2 and 4 to obtain:

$$L_T(t) = I_D(t) + I_{Em}\,\frac{M\,S_D(t) + 1}{1 - M\,S_{Em}} \qquad 0 \le S_D(t) \le \frac{\delta_{min}(1 - M\,S_{Em}) - 1}{M} \qquad \text{(Eq. 14)}$$

$$L_T(t) = I_D(t) + \delta_{min}\,I_{Em} \qquad S_D(t) > \frac{\delta_{min}(1 - M\,S_{Em}) - 1}{M} \qquad \text{(Eq. 15)}$$

Closed-Loop Proportional Control

A closed-loop proportional control system adjusts the electric light level so that $\delta(t)$ is a linear function of the difference between $S_T(t)$ and S_{Em}:

$$\delta = M\,(S_T(t) - S_{Em}) + 1 \qquad \text{(Eq. 16)}$$

A simplified circuit diagram for the closed-loop proportional control system is given in Figure 3-4. This circuit is similar to the open-loop circuit in that the control photosensor output is fed into the summing node of a negative-feedback, variable-gain operational amplifier. However, unlike the OLC circuit, which permits adjustment only of the system gain, the closed-loop proportional control circuit permits adjustments of both system gain and the offset on the noninverting input. During daytime operation, the output from the control photosensor drives the inverting input high. The op amp will produce whatever output is required to keep the potential at the inverting input equal to the potential at the non-inverting input. The relative change in op amp output for a given change in photosensor input is governed by the values of the feedback resistor (and other circuit resistances).

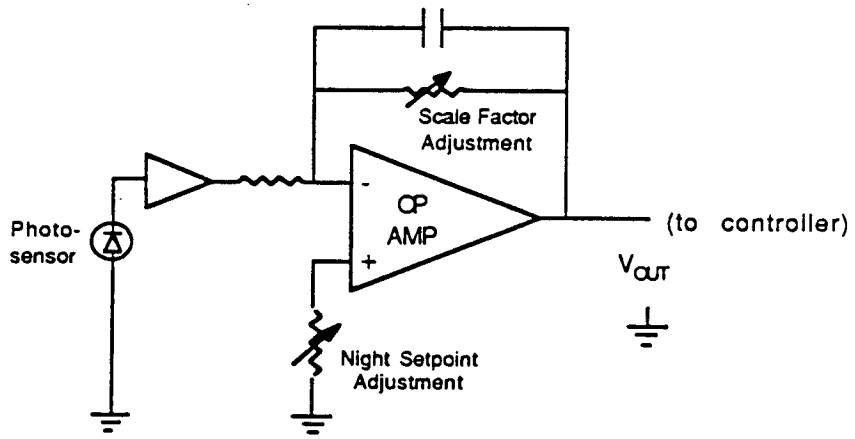

Figure 3-4. Generic circuit of closed-loop proportional control

Closed-loop proportional control is similar to open-loop proportional control except that the former permits adjustment of both the system gain (M) *and* the nighttime offset level (S_{Em}). To express δ as a function of the independent parameter $S_D(t)$, we substitute Eqs. 1 and 2 into Eq. 16. Rearranging and solving for δ yields:

$$\delta = \frac{1 + M\,(S_D(t) - S_{Em})}{1 - M\,S_{Em}} \qquad 0 \le S_D(t) \le \frac{\delta_{min}(1 - M\,S_{Em}) - 1}{M} + S_{Em} \qquad \text{(Eq. 17)}$$

When $S_D(t)$ exceeds the range given in Eq. 17, δ is simply given by:

$$\delta = \delta_{min} \qquad S_D(t) > \frac{\delta_{min}(1 - M\,S_{Em}) - 1}{M} + S_{Em} \qquad \text{(Eq. 18)}$$

As in the open-loop control case, the value of M in the above expressions is determined by calibrating the response of the lighting system during the day. Assuming that the lighting is calibrated so that at the time of calibration, t_c, the design level I_{Em} is obtained at the task, one can solve for M in terms of the daylight conditions obtained at t_c using Eqs. 2 and 4 with Eq. 17:

$$M = \frac{I_D(t_c)}{I_D(t_c)\,S_{Em} - I_{Em}\,S_D(t_c)} \qquad \text{(Eq. 19)}$$

Finally, to obtain the total illuminance at the workplane for the closed-loop proportional control system, we use Eqs. 2 and 4 with Eqs. 17 and 18 to obtain:

$$I_T(t) = I_D(t) + I_{Em}\frac{1 + M\,(S_D(t) - S_{Em})}{1 - M\,S_{Em}} \qquad 0 \le S_D(t) \le \frac{\delta_{min}(1 - M\,S_{Em}) - 1}{M} + S_{Em} \qquad \text{(Eq. 20)}$$

and:

$$I_T(t) = I_D(t) + I_{Em}\,\delta_{min} \qquad S_D(t) > \frac{\delta_{min}(1 - M\,S_{Em}) - 1}{M} + S_{Em} \qquad \text{(Eq. 21)}$$

Eqs. 8, 14, and 20 express the total workplane illuminance as a function of $S_D(t)$ and $I_D(t)$ for the integral reset, open- and closed-loop proportional control algorithms, respectively. Armed with these expressions, we can now calculate what proportionality constant relates $I_D(t)$ to $S_D(t)$ *assuming the daylighting control objective is acheived.* This is done by setting $I_T(t)$ equal to the design light level (I_{Em}) in Eqs. 8, 14, and 20 and solving for $I_D(t)/S_D(t)$.

Table 3-1 summarizes the preceding analysis by presenting, for each algorithm, the algorithm's transfer function, an expression for task illuminance as a function of the daylight component of the photosensor signal, and the proportionality constant that must relate $I_D(t)$ to $S_D(t)$ if the particular algorithm is to achieve the daylighting control objective.

Table 3-1. Operational equations for different control algorithms

Control Algorithm	Transfer Function	Task Illuminance	Conditional Expression
Integral Reset	$S_T(t) = S_{Em}$	$I_T(t) = I_D(t) + I_{Em}\left(1 - \frac{S_D(t)}{S_{Em}}\right)$	$\frac{I_D(t)}{S_D(t)} = \frac{I_{Em}}{S_{Em}}$
Open-Loop Proportional	$\delta = MS_T(t) + 1$	$I_T(t) = I_D(t) + I_{Em}\frac{1 + MS_D(t)}{1 - MS_{Em}}$	$\frac{I_D(t)}{S_D(t)} = \frac{I_D(t_{cal})}{S_D(t_{cal})}$, $S_{Em} \approx 0$
Closed-Loop Proportional	$\delta = M(S_T(t) - S_{Em}) + 1$	$I_T(t) = I_D(t) + I_{Em}\frac{1 + M(S_D(t) - S_{Em})}{1 - MS_{Em}}$	$\frac{I_D(t)}{S_D(t)} = \frac{I_D(t_{cal})}{S_D(t_{cal})}$

From the conditional expressions given in the Table 3-1, it is apparent that all algorithms require that the ratio between the daylight component of the photosensor and daylight on the task surface, $I_D(t)/S_D(t)$, remain constant for all daylighting conditions. (For the sake of brevity, the ratios $I_D(t)/S_D(t)$ and I_E/S_E are hereafter referred to as the *task-sensor ratios* for daylight and electric light, respectively). For an integral reset system, constant illumination on the task will only be achieved if the task-sensor ratio for daylight is equal to the task-sensor ratio for electric light. Open- and closed-loop proportional systems will only achieve the control objective if the task-sensor daylight ratio is always equal to the *particular* task-sensor daylight ratio obtained at the time of daytime calibration (t_c).

The equations derived above show that we can determine how well a given control system performs by measuring just the daylight on the task and the photosensor at various times throughout the day. In the following section, we describe the scale model used to obtain values of $S_D(t)$ and $I_D(t)$ under real skies.

Section 4

DEVELOPMENT OF THE SCALE MODEL

The physical principle behind scale models is straightforward: because the illumination at any point in a room is simply the sum of the contributions of the room surface and sky brightnesses, changing the scale of a room does not affect the light levels. Since measurements in a scale model of a room are essentially identical to measurements in the real room, the use of scale models under real sky conditions is a powerful predictive design tool.

Historically, physical scale models have played an important role in daylighting studies, but have not been used for studying electric light. Employing a scale model for investigating the effects of photosensor placement and control has several advantages over other methods, i.e., taking measurements in actual buildings or purely computational techniques. A scale model avoids the problems and expense of obtaining data in a building where people must work, and allows much greater control of the experimental variables. Moreover, an appropriately designed model can simulate rooms of various shapes (i.e., room cavity ratios) and various window management strategies, providing some of the flexibility and advantages of computer modeling techniques.

DESIGN SPECIFICATIONS

The scale model developed for this project was designed to meet the following specifications:

1) Permit measurement of daylight and electric light distributions at the workplane of the modeled building space.
2) Permit modeling of rooms having various shapes (i.e., room cavity ratios).
3) Permit testing of various window sizes, transmittances, and shading devices.
4) Permit examination of rooms facing in different directions.
5) Permit simulation of various lighting layouts.
6) Permit direct control of the electric light levels in the modeled space from any ceiling or wall-mounted control photosensor.

PHYSICAL DESCRIPTION OF SCALE MODEL

To meet the above specifications, it was necessary to design a model that would be flexible in function. The design chosen consisted of a wooden, cubic-shaped enclosure with one removable wall and movable internal partitions for the ceiling, walls, and floor. The floor

and ceiling were mounted on bookshelf-style support tabs so that their relative positions could be adjusted to model rooms of various sizes.

Model Room Configurations

We elected to model two different room shapes: the first, a small 15- x 15-ft office with modestly sized window; the second, a very long room of 30 ft depth with the long dimension of the room parallel to the window. The small office was modeled at 1:3 scale, while the long room was modeled at 1:6 scale.

Figure 4-1 is an exploded view of the small office scale model. Figure 4-2 provides a similar view of the model configured as a very long room. By using mirrored surfaces as shown in Figure 4-2, we were able to model a room of effectively infinite length parallel to the window. The wall, ceiling, and floor reflectances used for all the tests are indicated in the figures.

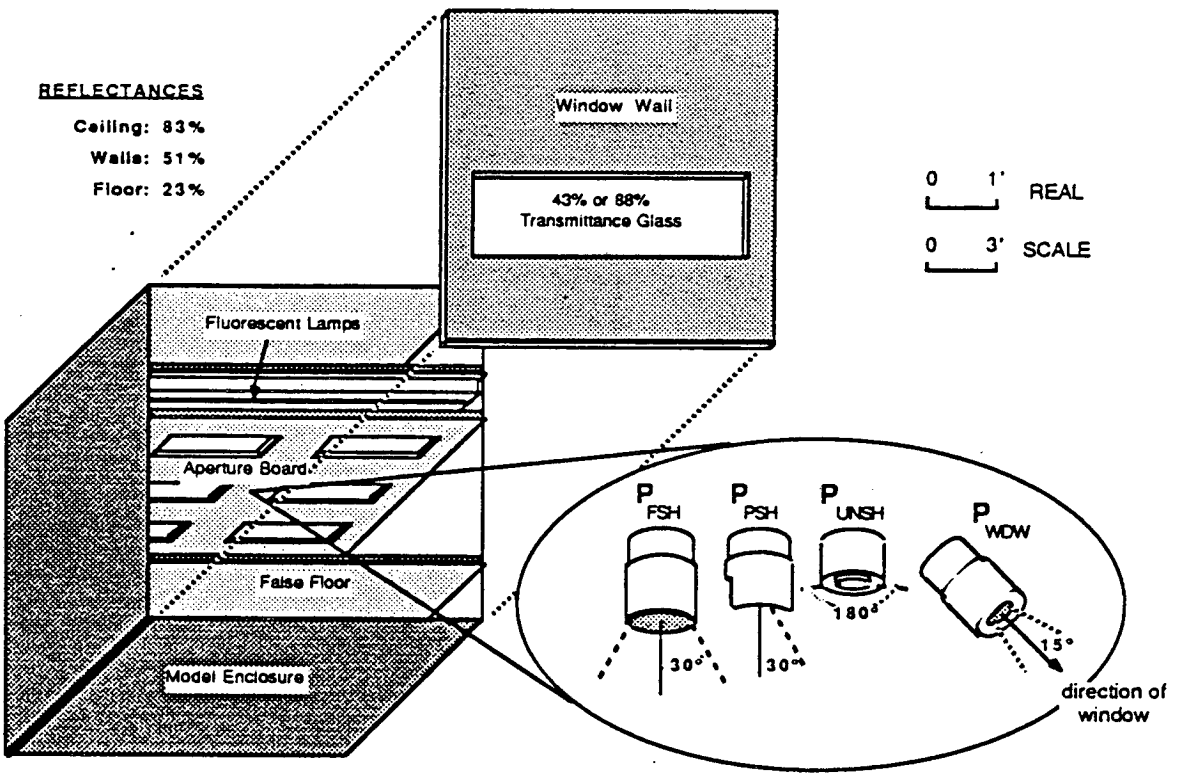

Figure 4-1. Exploded view of scale model of small office

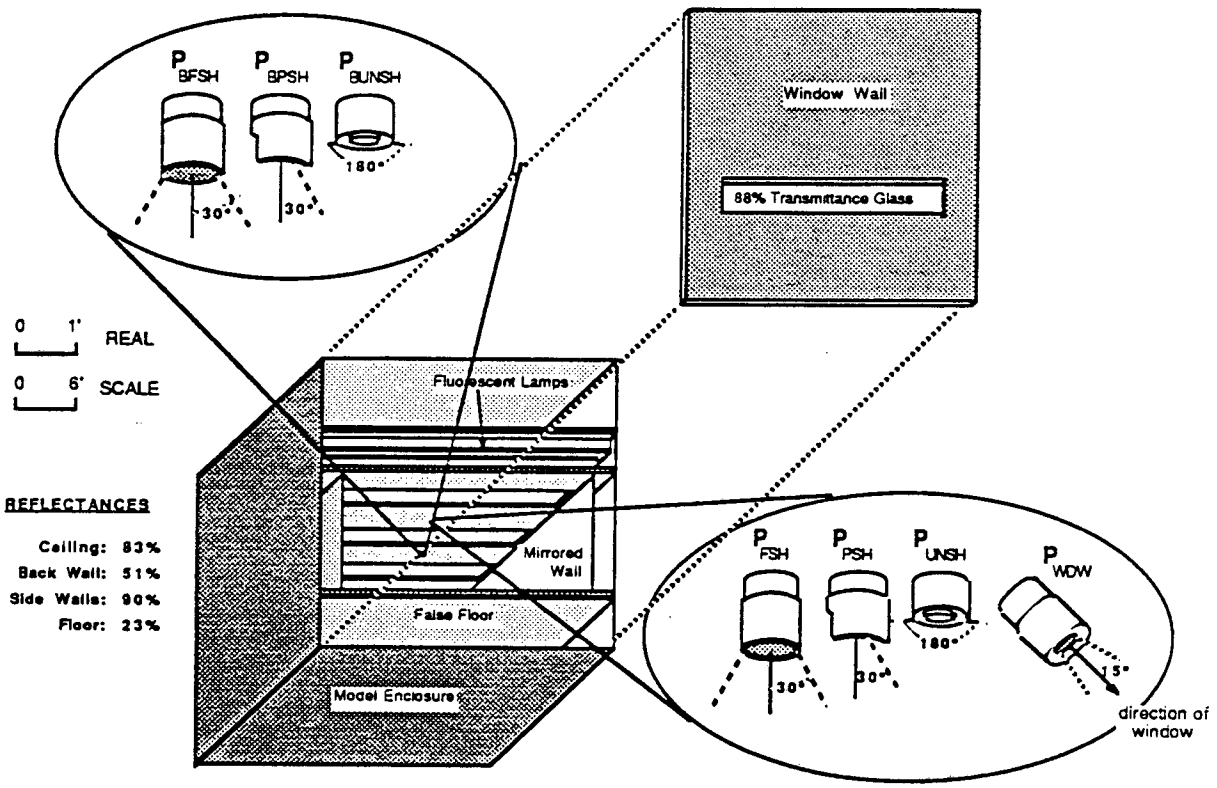

Figure 4-2. Exploded view of scale model of semi-infinite building space

The entire model could be rotated about a central pivot so that the window wall could be oriented towards any direction. This capability is critical to daylighting scale model studies because of the sensitivity of the daylight resource to room orientation.

Window System

Since the window size and transmittance and the type of shading device used are the most important determinants of the quantity and distribution of daylight within the room, the window-wall (the wall that contains the window) of the model was removable, allowing us to test different fenestration strategies. For the single office model, we used a window with a 1:3 window-to-wall ratio (the ratio of the area of the window to the area of the entire window-wall as measured from inside the model room) and examined two types of glass: 43% and 88% transmittance (Fig. 4-1). For the semi-infinite room model, we used clear glass (88% transmittance) with a window-to-wall ratio of 1:2 (Fig. 4-2).

Automatic shading device. To prevent direct sunlight from entering into the model space, an operable slat-type shading device (venetian blinds) was used for some of the tests. The venetian blind slats were 3/4" wide and were a neutral gray color of approximately 50%

reflectance. A small motor was employed to automatically control the blind blade angle. The motor was triggered by an external clock which incremented the blade angle a given angle either 30° every two minutes (Schedule A) or 10° every minute (Schedule B). This technique allowed us to test up to 10 different blade angles during a single day's test. However, because of mechanical limitations, the total maximum angular deflection possible was only 90°. The different blind blade angles tested are shown schematically in Figure 4-3, Schedules A and B.

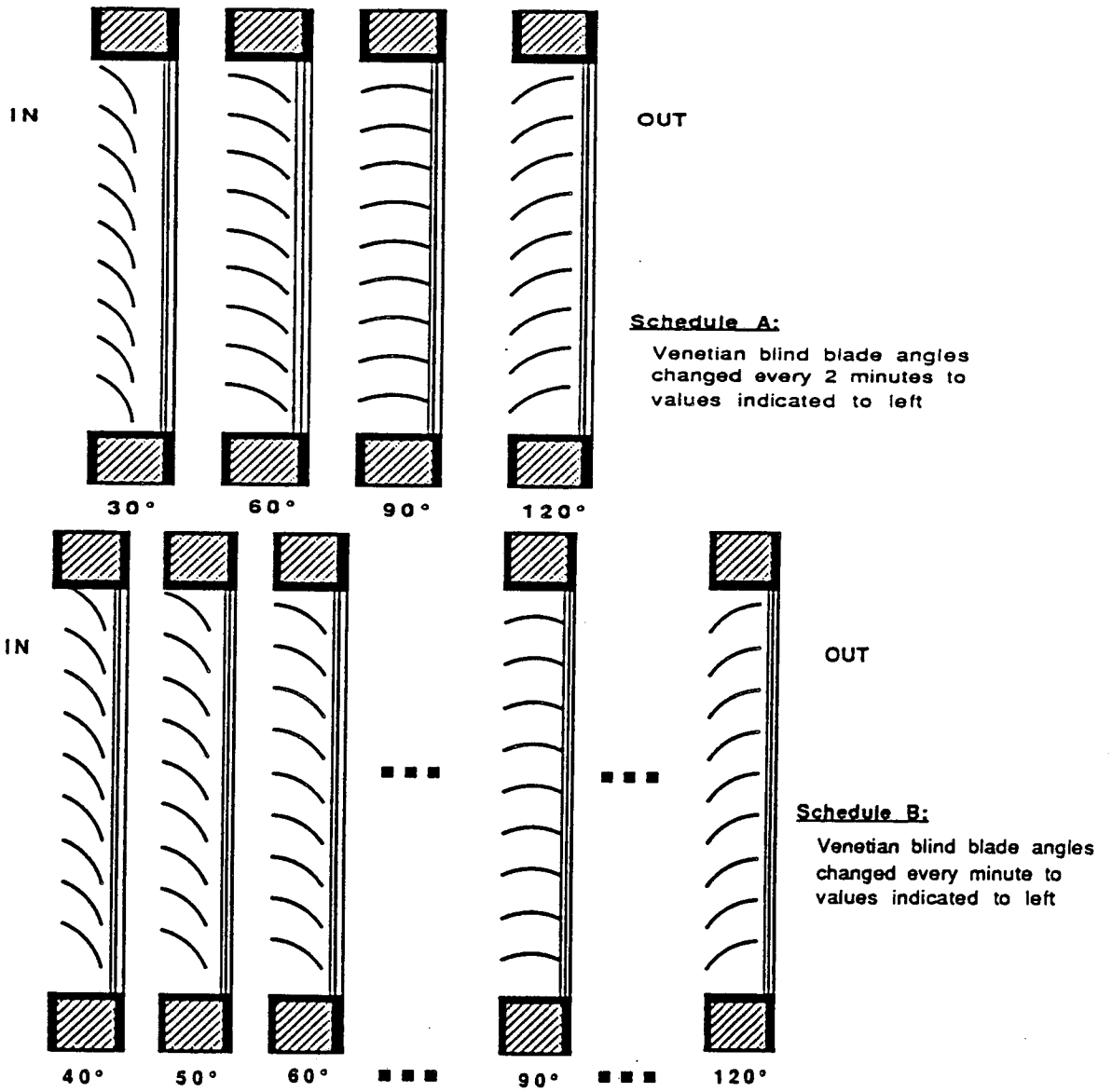

Figure 4-3. Venetian blind blade angles used in testing (two schedules)

Electric Lighting System

The electric lighting system consisted of three two-lamp strip fixtures mounted to the underside of the fixture board with an aperture board below it (Figs. 4-1 and 4-2) to simulate the appearance and light distribution properties of a typical ceiling system. For the small office model, the aperture board consisted of six appropriately scaled rectangular apertures fitted with industry-standard prismatic lens material to simulate standard 2- x 4-ft fluorescent troffers (Figs. 4-5 and 4-1). For the semi-infinite room model, we simulated 3 continuous rows of fluorescent fixtures on 10 foot centers as shown in Figures 4-6 and 4-2. To prevent light from one pair of lamps from spilling out through an adjacent "fixture" into the room space, baffles are interposed between the fixtures as shown in Figures 4-1 and 4-2.

The 6 lamps used were selected from a group of 24 F40T12 cool-white lamps (burned-in for 1000 hours) on the basis of similar lumen output. They produced an average of 2970 lumens with a standard deviation of less than 0.5%.

The lamps were operated by continuously dimmable, high-frequency ballasts controlled by a low-voltage control circuit. The ballasts and associated controls are commercially available but modifications to the control circuitry were necessary to adapt the system to our purposes. Specifically, we added proportional control to the integral reset controller by adding electrical components as shown in Figure 3-4. In addition, because we used control photosensors that were less sensitive (though more accurate) than the commercially provided ones, we increased the gain of the photosensor amplifiers built into the controller.

The ballast and control circuitry for each two-lamp fixture could be wired separately to permit testing of graded control techniques (viz. allowing the fixtures near the window to dim more than the fixtures further in). However, we restricted our investigation to uniformly dimming systems, so all three fixtures were operated by a single control module.

The efficiency of photoelectric dimming systems is determined by examining the relationship between the input power to the lamp/ballast system and the relative light output over the full control range. The power/light curve for the electronically ballasted system used in these experiments was determined by manually operating the lights in the model at night and simultaneously measuring the power input to the lights and the illuminance at the workplane. The power/light relationship for this system is linear but not proportional. At minimum light output (10%), the system draws 27% of the maximum wattage. (This loss in system efficacy with increased dimming is typical of well-designed systems that do not reduce filament voltage when dimming.)

INSTRUMENTATION

The scale model was extensively instrumented for photometric, electrical, and temperature measurements.

Photometric Instrumentation

The scale model was equipped with 26 photometers to measure light both inside and outside the model. Some of these photometers were optically modified to use as control photosensors for the dimmable electric lighting system. To ensure precise measurements, all photometers were required to meet the following specifications:

- Small physical size (< 1-in. diameter)
- Rugged and weather-resistant
- Good spectral response (conformance to the V_λ curve to within 2% of area under curve)
- Good spatial response (cosine-corrected to within 5% at all angles < 85° off axis)
- Good linearity over large dynamic range (linearity error < 2%)
- Output compatibility with existing multi-channel data acquisition system.

We used the Li-Cor model #LI-210SB: small, rugged, relatively inexpensive, and acceptably accurate photometric probes. However, these had to be modified to precisely measure the low light levels in the model under minimum daylight conditions.

A circuit for amplifying the electric current from the photometers was developed and fabricated at LBL (see Fig. 4-4). The photometer current is fed into a thermally stable operational amplifier operating in the transimpedance mode, which converts the input current (typically 0.2 nanoamp/lux) into a voltage signal measurable by the data acquisition system. To accommodate the large differences in light levels measured by the internal and external photometers, two different amplifier configurations were required. The amplifiers for the internal photometers, had 10 times the gain of the amplifiers for the external photometers.

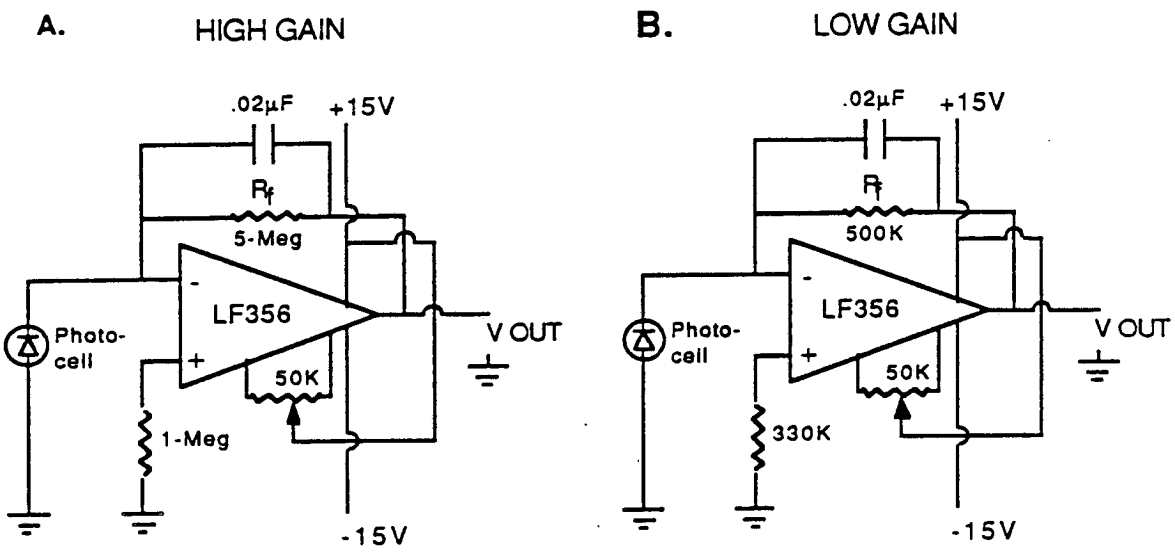

Figure 4-4. Circuit diagrams of photocell amplifiers used in scale model

Calibration. To ensure accurate and precise measurements over the entire anticipated range of light levels, the photometer/amplifier combinations were calibrated using a miniature 12-volt, narrow-beam, halogen projector lamp for the calibration source, with a regulating feedback circuit to keep the light output constant. The output of each photometer and amplifier was compared to the reading from a calibrated laboratory-grade photometer at a minimum of three different light levels to check linearity. To vary light level, neutral density filters were interposed in the beam path, to avoid changing the spectral distribution of the lamp by dimming.

The external photometers had to read accurately to at least 100,000 lux (10,000 fc), which is equivalent to full sun and sky illuminance. Since the calibration set-up described above could not provide such high illuminances, the calibration constants for the external photometers were determined under real sun and sky conditions using a research-grade photometer as the calibration reference.

Modifications for control photosensor (small office model). Several photometers were specially modified and mounted in the model ceiling to mimic the spatial response characteristics of typical commercially available control photosensors or to measure certain specific luminous quantities. In the former category, three sensors, designated P_{unsh}, P_{psh}, and P_{fsh}, were designed to be attached flat to the center of the ceiling. The P_{unsh} (unshielded) photosensor was an unmodified, cosine-corrected photometer; it measured the illuminance incident on the ceiling. The P_{psh} (partially-shielded) photosensor was equipped with an opaque baffle that shielded it from direct light from the window but otherwise allowed the photosensor a view of the floor and the three non-window-walls.

The photosensor designated P_{fsh} (fully-shielded) was fitted with a Gerschun tube that restricted its field of view (FOV) to a cone of 40° semi-angle allowing the sensor to measure light reflected from most of the floor while preventing the sensor from directly detecting light from any of the four walls. The output of this photosensor was roughly proportional to the average luminance of the floor below.

Four other photometers were fitted with Gershun tubes that restricted the angle of view of each photometer to a cone of 15° semi-angle. This FOV was selected so that each photometer when appropriately aimed would only be able to detect light reflected from that wall. These four photosensors measured a physical quantity that was closely related to but not identical to average wall luminance (or brightness). Note that the photosensor designated P_{wdw} was aimed so that it pointed at the centerpoint of the window (Figs. 4-1 and 4-2). Therefore the output of this photosensor was roughly proportional to the luminance of the horizontal plane outside the model (i.e., the ground plane) as viewed from the model ceiling.

Another photosensor was attached to the rear wall of the model and aimed at the window. By fitting this photosensor with a specially modified Gerschun tube, its field of view was restricted to the window only, and its output was proportional to the average window luminance measured normal to the window.

Semi-infinite room model. The control photosensors used for the semi-infinite room model were similar to those described above with the following differences. Two ceiling-mounted control photosensor clusters were used rather than the single cluster used in the small office model. These clusters were mounted as shown in Figure 4-2. Using two clusters allowed us to assess how important it was to place the ceiling-mounted photosensors near the workplane location where one wants to maintain the control criterion. Another difference between the two models was that we eliminated the three photosensors that measured the luminances of the three non-window-walls. (Analysis showed that these sensors provided consistently poor correlations with workplane illuminance).

Workplane photometers. Sixteen cosine- and color-corrected photometers were installed in the small office model to measure the illuminance distribution at the workplane. As shown in Figure 4-5, these photometers were arranged in a regular 4 x 4 array on 16-in centers 10 inches above the floor. Since the small office model was scaled at 1:3, this height is equivalent to 30 inches, where photometric measurements are typically made. The framework on which the photometers were mounted was painted the same color as the floor to minimize its effect on the light measurements.

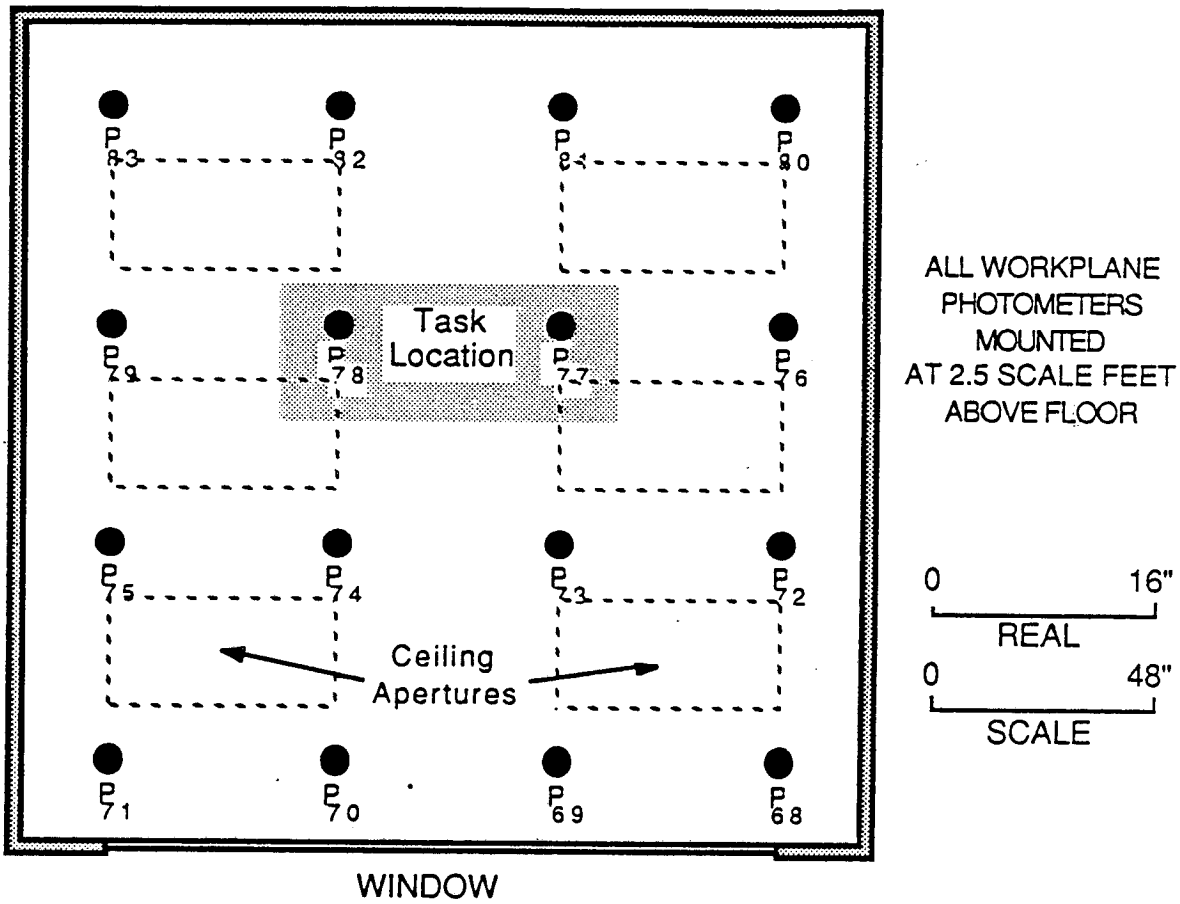

Figure 4-5. Floor plan and reflected ceiling diagram of small office model

For the semi-infinite room model, we used a linear array of fifteen photometers for measuring the workplane illumination with the photometers oriented with respect to the window as shown in Figure 4-6. (Because of the side wall mirrors used to simulate the infinite room length parallel to the window, it can be shown that only measurements along the room centerline are meaningful in this context).

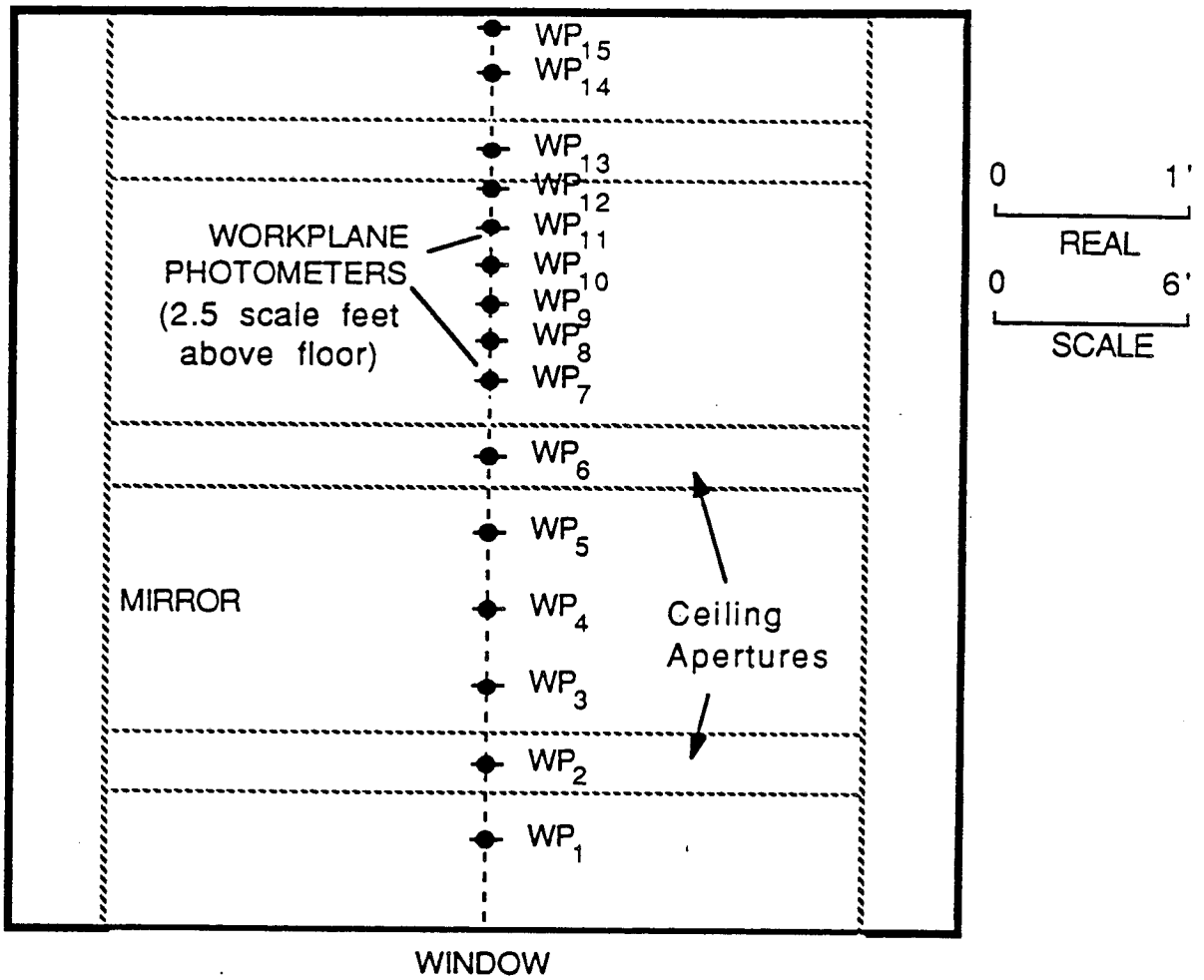

Figure 4-6. Floor plan and reflected ceiling diagram of semi-infinite room

External photometers. Two additional photometers, designated P_{gbl} and P_{dif} (global and diffuse), were mounted outside the model on a horizontal platform about 5 meters away from the scale model. These photometers were used to measure the horizontal illuminance (i.e., illuminance falling on a horizontal surface) due to the sun and sky and from the sky alone. The latter measurement was accomplished by placing the P_{dif} photometer under a shadow band that always shielded the photometer from direct sun. The positioning of the photometer relative to the shadow band and the angle of the shadow band was adjusted weekly to account for diurnal variations in sun position.

Electrical Instrumentation

Input power to each of the strip fixtures (lamp and ballast system wattage) was measured with small industrial watt transducers (F.W. Bell Industrial Watt Transducer #PX-2202B). The transducers were calibrated in terms of watts using incandescent lamps of various

wattage as test loads and comparing the transducer output to the wattage as measured by a laboratory-grade watt-meter (rated accurate to 1%).

Temperature Instrumentation

The light output and power input properties of fluorescent lamps are significantly affected by the temperature of the air surrounding the lamps. In addition, the accuracy of the photometric instrumentation is influenced by the temperature of the probes. Since we anticipated that the lamps and the photometers in the scale model might be subjected to substantially elevated temperatures on hot days, two thermocouples were installed to measure the temperature of the air surrounding the lamps and the air temperature within the room space. The calibration factors for the thermocouples were obtained from the manufacturer's calibration data.

DATA ACQUISITION SYSTEM

Amplified signals from all the photometers and watt transducers were fed into a multi-channel data acquisition control unit (Hewlett-Packard 3497A Data Acquisition and Control Unit). This unit incorporates a 5-1/2 digit auto-ranging voltmeter for precise voltage measurements. The operation of the 3497A Control Unit was programmed by an Osborne 1 microcomputer running under the CP/M operating system. The data collection programs were written in the C programming language.

Data were recorded onto 5 in. floppy disks in compacted form for efficient storage. Filled disks were then uploaded to the LBL VAX 11/780 computer for subsequent data analysis and reduction.

The data collection apparatus is shown schematically in Figure 4-7.

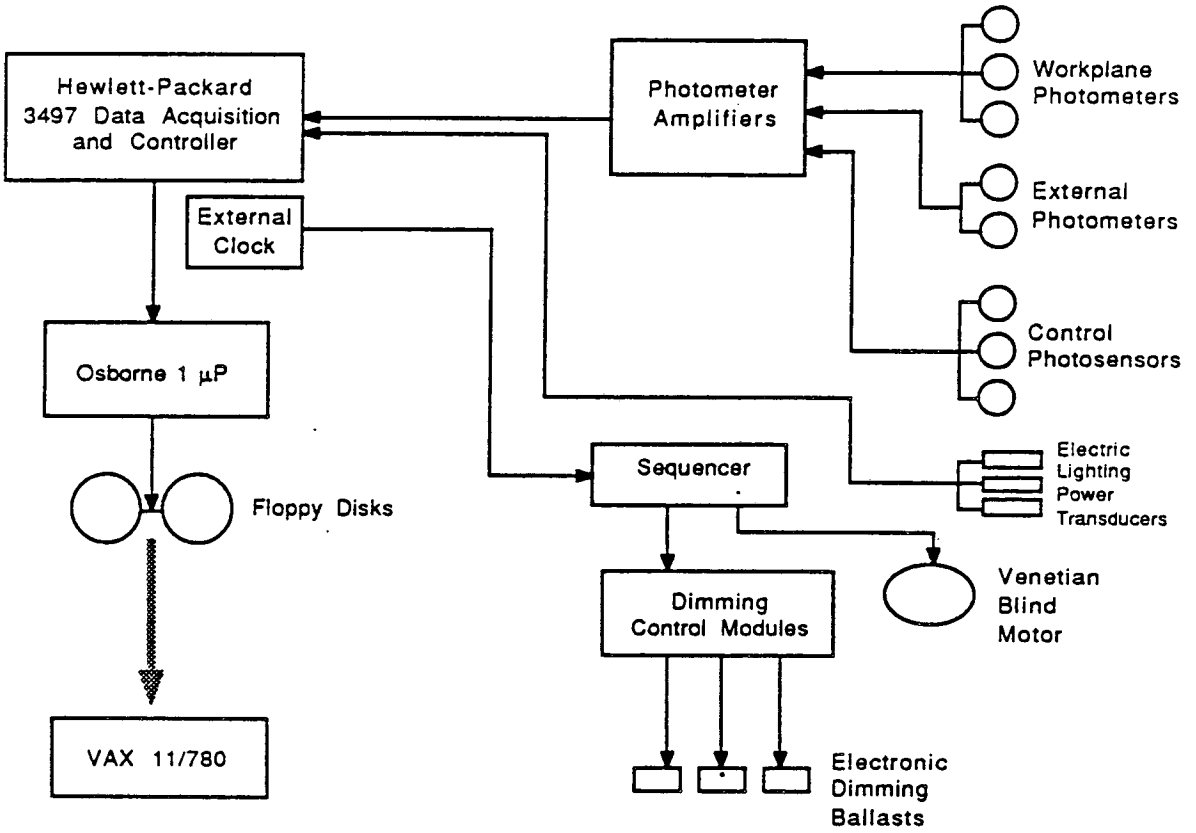

Figure 4-7. Schematic of data collection apparatus

TEST SITE DESCRIPTION

The scale model was located on the roof of the third floor roof of Building 90 at Lawrence Berkeley Laboratory. The model was anchored to a wood deck of 20-40% reflectance. The model had an unobstructed view of the sky when aimed in the west or south directions. Towards the east, the tops of two evergreen trees obstructed part of the sky. As shown in Figure 4-8, the fourth floor blocked much of the view north. The Berkeley hills that run NW to SE behind the building also blocked some of the lower portion of the sky to the north or east.

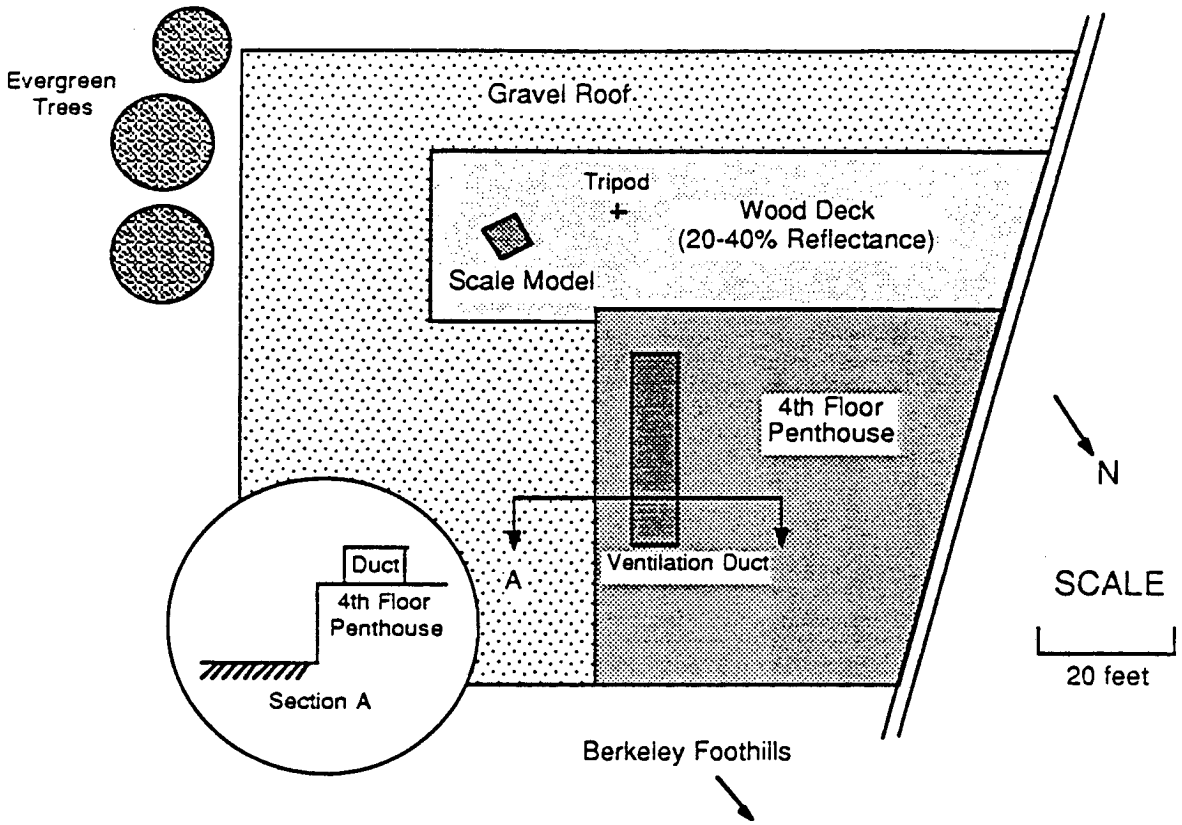

Figure 4-8. Plan view showing location of scale model test site

GENERALIZED SYSTEM MODEL

Figure 4-9 presents a schematic showing the relationship between the control system components and the other physical processes that make up the complete daylighting system in the scale model. In the diagram, each block represents a major system component or process; the direction of the signal flow is given by lines with arrows connecting the different blocks. Appropriate signal paths are labeled in accordance with the nomenclature presented in Section 3. Some of the blocks correspond to specific electric circuits (such as the controller). Others refer to physical processes such as the "fixture-to-workplane" block, which symbolizes the transfer function that expresses how electric light generated by the ceiling fixtures reaches the workplane station point. Ideally, these blocks are functionally equivalent to simple amplifiers in that the output of the block is simply the input multiplied by some scale factor, denoted by K. However, in some cases, such as the "window-to-sensor" block, the transfer function will be very complex in form because it must describe not only how direct window light illuminates the sensor but also how the window light reflected within the room affects the sensor. Also, as indicated in the diagram, many system elements are affected by uncontrollable variables such as dirt depreciation and other factors which, in turn, affect the operation of the entire system.

As shown in Figure 4-9, the photosensor signal goes to the controller summing node, where its value is compared to the setpoint level (S_{Em}). The difference, ε, is scaled by the integral or proportional gain factor, K_I or K_P, and is then compared to the maximum fractional dimming level ($\delta_{max} = 1$, as given in Section 3). This difference, δ, is the controller output and corresponds directly to the fractional dimming level that the system provides given these conditions. If the "fixture-to-sensor" gain, $K_{F\text{-}S}$, is not zero (i.e., some light from the fixtures reaches the photosensor), then the total photosensor signal $S_T(t)$ will consist of an independent component, $S_D(t)$, and a dependent component, $S_E(t)$, as described previously.

The major independent input to the daylighting control system, of course, is the daylight coming through the window. For analytical purposes, daylight is often divided into two components: the direct solar beam and the diffuse radiation from the sky. The direct beam radiation is generally an order of magnitude larger than the diffuse sky component and is very directional in nature. Because of its intensity, direct beam radiation is usually excluded from interior building spaces by means of solar controls (e.g., window blinds). Direct solar radiation, however, may penetrate into the space after bouncing off one or more reflecting surfaces (such as the slats on the blinds or the ground plane outside the building). This can contribute significantly to the daylight in the building space, and its spatial distribution is highly dependent on specific building and window factors. The radiation from the sky is more useful than direct sun as a source of illumination for buildings because it is diffuse in nature. However, the intensity of the diffuse component inside a side-lit room decreases rapidly as one moves away from the window. A more complete treatment of the daylighting phenomenon is given in Reference 6.

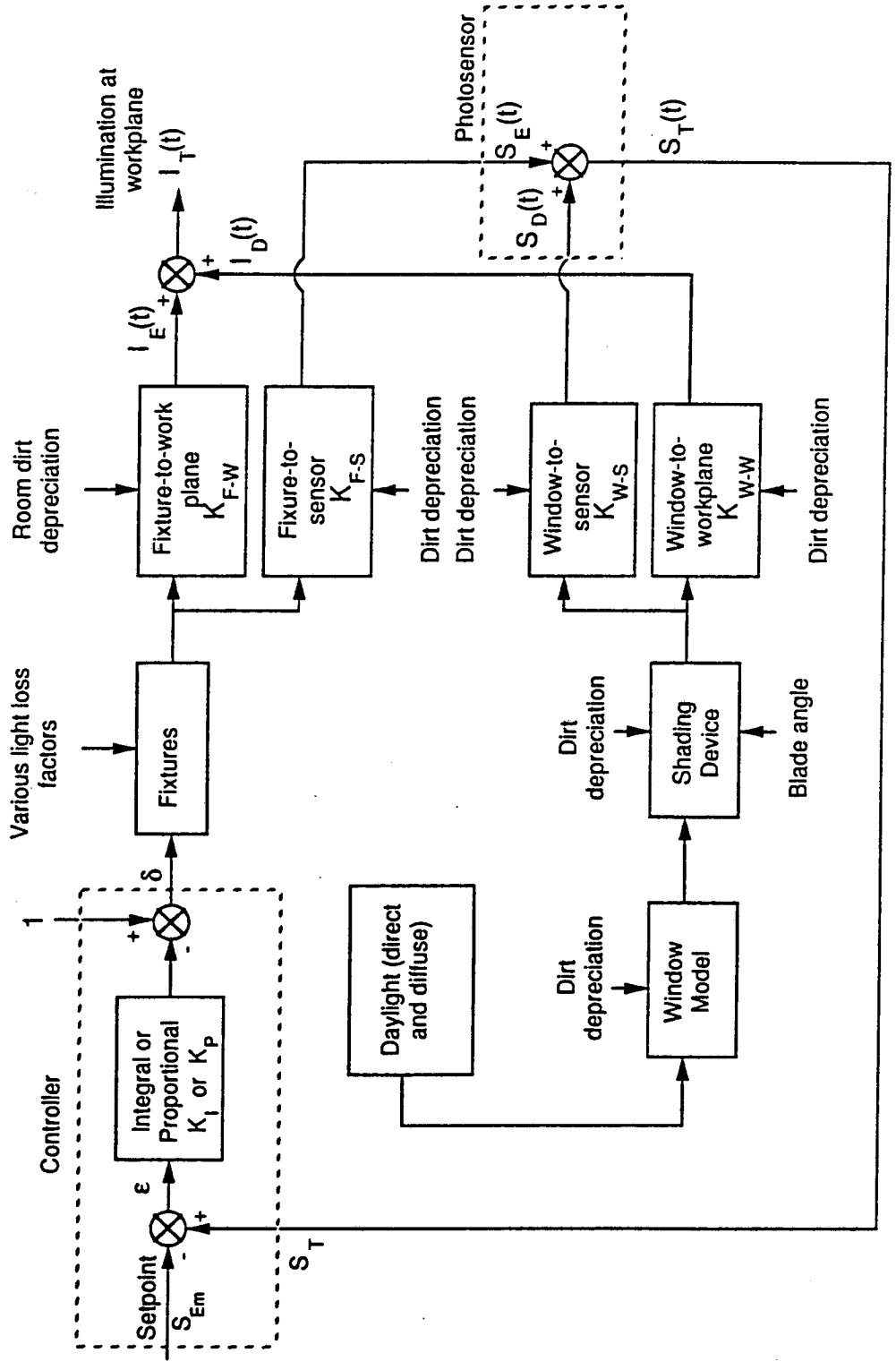

Figure 4-9. Block diagramof daylight-following system.

Section 5

DATA COLLECTION AND ANALYSIS

TESTING PROCEDURES

Between February 1984 and December 1986, data were taken periodically for two to five days at a time, depending on weather and test conditions. Before a test, the model was pointed in a particular direction (i.e., north, east, south, or west) and the data acquisition system programmed to take data scans at regular intervals (typically once every five minutes). During a data scan, the outputs of all 29 photometric and power transducers were rapidly read and recorded (in less than 2 seconds), ensuring effectively simultaneous reading of all data channels. The computer was programmed not to collect data during the hours between 8 pm and 4 am. After from two to five days, the data acquisition system was stopped and the model rotated to another direction for the next round of data collection.

Table 5-1 lists the number of days that data was taken for each month and direction and specifies the particular test conditions. During these three years we took data for approximately 390 days; thus we collected data on 35% of the maximum possible number of days, ensuring adequate sampling of the diverse daylight conditions and seasonal effects.

Testing Techniques

As indicated in Table 5-1, between February and September, 1984, we used an electronic sequencing device to switch the electric lighting system on and off at regular intervals (typically on for one minute and off for nine minutes). This allowed data collection for different modes of the lighting system operated under identical sky conditions. Measurement scans timed to occur when the lights were off provided baseline measurements of the daylight on all the photometers and photosensors within the model without the influence of electric lights. Scans that took place when the electric lights were on provided direct measurements of the combined effect of daylight and electric light controlled according to a particular control algorithm and with a selected photosensor. Between February and June,1984, the electric lights were controlled by the workplane photometer at P_{77} (Fig. 4-5) using the integral reset control algorithm. Between June and September, 1984, the electric lights were controlled by the P_{unsh} photosensor using the proportional control algorithm. These data were taken to demonstrate 1) that we could easily modify an existing

TABLE 5-1
Test Conditions and Number of Days Data Were Collected

Test Date	Model Type	Window Transmttce	Ven.Blind Schedule[A]	Data Type[B]	# Days in Direction N	E	S	W
2/84-6/84	Sm. Office	43%	None	I	14	16	8	14
6/84-7/84	Sm. Office	43%	None	$P(P_{unsh})$	0	0	0	11
8/84-9/84	Sm. Office	43%	None	$P(P_{unsh})$	5	15	6	6
9/84	Sm. Office	43%	None	$P(P_{unsh})$	4	0	5	8
10/85	Sm. Office	43%	A	DL Only	0	0	5	7
11/85-1/86	Sm. Office	43%	A	DL Only	15	18	6	10
1/86-4/86	Sm. Office	88%	A	DL Only	29	13	4	9
4/86	Sm. Office	88%	A	DL Only	0	7	0	0
4/86-7/86	Sm. Office	88%	A	DL Only	13	11	9	3
6/86-7/86	Sm. Office	88%	A	DL Only	3	11	6	3
6/86-8/86	Sm. Office	88%	A	DL Only	4	14	7	9
9/86-10/86	Sm. Office	88%	B	DL Only	0	0	2	9
9/86-10/86	Sm. Office	88%	B	DL Only	0	0	14	5
11/86	Semi Inf. Room	88%	B	DL Only	6	6	6	6
12/86	Semi Inf. Room	88%	B	DL Only	2	2	0	4

[A]See Fig. 4-3 for venetian blind schedule definitions

[B]During this time, the electric lights were controlled alternately every 2 minutes by the P_{unsh}, P_{psh}, and P_{fsh} photocells using integral reset control.

integral reset type controller to use proportional control, 2) that the modified control circuit operated as predicted, and 3) that the total maintained light levels at the workplane (i.e., daylight plus supplied electric light) could be computed based entirely on the daylight-only data and an understanding of how the various control algorithms operated (expressed mathematically in Eqs. 3-8, 9, 14, 15, 20, and 21). This third point is particularly important since it would be impossible to adequately test and compare every combination given the number of control photosensors and algorithms to choose from.

Except for periodic nighttime baseline measurements of the electric lighting level in the model, all the data after September 1984 were taken with the electric lights off. The venetian blinds were controlled automatically using two different schedules as illustrated schematically in Figure 4-3. Between June and October 1986 we alternately covered the wooden deck outside the model window with white and black cloth to test the impact of varying ground plane reflectance on the measured data.

DATA ANALYSIS

Understanding how changing daylight conditions and seasons affect the performance of photoelectric control systems generally requires collecting a large amount of data. To efficiently process and reduce these data, a series of computer programs were developed to run on the LBL VAX 11/780 computer operating under the UNIX operating system. These programs could be linked together in a "pipeline" to achieve various data reduction functions such as applying calibration factors to the raw data, plotting the results from a particular channel as a function of time of day, and averaging results from many days to obtain a statistically significant picture. In the following section, we describe some of the data analysis programs used to process the experimental data.

Simulation Programs

Three simulation programs were developed to model the response of lighting control systems obeying the three control algorithms described in Section 3. These programs compute how much electric light each modelled system would supply by inputting the daylight-only measurements from the model's control photosensors and workplane photometers into Eqs. 3-8, 9, 14, 15, 20, or 21 to compute the total illuminances at points on the workplane. Although this computational technique is, in the strict sense, a simulation, the program should accurately predict how a real system would perform because it uses the measured daylight data as input.

The two simulation programs that predict the response of integral-reset and proportional-control systems must also be given measured values of S_{Em}, the control photosensor signals obtained with no daylight and the electric lights at full light output, for each control photosensor. These values were obtained by reading the output from each control photosensor at night with the electric lights set to maximum brightness (Table 6-1 for the small office model and Table 6-2 for the semi-infinite room model).

Because closed- and open-loop proportional control systems require the system gain to be adjusted according to room and daylight conditions, their simulation programs must be given scale-factor values (the M terms in Eqs. 3-19 and 3-13). Choosing a scale factor is equivalent to specifying the conditions under which the system is calibrated. Scale factors for each photosensor/algorithm simulation were computed (Table 6-1 for the small office model data and Table 6-2 for the semi-infinite room model) by fitting the workplane daylight illuminance data and photosensor data to a line and computing the slope of the line. For each photosensor/algorithm/orientation combination in the small-office model, we selected two sunny days from the winter and summer for this calculation to ensure adequate representation of the diverse possible daylight conditions. For the semi-infinite room model, only the data from a typical sunny winter day was used.

Sky Condition Analysis Program

To show how the intensity of the direct sun can influence photosensor performance, a program was written to computationally classify each measured data point as "sunny" or "not sunny." The program classified each data point using the data from the external photometers to compute the intensity of the direct normal solar component outside the model at the time of measurement by means of the following criteria:

$$\text{not sunny:} \quad \frac{E_g - E_d}{\sin \theta} < 20{,}000 \text{ lumens/meter}^2$$

$$\text{sunny:} \quad \frac{E_g - E_d}{\sin \theta} > 20{,}000 \text{ lumens/meter}^2$$

where E_g is the total horizontal illuminance from the sun and unobstructed sky; E_d is the illuminance due only to the sky; and θ, the solar altitude (measured from the horizon), is computed from the time of day. The above criterion for differentiating sunny and not sunny conditions was selected to be consistent with measurements from the Campbell-Stokes sunshine recorder, which has often been used for recording the number of hours of sunshine. Readings obtained from the external unshielded photometer, P_{glob}, were used for E_g, and E_d was approximated using the reading from the external photometer, P_{dif}, that was equipped with a shadow band to shield it from direct sun. Readings from P_{dif} are not strictly equal to E_d because of the error introduced by the portion of the shadow band that obstructs the sky but not sun but the error is acceptably low for our purposes. The program also filtered out data points obtained when the sun was below 6 degrees from the horizon since the above method of calculating direct normal solar intensity is inaccurate at low solar altitudes.

Direct Sun Exclusion Program

Because direct sun is usually prevented from entering a real building space by means of solar controls on the window, we developed a computer program that threw out data points for which the venetian blind blade angle and/or the location of the sun relative to the window was such to allow direct sun penetration. The mathematical formulation for this program is given in Reference 7.

Task Location

Our analysis presupposes that there is a point or points on the workplane where we want to achieve our objective of maintaining a minimum specified illuminance level. In a real

building, these points would usually be at the location of visual tasks. Since there were no explicit visual task locations in the scale model, we had to choose a location or locations at which to perform the analysis. For the small office model, we posited a task located approximately 2/3 of the way in from the window as shown in Figure 4-5 and took the task illuminance to be the average illuminance of the two workplane photometers symmetrically located about the room centerline as indicated. For the semi-infinite room case, we took the task illuminance of the front portion of the room to be the illuminance measured by the workplane photometer at position WP_4 and the task illuminance at the rear to be that measured at WP_9 as shown in Figure 4-6.

Section 6

EXPERIMENTAL RESULTS

INTRINSIC CONTROL PHOTOSENSOR PERFORMANCE

By examining the relationship between the daylight illuminance at the workplane and the daylight striking the photosensor, one can analyze the performance of any control photosensor somewhat independently of the specific characteristics of its control system.

Small Office Model

These relationships are plotted as scatter plots for typical clear days for the small office model both with and without the operable venetian blind shading system in Figure 6-1 (west), Figure 6-2 (north), Figure 6-3 (east), and Figure 6-4 (south) for the (A and B) unshielded, (C and D) partly shielded, (E and F) fully shielded, and (G and H) window-aimed photosensors. Every data point on these scatter plots represents a simultaneous measurement of the daylight on the photosensor (horizontal axis) and the daylight illuminance at the workplane (vertical axis). (Workplane daylight illuminance is defined as the average daylight illuminance at workplane points WP_{78} and WP_{77}). Because direct sun would enter the unshaded model (Figs. 6- A, C, E, and G) when the sun was shining and within 90° from normal to the window, data points taken under such conditions were excluded from the graphs. For the model with the operable shading device installed (Figs. 6- B, D, F, and H), we computationally excluded those data points for which the blade angle was such as to allow direct solar penetration. This treatment is justifiable because, in any realistic building application, direct sun would be excluded by appropriate use of a shading device.

Table 6-1 presents statistics that summarize the degree of correlation between workplane illuminance and photosensor signal for each control photosensor and direction. Fitting coefficients, b, were determined by applying least-squares fits to each of the scatter plots shown in Figures 6-1 through 6-4 and constraining the fitted lines to pass through the origin. These fitted coefficients are given in the bold-face column in Table 6-1 labeled "Task-Sensor Ratio I_D/S_D." The standard error of the estimate (SE) and correlation coefficient (r) are measures of how well the data can be fitted to a line with slope b passing through the origin. (For a perfect fit, SE = 0 and r=1).

While the details of the data vary depending on the direction and photosensor, several major trends are evident. Except for the north-facing window, it is clear that the signal from the partially shielded photosensor, P_{psh}, is best correlated with the illuminance at the workplane. Even when comparing different seasons and with and without the shading

device, P_{psh} outperforms all the other photosensors. The fully shielded photosensor, P_{fsh}, also performs reasonably well, as indicated by the relatively high correlation coefficients and low standard error values; however, it consistently scores lower than the partially shielded photosensor. It is significant that the fitted slope, b, for these photosensors does not change significantly between different seasons or with different venetian blind blade angles, because this invariance implies that calibrating the response of the photocontrol system need only be performed once.

The unshielded photosensor, P_{unsh}, shows much more scatter than either the fully or partially shielded photosensors, indicating that the signal from this photosensor is only a fair indicator of workplane illuminance. Furthermore, the slope of the best-fit line for this photosensor is more sensitive to different seasons and different venetian blind blade angles than the P_{psh} or P_{fsh} photosensors. The data for the north-facing model without venetian blinds is the one exception to these trends. In this one case, the signal from the P_{unsh} photosensor is more closely correlated to workplane illuminance than that of any other tested photosensor.

The scatter plots of the response for the window aimed photosensor, P_{wdw}, show that the output of this photosensor is a poor indicator of the illuminance at the workplane. The relationship between sensor output and workplane illuminance is highly sensitive to the season and blade angle. For most orientations, the correlation coefficients for the best-line fit are so low that one cannot reject the hypothesis that there is *no* correlation between workplane illuminance and photosensor output.

Table 6-1. Correlation Statistics and Calibration Factors for Control Photosensors in Small Office Model

	ELECTRIC LIGHT		DAYLIGHT MEASUREMENTS							CALCULATED SCALE FACTORS		
Photo-sensor	Night Setpnt. S_{Em} (lux) (1)	Task-Sensor Ratio (2) I_{Em}/S_{Em}	Test Date	Direc-tion	Venetian Blinds Schedule (3)	Num. Data Point N	Task-Sensor Ratio (4) I_D/S_D	Stand. Err. of Est. SE (5)	Correl. Coeff. r	Ave. Ratio <b> (6)	M_{CL} (7)	M_{OL} (8)
P_{unsh}	140	5.14	4/7/84	W	no blinds	54	0.65	78.2	0.89	0.592	-0.000944	-0.000822
	140	5.14	12/9/85	W	Sch. A	118	0.592	55.5	0.683			
	140	5.14	7/5/86	W	Sch. A	153	0.588	153.0	0.748			
P_{fsh}	60.5	11.9	4/7/84	W	no blinds	54	8.18	29.4	0.985	8.323	-0.0386	-0.0116
	60.5	11.9	12/9/85	W	Sch. A	118	8.54	19.4	0.967			
	60.5	11.9	7/5/86	W	Sch. A	153	8.25	68.6	0.955			
P_{psh}	99	7.27	4/7/84	W	no blinds	54	3.83	20.2	0.993	3.82	-0.0112	-0.00531
	99	7.27	12/9/85	W	Sch. A	118	3.73	11.7	0.988			
	99	7.27	7/5/86	W	Sch. A	153	3.9	39.3	0.985			
P_{wdw}	1	720.0	4/7/84	W	no blinds	54	3.13	149.7	0.486	2.613	-0.00364	-0.00363
	1	720.0	12/9/85	W	Sch. A	118	2.29	74.1	0.22			
	1	720.0	7/5/86	W	Sch. A	153	2.42	196.8	0.522			
P_{unsh}	140	5.14	6/8/84	N	no blinds	75	0.461	23.6	0.978	0.592	-0.000944	-0.000822
	140	5.14	12/11/85	N	Sch. A	143	0.872	30.9	0.694			
	140	5.14	5/16/86	N	Sch. A	139	0.442	78.9	–			
P_{fsh}	60.5	11.9	6/8/84	N	no blinds	75	5.38	51.9	0.891	6.697	-0.0229	-0.0093
	60.5	11.9	12/11/85	N	Sch. A	143	7.99	15.37	0.934			
	60.5	11.9	5/16/86	N	Sch. A	139	6.72	64.19	–			
P_{psh}	99	7.27	6/8/84	N	no blinds	75	2.84	57.7	0.864	3.367	-0.00889	-0.00468
	99	7.27	12/11/85	N	Sch. A	143	3.79	7.3	0.985			
	99	7.27	5/16/86	N	Sch. A	139	3.47	41.8	0.737			
P_{wdw}	1	720.0	6/8/84	N	no blinds	75	0.91	59.1	0.856	2.183	-0.00304	-0.00303
	1	720.0	12/11/85	N	Sch. A	143	3.79	48.7	–			
	1	720.0	5/16/86	N	Sch. A	139	1.85	104.2	–			

continued

Table 6-1 (Contd). Correlation Statistics and Calibration Factors for Control Photosensors in Small Office Model

Photo-sensor	ELECTRIC LIGHT		DAYLIGHT MEASUREMENTS							CALCULATED SCALE FACTORS		
	Night Setpnt. S_{Em} (lux) (1)	Task-Sensor Ratio (2) I_{Em}/S_{Em}	Test Date	Direc-tion	Venetian Blinds Schedule (3)	Num. Data Point N	Task-Sensor Ratio (4) I_D/S_D	Stand. Err. of Est. SE (5)	Correl. Coeff. r	Ave. Ratio <b> (6)	M_{CL} (7)	M_{OL} (8)
P_{unsh}	140	5.14	4/3/84	E	no blinds	39	0.602	41.5	0.938			
	140	5.14	12/16/85	E	Sch. A	116	0.657	36.7	0.657	0.6	-0.000945	-0.000834
	140	5.14	4/29/86	E	Sch. A	113	0.543	125.0	0.626			
P_{fsh}	60.5	11.9	4/3/84	E	no blinds	39	6.99	20.6	0.985			
	60.5	11.9	12/16/85	E	Sch. A	116	7.66	15.3	0.949	7.183	-0.0254	-0.00998
	60.5	11.9	4/29/86	E	Sch. A	113	6.9	67.5	0.907			
P_{psh}	99	7.27	4/3/84	E	no blinds	39	3.72	15.13	0.992			
	99	7.27	12/16/85	E	Sch. A	116	3.71	10.4	0.977	3.713	-0.0105	-0.00516
	99	7.27	4/29/86	E	Sch. A	113	3.71	44.5	0.961			
P_{wdw}	1	720.0	4/3/84	E	no blinds	39	1.26	56.5	0.882			
	1	720.0	12/16/85	E	Sch. A	116	3.0	49.4	–	2.187	-0.00305	-0.00304
	1	720.0	4/29/86	E	Sch. A	113	2.3	167	–			
P_{unsh}	140	5.14	12/18/85	S	Sch. A	77	0.509	19.0	0.988	0.532	-0.000823	-0.000738
	140	5.14	5/24/86	S	Sch. A	136	0.554	178.8	–			
P_{fsh}	60.5	11.9	12/18/85	S	Sch. A	77	7.64	8.7	0.998	7.475	-0.028	-0.0104
	60.5	11.9	5/24/86	S	Sch. A	136	7.31	88.5	0.783			
P_{psh}	99	7.27	12/18/85	S	Sch. A	77	3.53	6.3	0.999	3.595	-0.00988	-0.00499
	99	7.27	5/24/86	S	Sch. A	136	3.66	49.4	0.938			
P_{wdw}	1	720.0	12/18/85	S	Sch. A	77	2.26	30.7	0.97	2.21	-0.00308	-0.00307
	1	720.0	5/24/86	S	Sch. A	136	2.16	228.2	–			

(1) Photosensor output at night with full electric light (δ=1).
(2) I_{Em}= 720 lux (ave. of illuminance at WP_{77} and WP_{78} for δ=1).
(3) Schedule A: 4 possible blade angles -- 30, 60, 90, 120°. Data points with interior direct sun excluded.
(4) Least squares estimate of b using I_D=b S_D.
(5) Standard error of estimate:
(6) Average of task-sensor ratios from column 8.
(7) Calculated from Eq. (3-19) using $<b> = I_D(t_c)/S_D(t_c)$.
(8) Calculated from Eq. (3-13) using $<b> = I_D(t_c)/S_D(t_c)$.

Table 6-2. Correlation Statistics and Calibration Factors for Control Photosensors in Semi-Infinite Room Model

Photo-sensor	Station point	ELECTRIC LIGHT: Night Setpnt. S_{Em} (lux) (1)	ELECTRIC LIGHT: Task-Sensor Ratio (2) I_{Em}/S_{Em}	DAYLIGHT MEASUREMENTS: Test Date (3)	Direc-tion	Num. Data Points N	Task-Sensor Ratio (4) I_D/S_D	Stand. Err. of Est. SE (5)	Correl. Coeff. r	CALCULATED SCALE FACTORS: M_{CL} (7)	M_{OL} (8)
P_{unsh}	WP4	182	3.94	1/15/87	W	231	1.29	125.0	0.864	-0.00268	-0.0018
P_{bunsh}	WP9	184	4.00	1/15/87	W	231	1.64	18.8	0.992	-0.00378	-0.00222
P_{fsh}	WP4	105	6.83	1/15/87	W	231	8.17	54.5	0.976	∞	-0.011
P_{bfsh}	WP9	102	7.22	1/15/87	W	231	6.385	17.4	0.993	-0.075	-0.0087
P_{psh}	WP4	164	4.37	1/15/87	W	231	4.838	36.47	0.989	∞	-0.0067
P_{bpsh}	WP9	118	6.24	1/15/87	W	231	4.391	19.8	0.991	-0.02	-0.006
P_{wdw}	WP4	4	179.25	1/15/87	W	231	1.432	210.0	0.530	-0.002	-0.002
P_{wdw}	WP9	4	184.00	1/15/87	W	231	0.853	125.6	0.538	-0.0012	-0.0012
P_{unsh}	WP4	182	3.94	1/16/87	N	323	1.316	70.65	0.832	-0.00276	-0.0018
P_{bunsh}	WP9	184	4.00	1/16/87	N	323	1.36	8.59	0.994	-0.0028	-0.0018
P_{fsh}	WP4	105	6.83	1/16/87	N	323	7.89	36.5	0.958	∞	-0.011
P_{bfsh}	WP9	102	7.22	1/16/87	N	323	6.17	13.1	0.987	-0.058	-0.0084
P_{psh}	WP4	164	4.37	1/16/87	N	323	4.73	21.2	0.986	∞	-0.0066
P_{bpsh}	WP9	118	6.24	1/16/87	N	323	4.46	12.9	0.987	-0.02	-0.006
P_{wdw}	WP4	4	179.25	1/16/87	N	323	1.61	107.2	0.539	-0.0023	-0.0022
P_{wdw}	WP9	4	184.00	1/16/87	N	323	1.06	55.3	0.736	-0.0015	-0.0014

continued

Table 6-2 (contd). Correlation Statistics and Calibration Factors for Control Photosensors in Semi-Infinite Room Model

Photo-sensor	Station point	ELECTRIC LIGHT: Night Setpnt. S_{Em} (lux) (1)	ELECTRIC LIGHT: Task-Sensor Ratio (2) I_{Em}/S_{Em}	DAYLIGHT MEASUREMENTS: Test Date	Direc-tion	Num. Data Points N	Task-Sensor Ratio (4) I_D/S_D	Stand. Err. of Est. SE (5)	Correl. Coeff. r	CALCULATED SCALE FACTORS: M_{CL} (7)	M_{OL} (8)
P_{unsh}	WP_4	182	3.94	1/14/87	E	263	1.27	77.8	0.858	-0.00261	-0.00178
P_{bunsh}	WP_9	184	4.00	1/14/87	E	263	1.39	6.62	0.995	-0.0028	-0.0018
P_{fsh}	WP_4	105	6.83	1/14/87	E	263	7.12	64.8	0.904	∞	-0.01
P_{bfsh}	WP_9	102	7.22	1/14/87	E	263	5.48	11.65	0.985	-0.031	-0.0074
P_{psh}	WP_4	164	4.37	1/14/87	E	263	4.47	59.9	0.919	∞	-0.0062
P_{bpsh}	WP_9	118	6.24	1/14/87	E	263	4.39	10.3	0.988	-0.0213	-0.0061
P_{wdw}	WP_4	4	179.25	1/14/87	E	263	1.88	118.1	0.626	-0.0026	-0.0026
P_{wdw}	WP_9	4	184.00	1/14/87	E	263	0.92	41.0	0.794	-0.0013	-0.00125
P_{unsh}	WP_4	182	3.94	2/18/87	S	164	1.27	78.4	0.98	-0.00261	-0.00177
P_{bunsh}	WP_9	184	4.00	2/18/87	S	164	1.7	14.8	0.997	-0.004	-0.0023
P_{fsh}	WP_4	105	6.83	2/18/87	S	164	7.79	72.0	0.983	∞	-0.011
P_{bfsh}	WP_9	102	7.22	2/18/87	S	164	6.17	7.32	0.999	-0.059	-0.0084
P_{psh}	WP_4	164	4.37	2/18/87	S	164	4.89	56.4	0.99	∞	-0.0068
P_{bpsh}	WP_9	118	6.24	2/18/87	S	164	4.46	15.2	0.997	-0.021	-0.0061
P_{wdw}	WP_4	4	179.25	2/18/87	S	164	1.57	164.3	0.908	-0.0022	-0.0022
P_{wdw}	WP_9	4	184.00	2/18/87	S	164	0.77	94.0	0.878	-0.001	-0.001

(1) Photosensor output at night with full electric light (δ=1).
(2) I_{Em}= 720 lux (ave. of illuminance at WP_{77} and WP_{78} for δ=1).
(3) Schedule A: 4 possible blade angles -- 30, 60, 90, 120°. Data points with interior direct sun excluded.
(4) Least squares estimate of b using I_D=b S_D.
(5) Standard error of estimate:
(6) Average of task-sensor ratios from column 8.
(7) Calculated from Eq. (3-19) using $\langle b \rangle = I_D(t_c)/S_D(t_c)$.
(8) Calculated from Eq. (3-13) using $\langle b \rangle = I_D(t_c)/S_D(t_c)$.

Semi-Infinite Room Model

The relationships between photosensor signal and workplane illuminance are shown for the west, north, east, and south directions in Figures 6-5 through 6-8, respectively, for the semi-infinite room model fitted with a clear glass window and the operable venetian blind system operating under Schedule B (i.e., every 10° between 40° and 120°, as shown in Figure 4-3). The plots in the left-hand column of each of these figures (sub-figures A, C, E, and G for the P_{unsh}, P_{fsh}, and P_{psh}, and P_{wdw} photosensors, respectively) show the relationship between the aforementioned front cluster photosensors (Fig. 4-2) and the daylight workplane illuminance measured by the WP_4 workplane photometer (Fig. 4-6). The right-hand plots show the equivalent relationships between the rear photosensors and the WP_9 workplane photometer (Fig. 4-6). The WP_4 and WP_9 photometers were selected as indicators of the workplane illuminance in the front and rear portions of the room, respectively. In these scatter plots, we have excluded, using the program discussed in Section 5, data points that occurred when the blade angles were such that direct sun penetrated into the model interior.

Table 6-2 summarizes the best-line slopes, goodness of fit, and standard errors statistics for the scatter plots given in Figures 6-5 through 6-8.Qualitatively, in the front portion of the model, the correlations between the various control photosensors and workplane illuminance are similar to the small office model results. Photosensor output and workplane illuminance are best correlated for the partially shielded photosensor while there is poor correlation for the window-aimed photosensor. In the rear portion of the model, though, the unshielded photosensor performs generally as well, and for some orientations, better than the partially or fully shielded photosensors. Thus, there appears to be little advantage to shielding the control photosensor from direct window light, if the control photosensor is sufficiently distant from the window (i.e., greater than approximately 3 window heights).

EFFECT OF CONTROL ALGORITHM

In the preceding section, we compared the intrinsic performance of the control photosensors by examining how well they tracked the daylight illuminance at the workplane. In this section, we analyze the effect of the control circuit, which sets the electric light level based on the measured photosensor signal, and investigate how the choice of control algorithm affects overall control system performance with respect to maintaining a minimum workplane illuminance.

Simulated vs. Measured Electric Light Levels

To justify the use of simulated electric light levels, which, as discussed in the previous section, simplified the data acquisition process, we compare here measurements of controlled electric light to simulations of the same quantity. To accomplish this, we designed physical electronic circuits of the integral reset and closed-loop proportional control systems and used these to control the electric lights from the P_{unsh}, P_{fsh}, and P_{psh} photocells. As indicated in Table 5-1, we used integral reset control from the P_{unsh}, P_{fsh}, and P_{psh} photocells in the spring of 1984 and closed-loop proportional control from the P_{unsh} photosensor in the fall of 1984. The accuracy of the simulation method is demonstrated in Figure 6-9 for the west-facing model with 43% transmittance window and no shading device. The curve labeled "actual" indicates the measured total workplane illuminance (daylight plus controlled electric light) at the P_{77} workplane photometer (see Fig. 4-5) when the integral-reset system was controlled by the partially shielded (P_{psh}) control photosensor. The curve labeled "simulation" gives the illuminance at the same point as computed by the simulation program modelling the "real" system. The actual and simulated workplane illuminance and electric lighting power use for the closed-loop proportional system controlled by the P_{unsh} photosensor are given in Figures 6-10 through 6-12 for the west, north, and south directions, respectively.

The results obtained with the physical circuits correspond closely to the simulations in terms of overall shape, although there are discernible differences in the fine-scale details for two reasons. The small-scale differences reflect the limitation in how the data for the curves are collected. Because the data from which the "actual" curve is constructed is collected two minutes earlier than the "daylight only" data, short-term changes in daylight levels cause small differences between the actual and simulated curves. The longer-term discrepancies result from elevated temperatures in the model reducing the light output and efficacy of the real fluorescent lighting system. The simulations do not account for this thermal effect and make the simulated light levels slightly higher, and the simulated power levels slightly lower than those measured in the model. These differences would be smaller in a realistic building environment where the air temperature is controlled by the building cooling system.

Integral-Reset Systems

Small office model. The simulation results for control photosensors P_{unsh}, P_{psh}, and P_{fsh} driving integral-reset control systems (subfigures A, C, and E, respectively) are given in Figures 6-13 (for winter) and 6-14 (for summer) for the small office model facing west. Similar sets of figures are given for the north (6-15 and 6-16), east (6-17 and 6-18), and south (6-19 and 6-20).

Semi-infinite room model. The simulations for the front control photosensors P_{unsh}, P_{psh}, and P_{fsh} controlling integral-reset systems (subfigures A, C, and E, respectively) are shown in Figure 6-22 for the front portion of the semi-infinite room facing west. Figure 6-23 shows the equivalent results in the rear portion of the model for integral-reset systems controlled by the rear photosensors P_{bunsh}, P_{bpsh}, and P_{bfsh}. Comparable graphs are shown in Figures 6-24 through 6-29 for the north, east, and south directions.

The grey shaded area in each graph shows the contribution of daylight to the total illuminance at the indicated workplane point(s) as a function of time of day for the indicated test day. The cross-hatched area indicates the contribution of supplied electric light to the workplane illuminance for the indicated control photosensor and algorithm. The upper boundary of the cross-hatched area therefore corresponds to the total illuminance at the workplane. In each graph, the dashed curve gives the blade angle of venetian blind system as a function of time of day. The blade angles shown are those slat angles that excluded direct sun from penetrating the model while permitting maximum slat openness. Thus, for the example of the west-facing model, the 90° blade angle data (see Fig. 6-13) was used until approximately 2:00 pm after which the 60° blade angle data was used because the 90° blade angle was insufficient to block the sun. Similarly, from approximately 4:00 pm until sunset, the 30° blade angle data was used since direct sun could penetrate with the blades at 60° (or 90°). We selected this venetian blind control strategy for the small office model simulations to mimic the way the room occupant might realistically use the blinds (i.e., periodically adjusting the venetian blinds to provide a reasonable external view while preventing uncomfortable direct sun from penetrating the room). A similar, but more refined control strategy was used for the semi-infinite room case. In this case, the blade angles could vary in 10° rather than 30° increments. Thus the semi-infinite room simulations are more indicative of what might be expected in a building with a completely automatic shading system designed to prevent direct solar penetration while providing maximum openness.

Small office model. Figures 6-13 through 6-20 show that integral reset systems controlled by the unshielded photosensor (P_{unsh}) consistently provide far less electric lighting than is required to meet the target light level. In several cases, (e.g., Figs. 6-13, 6-16, 6-18, and 6-19) the electric light levels are fully dimmed for much of the day even though the daylight contribution at the workplane only provided about 30% of the design light level. The poor performance of the P_{unsh} cell is particularly apparent for the north-facing model, when the electric lights are dimmed to minimum despite the small contribution of daylight to the workplane light level. Integral-reset systems driven by the partially- and fully-shielded photosensors (P_{psh} and P_{fsh}) also failed to provide sufficient electric light to meet the target level but consistently provided more light than equivalent systems driven by the unshielded photosensor. Systems driven by the P_{fsh} photosensor provided somewhat more electric

light than P_{psh}-driven systems. However, for the south and east-facing test days (Figs. 6-18, 6-19, and 6-20), the P_{fsh} and P_{psh}-driven systems allowed total light levels to fall roughly 25% and 45%, respectively, below the target light level for portions of the day. Thus, while it is apparent that shielding the ceiling-mounted photosensor from the window and vertical walls improves the performance of integral reset systems, it is important to note that none of the integral reset systems, regardless of direction or type of photosensor, provide sufficient illumination to satisfy the control system objectives.

Semi-infinite room model. Figures 6-23, 6-25, 6-27, and 6-29 show that the performance of integral reset control systems in the rear portion of the semi-infinite room are qualitatively similar to those of the small office model presented above. The total illuminance at the back part of the model (viz., at point WP_9 as shown in Fig. 4-6) was significantly below the design level (736 lux) when the integral-reset system was controlled by the rear unshielded photosensor, P_{bunsh}. Improved performance was evident for integral reset systems controlled by the rear partially- and fully-shielded photosensors, P_{bpsh} and P_{bfsh}. However, even in these cases, total illuminance at the rear of the room was at least slightly below the design level for substantial portions of the day.

In contrast to the results from the rear portion of the semi-infinite room, integral reset systems controlled by the front partially- and fully-shielded photosensors provided sufficient electric light at the front portion of the room to meet the design illuminance level throughout the day (Figs. 6-22, 24, 26, and 28, subfigures C and E) regardless of room orientation. The integral reset systems controlled by the front unshielded photosensor, P_{unsh}, however, provided substantially less illumination at the front of the room than required for all room orientations.

Closed-Loop Proportional Control Systems

For the small office model facing west, the simulation results for photosensors P_{unsh}, P_{psh}, and P_{fsh} driving closed-loop proportional control systems (subfigures B, D, and F, respectively) are given in Figures 6-13 (winter) and 6-14 (summer). Similar sets of figures are given for the north (6-15 and 6-16), east (6-17 and 6-18), and south (6-19 and 6-20). For the front portion of the semi-infinite room facing west, he simulations for the front control photosensors P_{unsh}, P_{psh}, and P_{fsh} controlling closed-loop proportional control systems (subfigures B, D, and F, respectively) are shown in Figure 6-22. Equivalent results for the rear portion of the model for closed-loop proportional control systems driven by the rear photosensors P_{bunsh}, P_{bpsh}, and P_{bfsh} are given in Figure 6-23. Results for the north, east, and south directions are presented in Figures 6-24 and 25 (north, front and rear), 6-26 and 27 (east, front and rear), and 6-28 and 29 (south, front and rear).

For all the small office data, closed-loop proportional control systems provide a total light level at the task much closer to the target level than comparable integral-reset systems. In every case, the use of proportional control causes task light levels to be within 10% of the target level. Because the unshielded photosensor, P_{unsh}, performed so poorly with an integral reset system, the improved performance of this photosensor with proportional control is most marked. However, performance was also significantly improved for the partially- and fully-shielded photosensors relative to integral reset control. The total light levels from these latter two systems are generally comparable for most of the test days shown. The simulations for the unshielded photosensor driving proportional controls show slightly inferior performance, with more variability in total light levels than either the P_{fsh} or the P_{psh} photosensors (see particularly Fig. 6-18). Also, the simulations from the unshielded photosensor often show this system providing more than the necessary amount of electric light to meet the target light level (e.g., Fig. 6-14B).

The closed-loop proportional control simulations for the rear portion of the semi-infinite room show characteristics similar to those of the proportional control simulations for the small office model. For the rear unshielded, partially- and fully-shielded photosensors, P_{bunsh}, P_{bpsh}, and P_{bfsh}, the use of proportional control provides a total light level in the rear of the room closer to the target light level than does the use of integral reset control. Total light levels are generally more constant with the partially- and fully-shielded photosensors compared to the results from the unshielded photosensor.

For the partially- and fully-shielded photosensors, the closed-loop proportional control simulations for the front portion of the semi-infinite room are identical to the results obtained with integral reset control. The simulations of the unshielded photosensor with closed-loop proportional control show total light levels at the workplane fairly constant throughout the day in marked contrast to the results obtained with integral reset control.

Open-Loop Proportional Control Systems

The simulation results for the P_{wdw} photosensor driving an open-loop proportional control system are shown in Figure 6-21 for the west-facing small office model in winter (A) and summer (B), north-facing (C & D), east-facing (E & F), and south-facing (G & H). Figure 6-30 shows the open-loop simulations for the P_{wdw} photosensor in the semi-infinite room model. The results for the front portion of the model are given for the west, north, east and south in subfigures A, C, E, and G, respectively with simulations for the rear portion of the model in subfigures B, D, F, and H. The graphs indicate that while open-loop proportional control clearly yields better results than integral reset control, there is a fair degree of variability in the maintained workplane light levels. In addition, the open-loop form of control provides more electric light than is necessary in some cases (Fig. 6-21 B, for example) while providing insufficient light in others (Fig. 6-21 G). Similar results

were found for the semi-infinite room example, with total light levels closer to the target level than integral reset systems, but showing more variability than the results obtained with the closed-loop proportional control.

The results show that an open-loop system controlled by the P_{wdw} photosensor outperforms any of the integral-reset systems in satisfying the control objectives. However, compared to closed-loop proportional control systems, open-loop control is more erratic, with the system often significantly overshooting or undershooting the design level.

PHOTOSENSOR LOCATION RELATIVE TO TASK LOCATION

One important issue in photoelectric controls is how close the ceiling-mounted photosensor should be to the task location where a minimum specified light level is to be maintained. We examined this question in the semi-infinite room model by performing least-squares fits to the measured signals from the partially- and fully-shielded photosensors relative to the measured illuminances at different points at the workplane. An example of the results of this analysis is given in Figure 6-31 for a clear winter day for the west-facing model at 11:00 am. In this figure we plot the goodness of fit (as measured by the standard error of the fit) for the P_{psh}, P_{bpsh}, P_{fsh}, and P_{bfsh} and P_{bunsh} photosensors versus the distance of the workplane point from the window. From the figure, it is seen that the best fit, i.e., the smallest standard error, occurs at the workplane point directly under the ceiling-mounted control photosensor. The goodness-of-fit for workplane points displaced to either side of the control photosensor decreases fairly rapidly. Other data (not shown) also indicated that the goodness of fit decreased more rapidly for the fully-shielded photosensor than for the partially-shielded or unshielded photosensors.

CALIBRATION

As discussed in Sections 3 and 5, the scale factor (i.e., the gain) for any proportional control system, whether closed- or open-loop, must be set by calibrating the system during the day. (Integral reset systems do not have adjustable gain and are designed to be calibrated only at night). The closed- and open-loop control simulations discussed above are based on the assumption that all systems are calibrated under comparable typical daylight conditions, with the best-fit slope to the data used for the computation of all the scale factors. In other words, we have assumed that all the simulated systems were calibrated under "typical" daylight conditions as determined by the available data. It is useful to ask what the results would be if the systems are calibrated under *atypical* daylight conditions (i.e., under a condition where the ratio of daylight on the workplane point and daylight on the photosensor is *not* typical). In Figure 6-32A, the north data for the P_{unsh}

photosensor (semi-infinite room, all allowable blade angles) is used to exemplify how calibration under atypical daylight conditions affects overall system performance. Superimposed on the daylight data are three possible slopes representing two extreme values and the best-fit slope value for this direction and photosensor. Figure 6-32B shows the total light levels at the task assuming system calibration under these three conditions. If the low slope value is used as the basis of the calibration then the system will, on the average, provide more electric light than that required to maintain the design light level. The reverse is true for the high slope value; in this case, the system significantly undershoots the target level. The curves given in Figure 6-32B indicate the importance of calibrating the system response under typical daylight conditions. If the system is calibrated under atypical conditions, then the response of the control system under more typical conditions will not be optimal. It is especially important to avoid calibrating the system at a time when the daylight workplane illuminance is unusually high relative the photosensor signal, since this will result in the system providing less light than required under most conditions. It should be noted however that the example shown above is a relatively extreme case since, as we have shown, the partially- and fully-shielded photosensors show a much better correlation between daylight workplane illuminance and photosensor signal than does the unshielded photosensor used in the example.

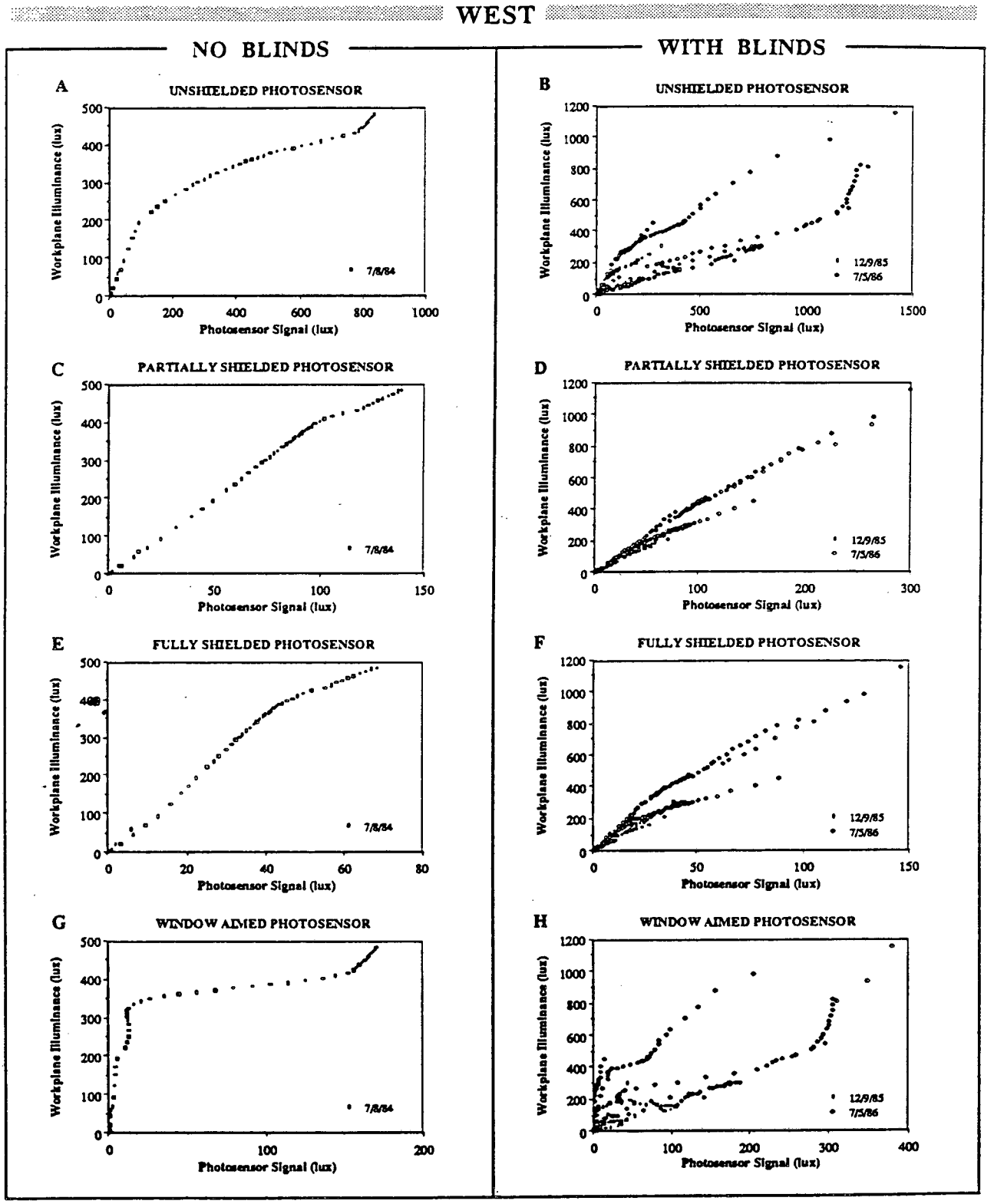

Figure 6-1. Scatter plots of daylight on control photosensors vs. daylight on workplane for small office model facing west with and without shading device. Data points representing direct solar penetration into interior space are excluded

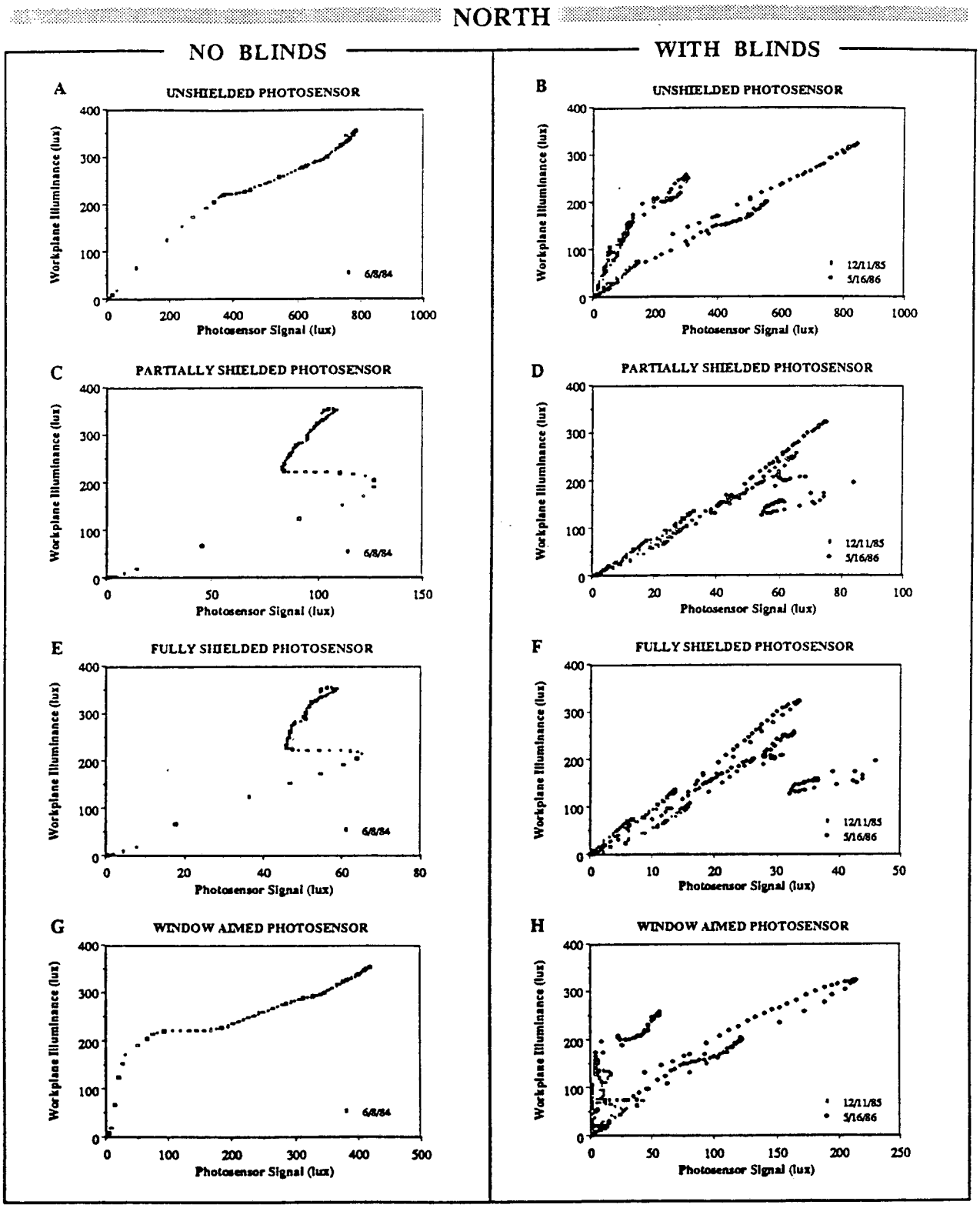

Figure 6-2. Scatter plots of daylight on control photosensors vs. daylight on workplane for small office model facing north with and without shading device. Data points representing direct solar penetration into interior space are excluded

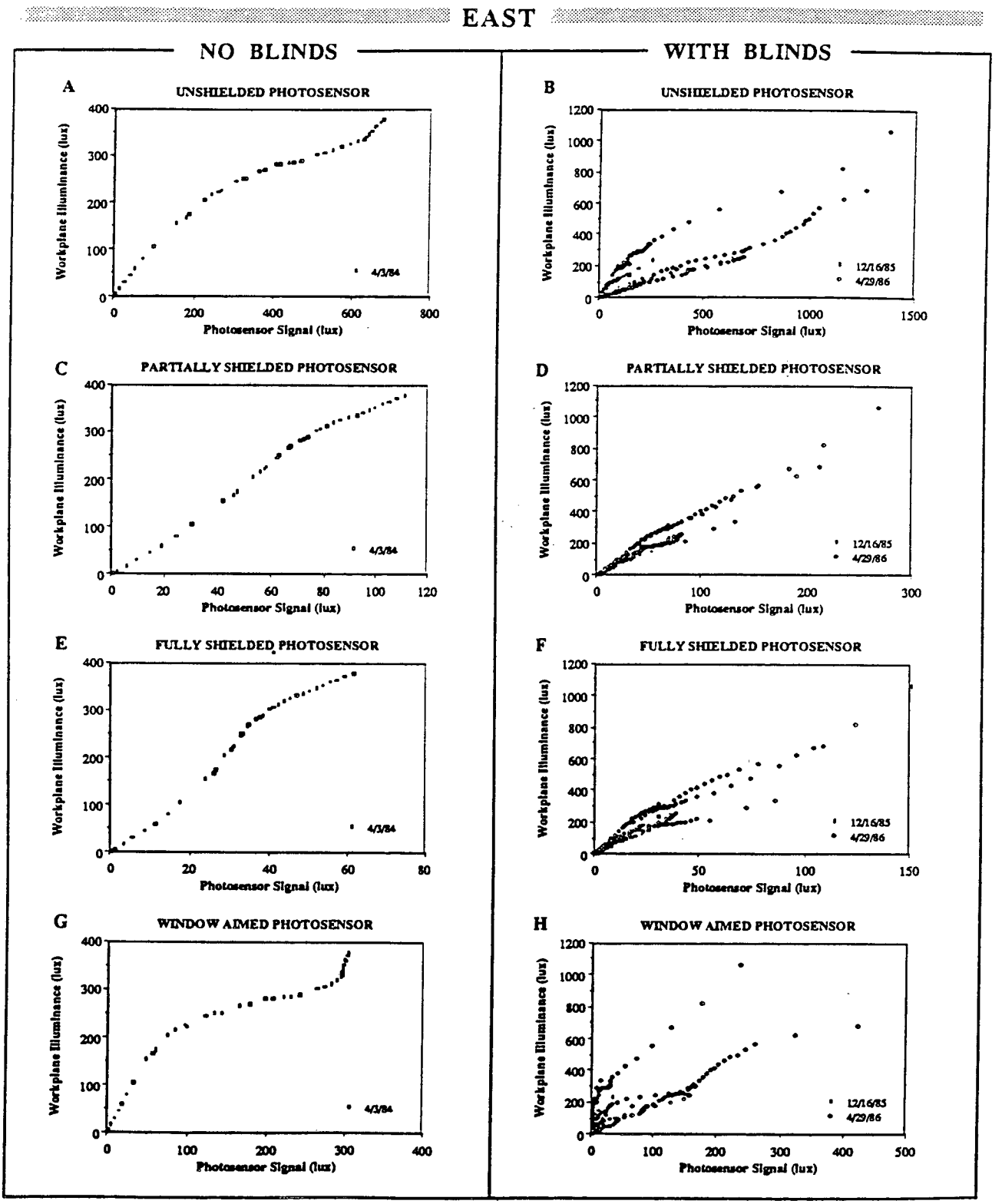

Figure 6-3. Scatter plots of daylight on control photosensors vs. daylight on workplane for small office model facing east with and without shading device. Data points representing direct solar penetration into interior space are excluded

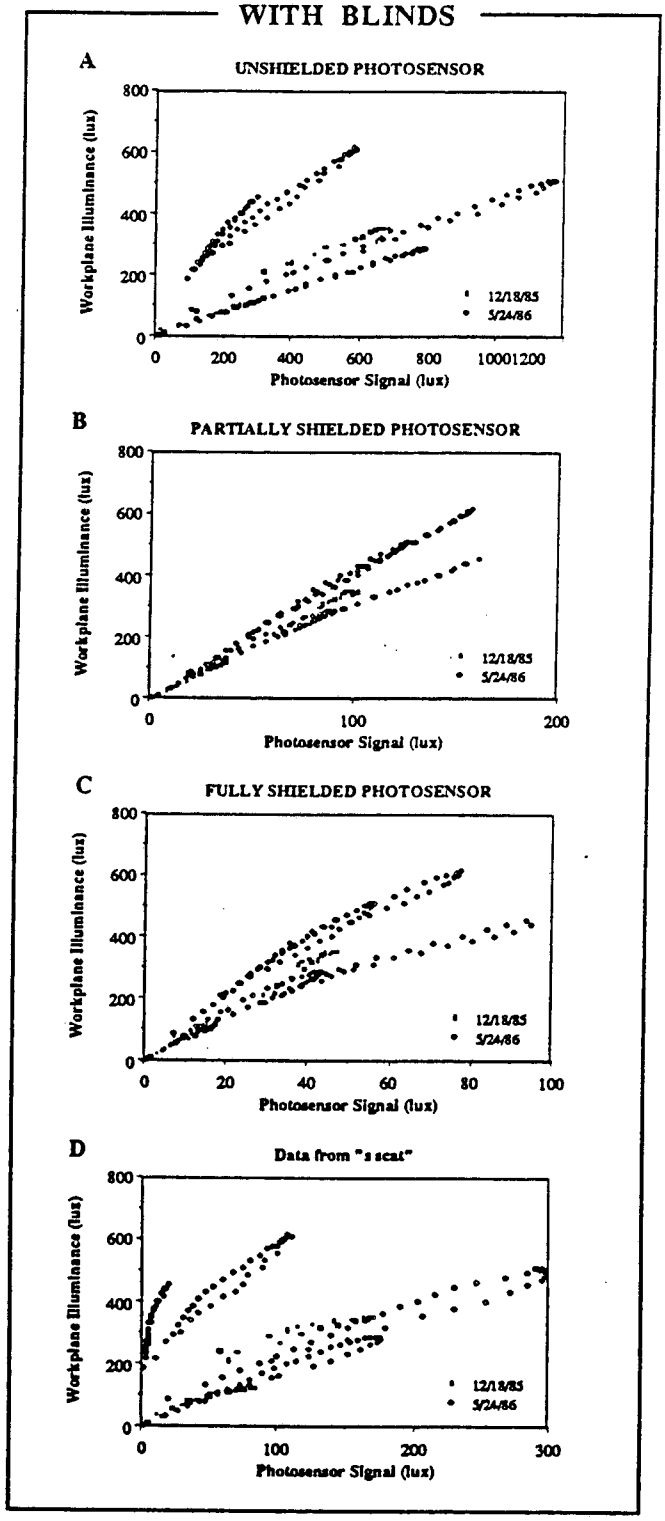

Figure 6-4. Scatter plots of daylight on control photosensors vs. daylight on workplane for small office model facing south with shading device. Data points representing direct solar penetration into interior space are excluded

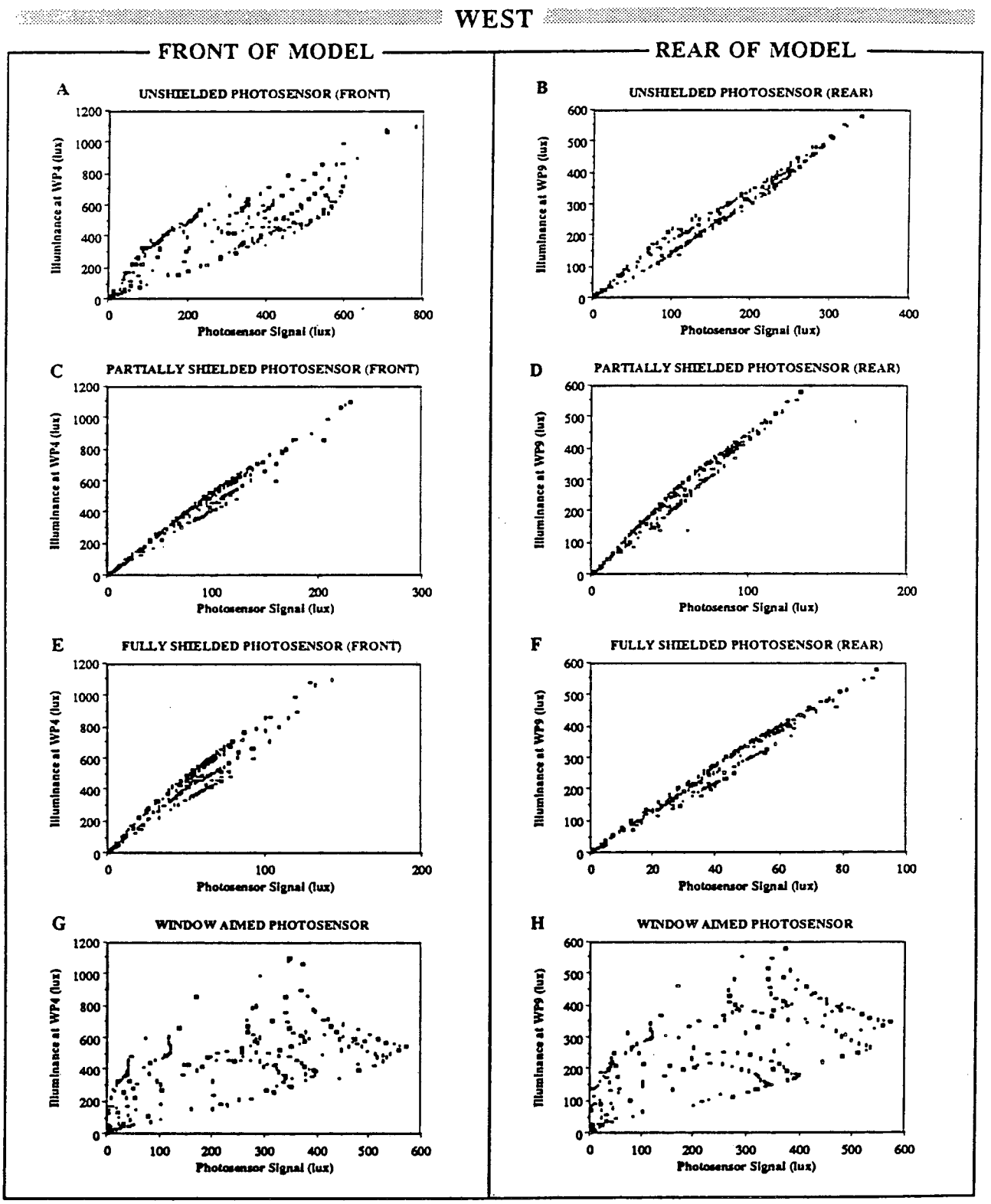

Figure 6-5. Scatter plots of daylight on control photosensors vs. daylight on workplane (front and rear of model) for semi-infinite room model facing west with shading device on clear, winter day. Data points representing direct solar penetration into interior space are excluded

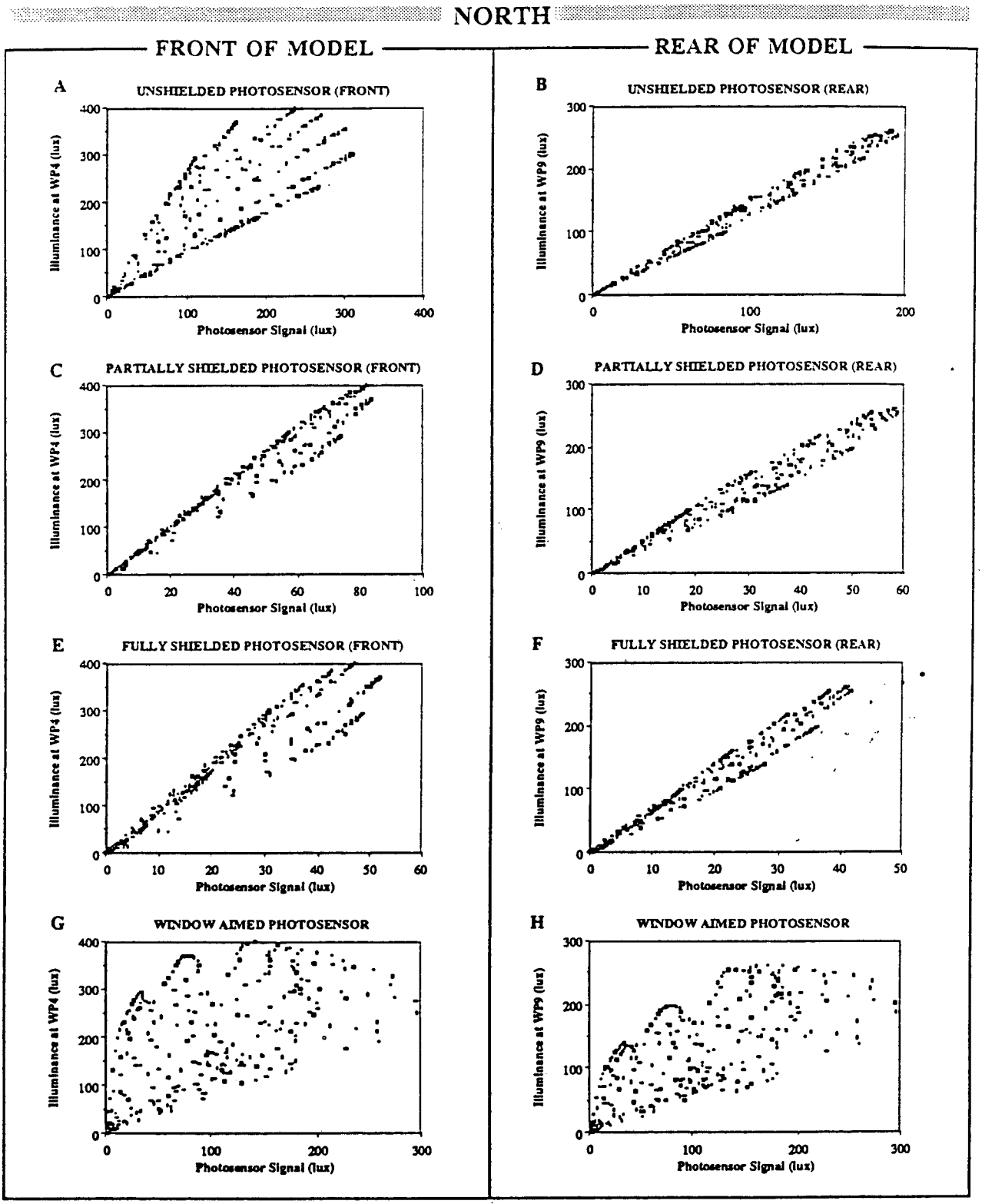

Figure 6-6. Scatter plots of daylight on control photosensors vs. daylight on workplane (front and rear of model) for semi-infinite room model facing north with shading device on clear winter day. Data points representing direct solar penetration into interior space are excluded

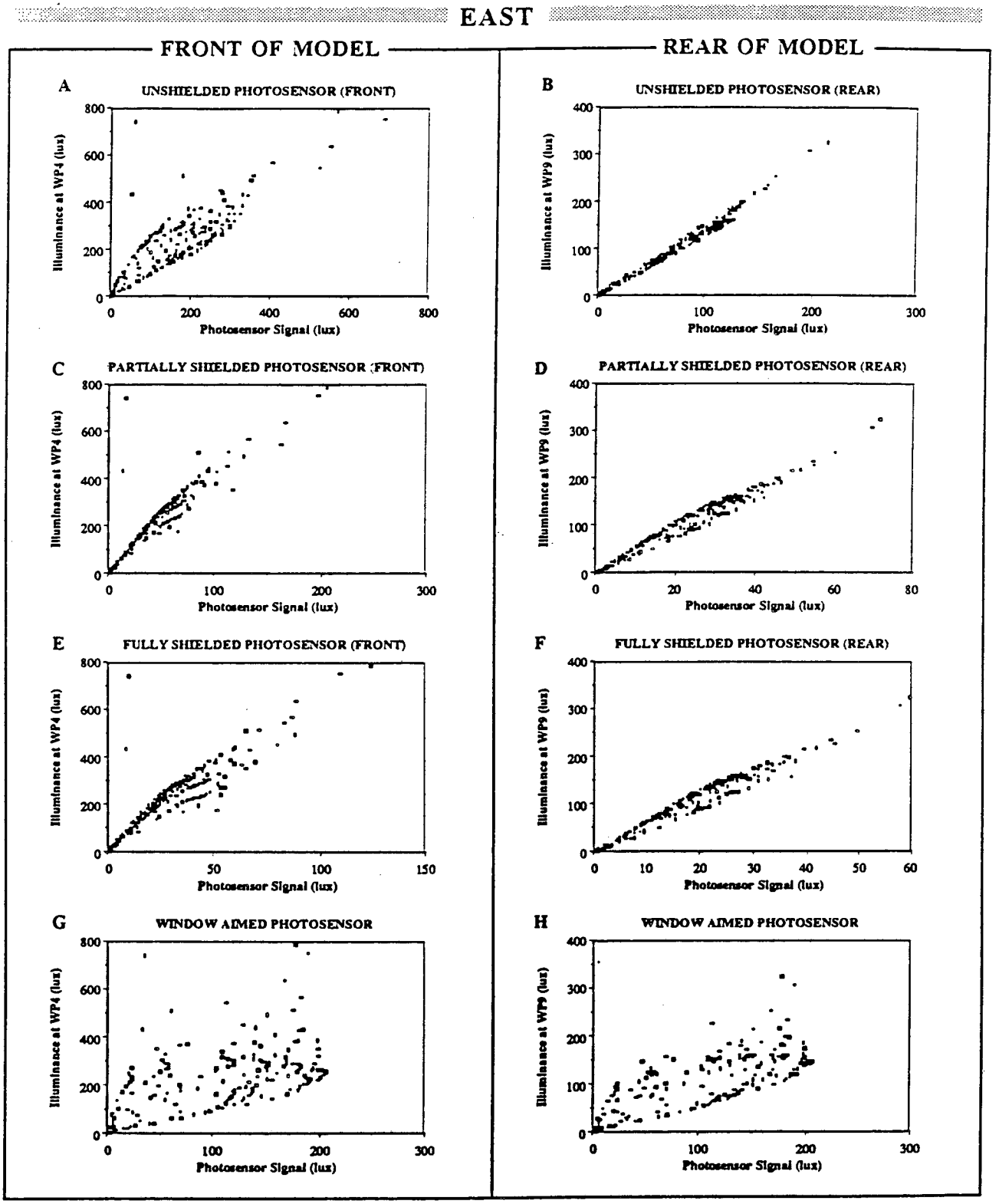

Figure 6-7. Scatter plots of daylight on control photosensors vs. daylight on workplane (front and rear of model) for semi-infinite room model facing east with shading device on clear, winter day. Data points representing direct solar penetration into interior space are excluded

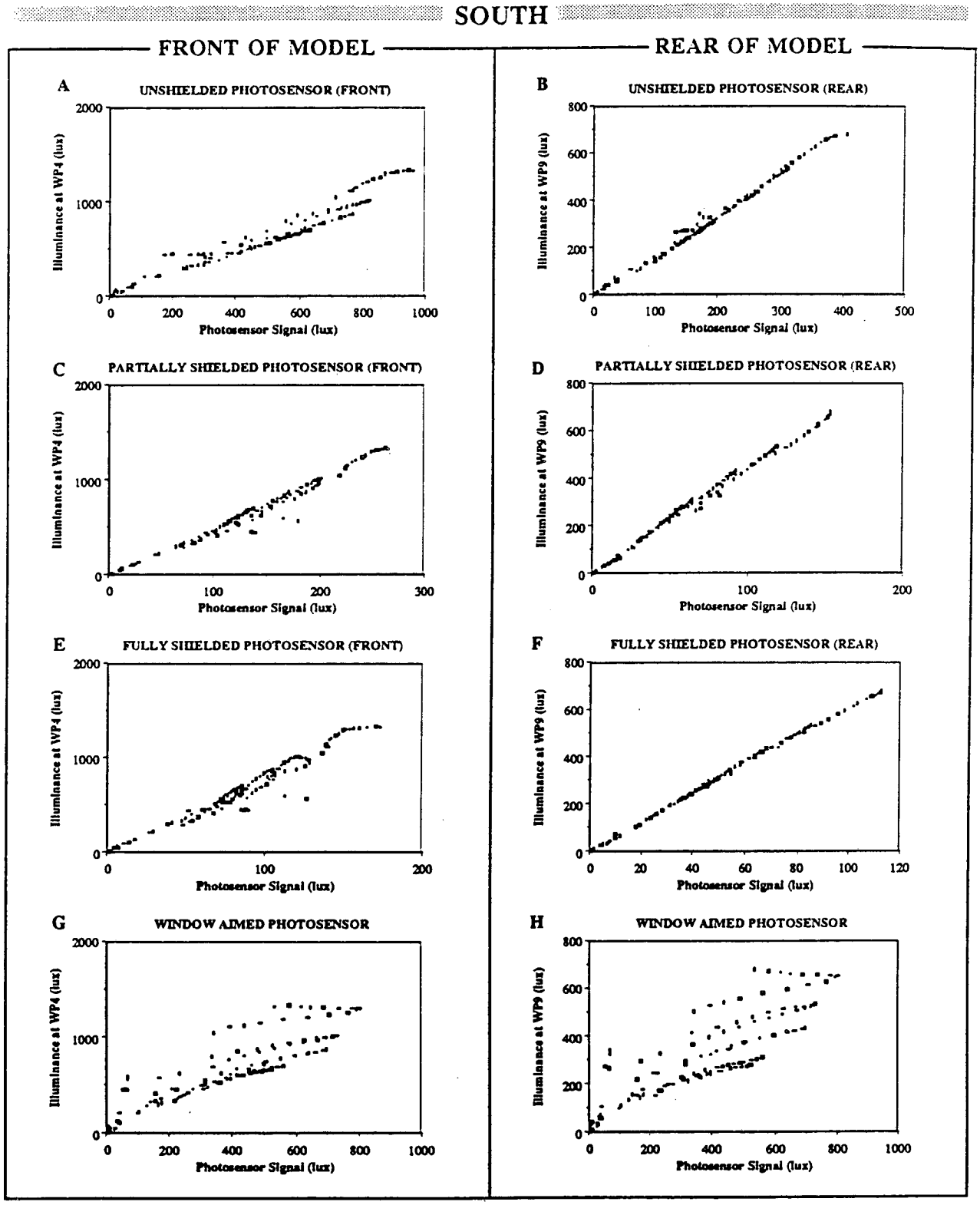

Figure 6-8. Scatter plots of daylight on control photosensors vs. daylight on workplane (front and rear of model) for semi-infinite room model facing south with shading device on clear, winter day. Data points representing direct solar penetration into interior space are excluded

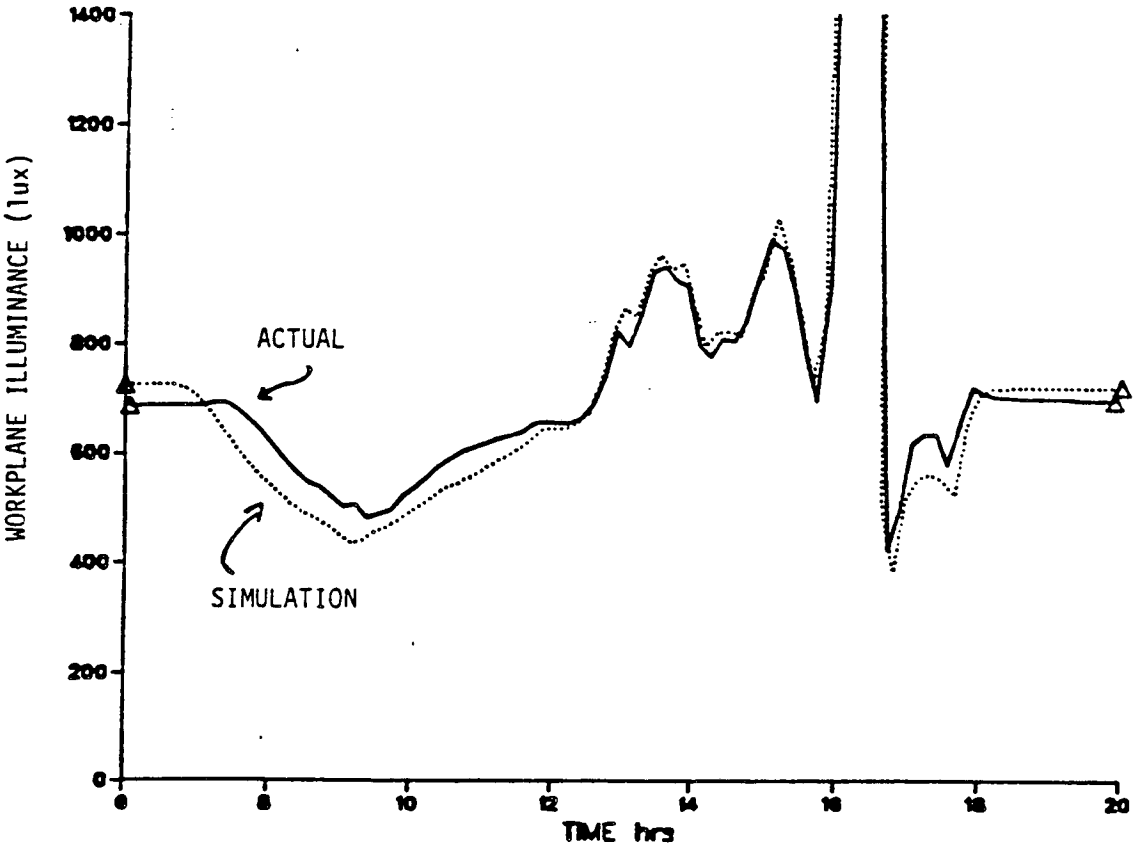

Figure 6-9. Total workplane illuminance (daylight plus controlled electric light) for an integral reset system controlled by the P_{77} photocell. Solid line is measured results for the real integral reset system. Dashed line represents the simulation assuming the same conditions. Data are for the model pointing west on Feb. 25, 1984

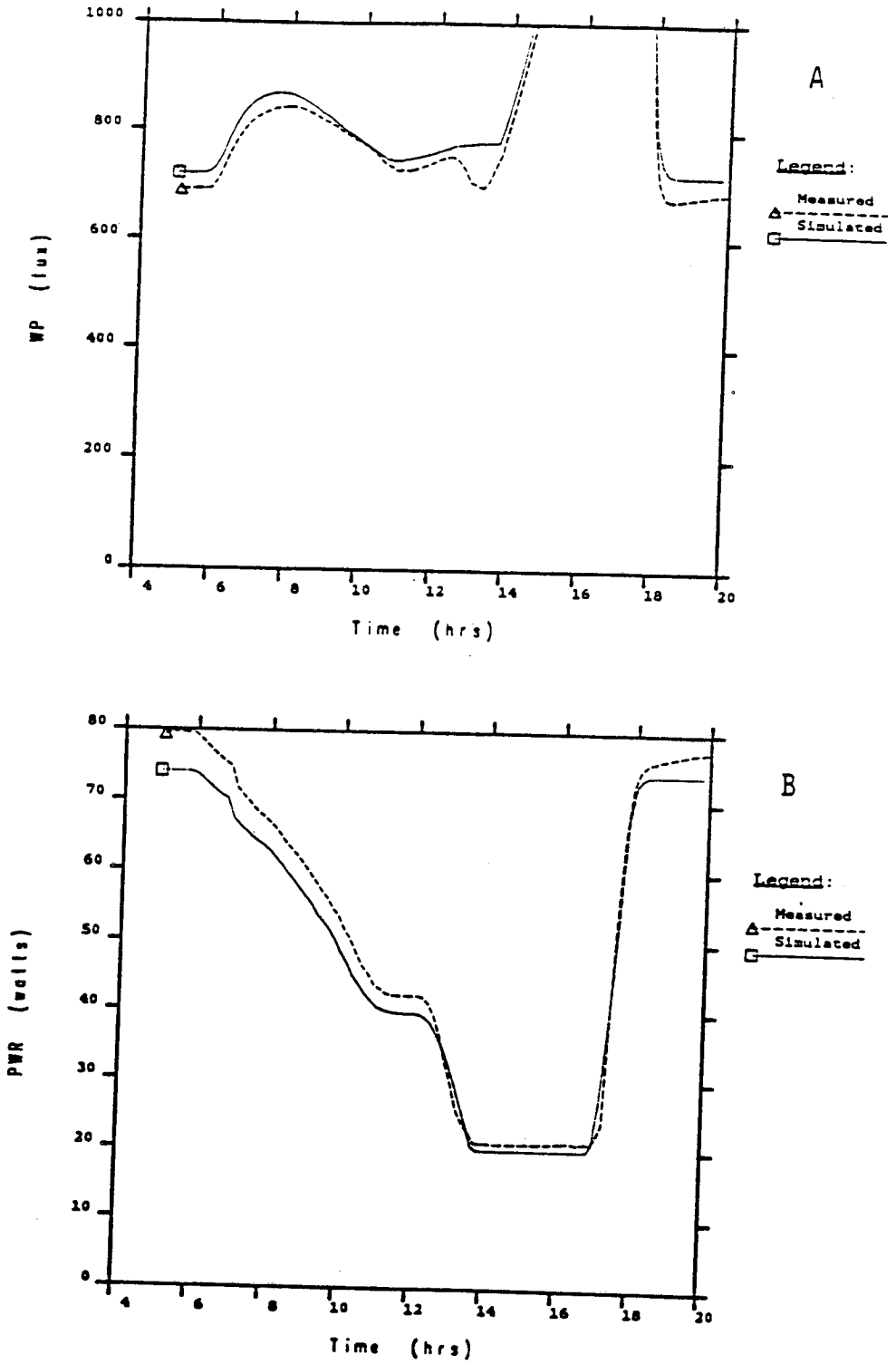

Figure 6-10. Total workplane illuminance (A) and electric lighting power per ballast (B) for proportional system controlled by the P_{unsh} photocell. Dashed line is measured results for the real proportional control system. Dotted line represents the simulation assuming the same conditions. Data is for the model pointing west on Sep. 23, 1984

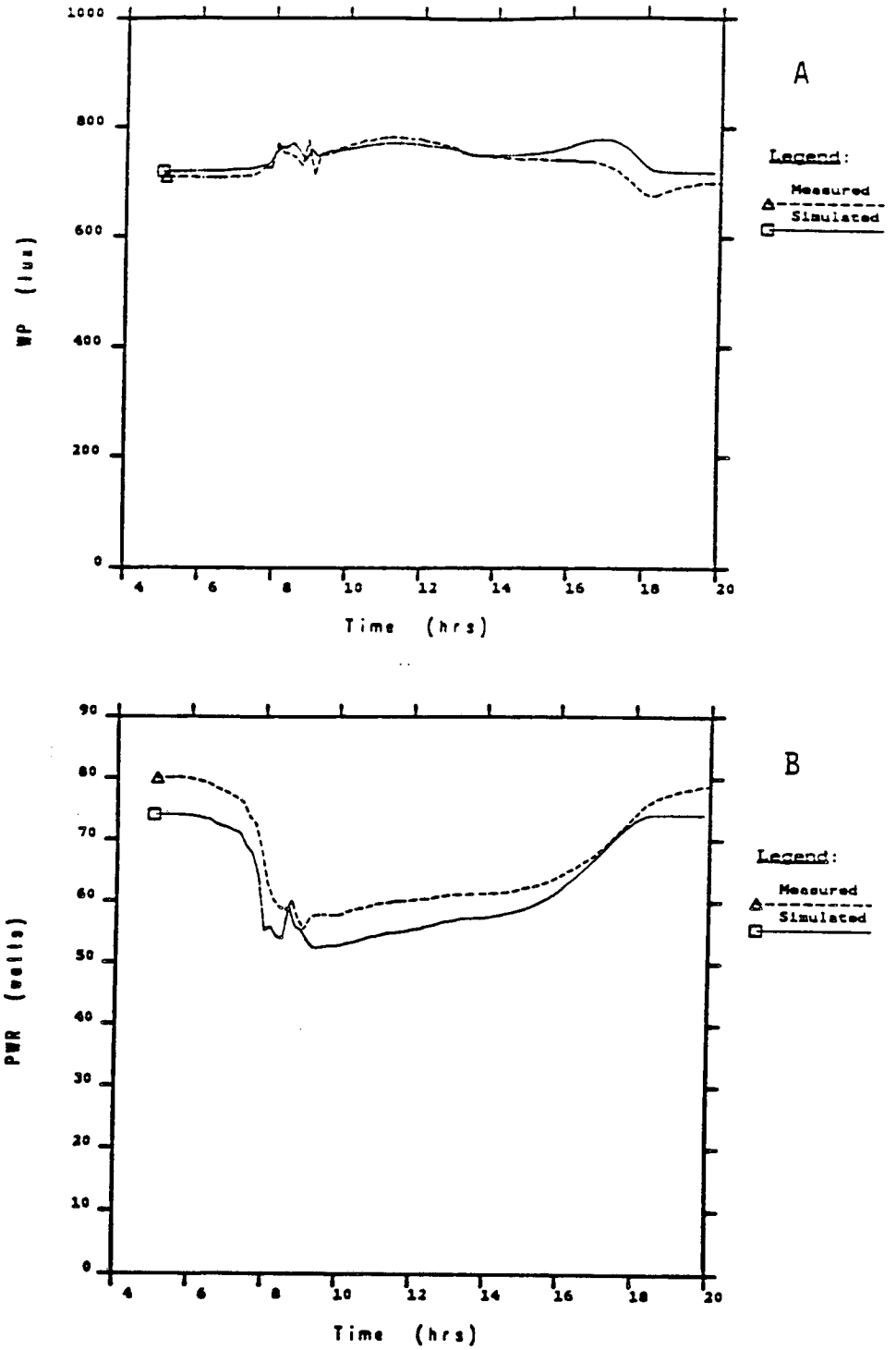

Figure 6-11. Total workplane illuminance (A) and electric lighting power per ballast (B) for proportional system controlled by the P_{unsh} photocell. Dashed line is measured results for the real proportional control system. Dotted line represents the simulation assuming the same conditions. Data is for the model pointing west on Sep. 15, 1984

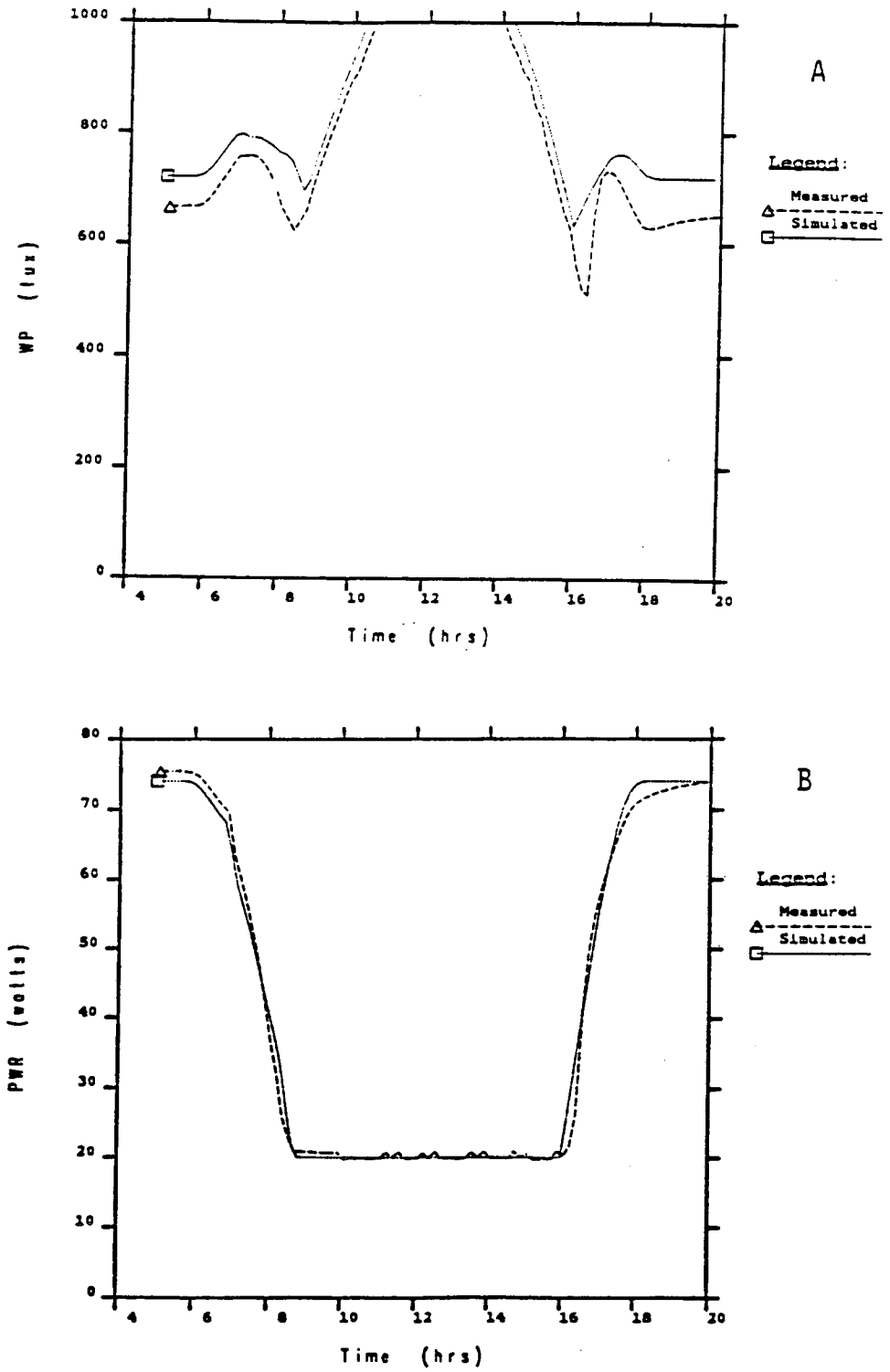

Figure 6-12. Total workplane illuminance (A) and electric lighting power per ballast (B) for proportional system controlled by the P_{unsh} photocell. Dashed line is measured results for the real proportional control system. Dotted line represents the simulation assuming the same

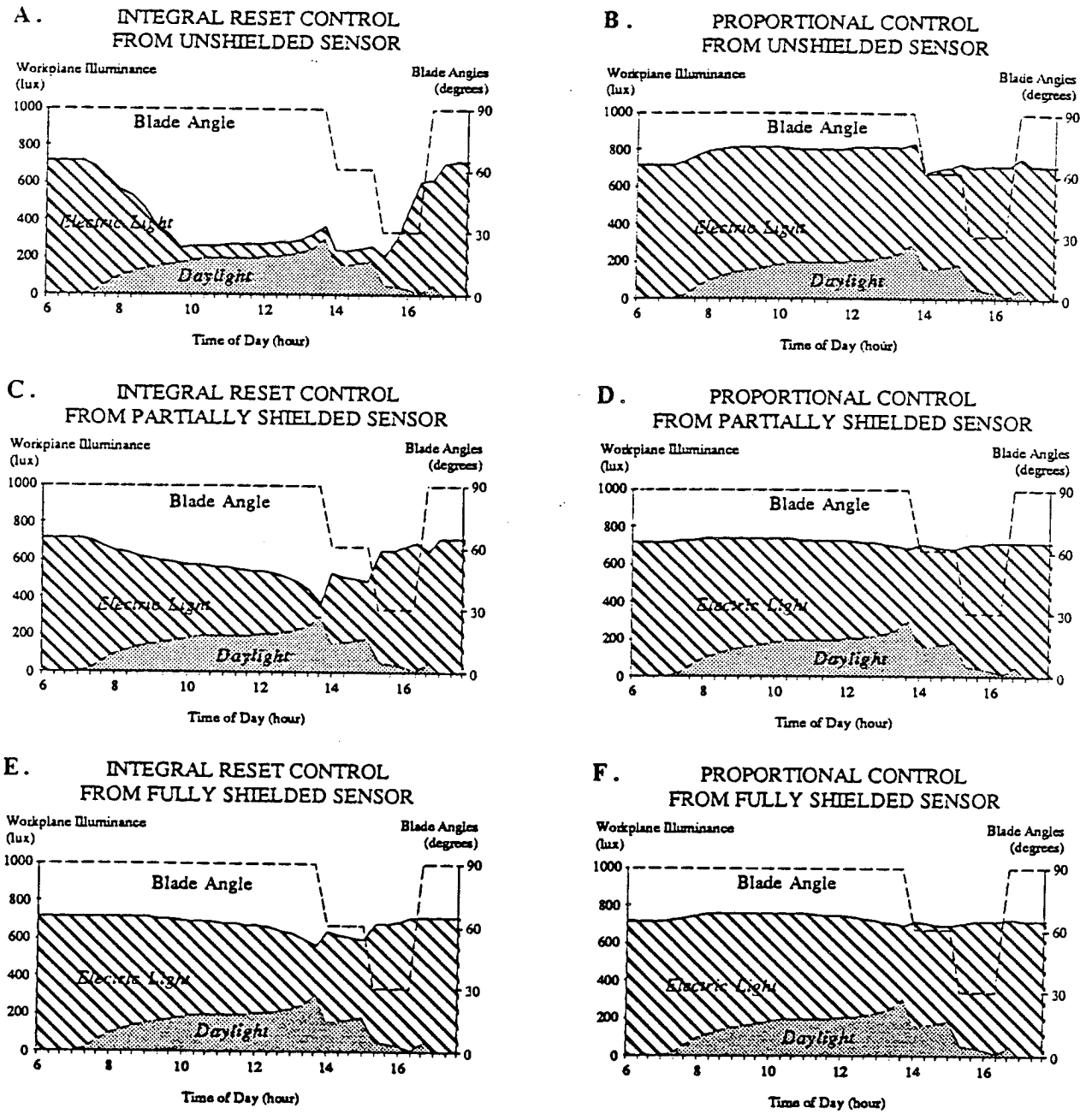

Figure 6-13. Light levels on workplane for integral reset and closed-loop proportional control systems controlled by three photosensors for small office model facing west on clear winter day

A. INTEGRAL RESET CONTROL FROM UNSHIELDED SENSOR

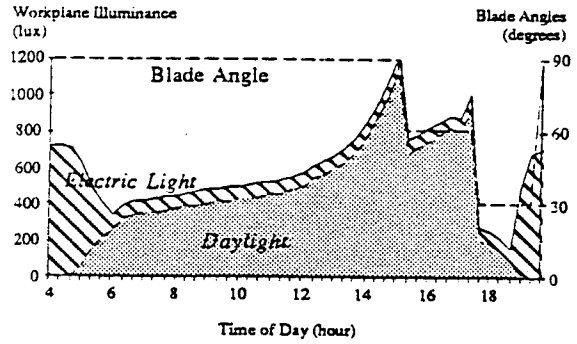

B. PROPORTIONAL CONTROL FROM UNSHIELDED SENSOR

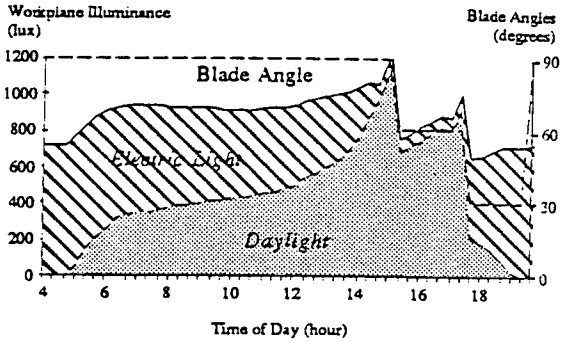

C. INTEGRAL RESET CONTROL FROM PARTIALLY SHIELDED SENSOR

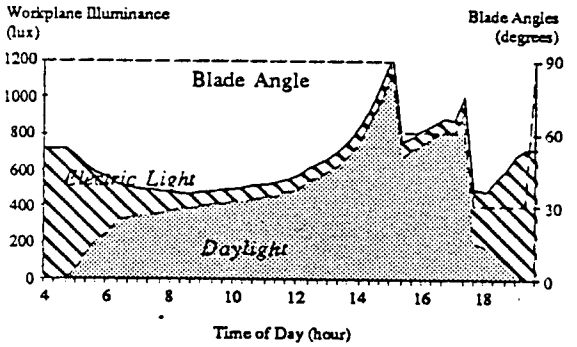

D. PROPORTIONAL CONTROL FROM PARTIALLY SHIELDED SENSOR

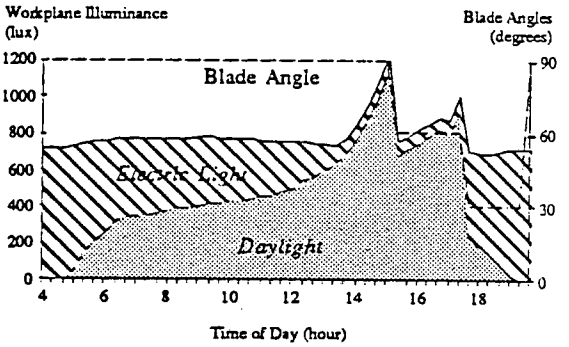

E. INTEGRAL RESET CONTROL FROM FULLY SHIELDED SENSOR

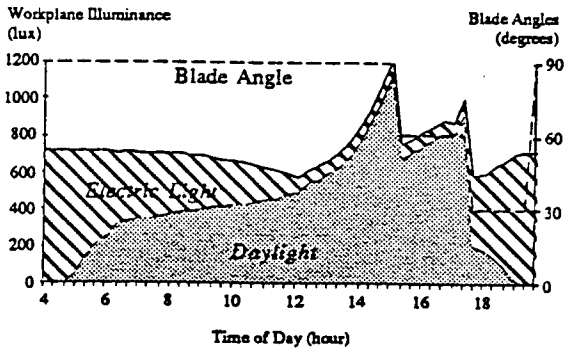

F. PROPORTIONAL CONTROL FROM FULLY SHIELDED SENSOR

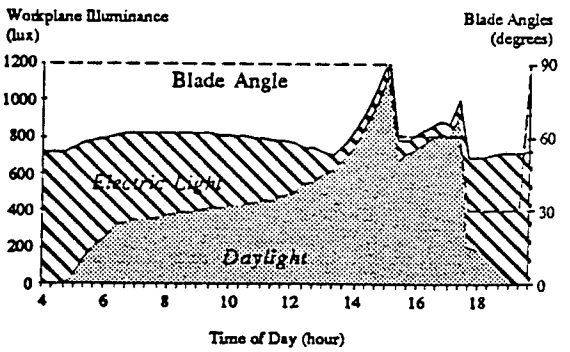

Figure 6-14. Light levels on workplane for integral reset and closed-loop proportional control systems controlled by three photosensors for small office model facing west on clear summer day

A. INTEGRAL RESET CONTROL FROM UNSHIELDED SENSOR

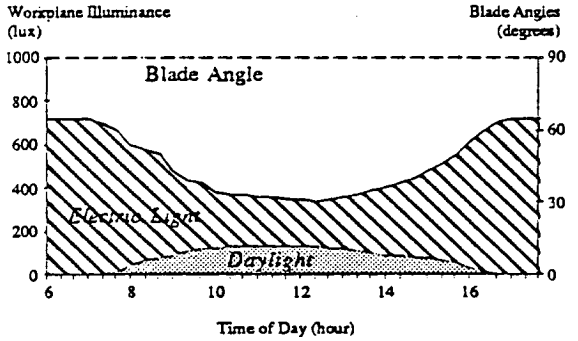

B. PROPORTIONAL CONTROL FROM UNSHIELDED SENSOR

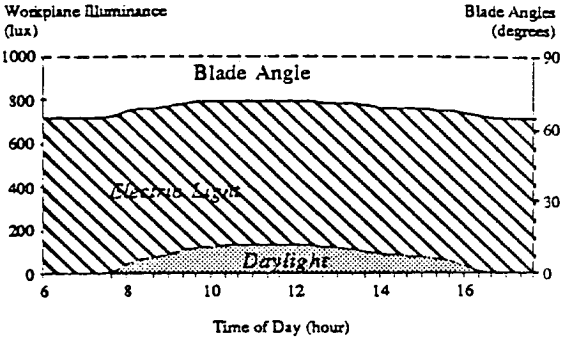

C. INTEGRAL RESET CONTROL FROM PARTIALLY SHIELDED SENSOR

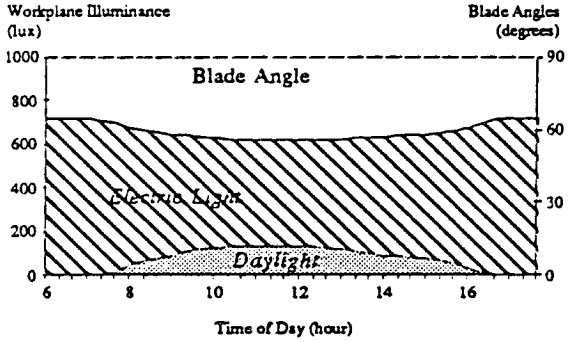

D. PROPORTIONAL CONTROL FROM PARTIALLY SHIELDED SENSOR

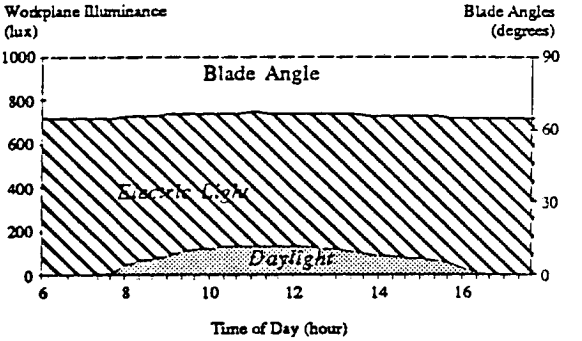

E. INTEGRAL RESET CONTROL FROM FULLY SHIELDED SENSOR

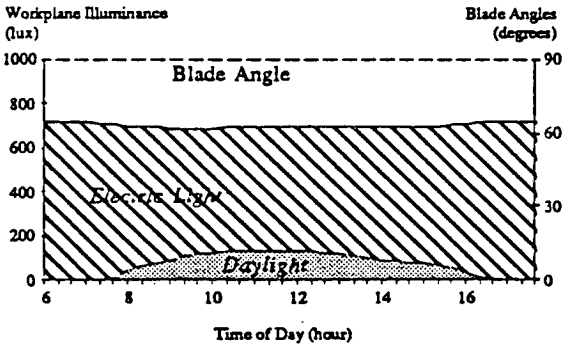

F. PROPORTIONAL CONTROL FROM FULLY SHIELDED SENSOR

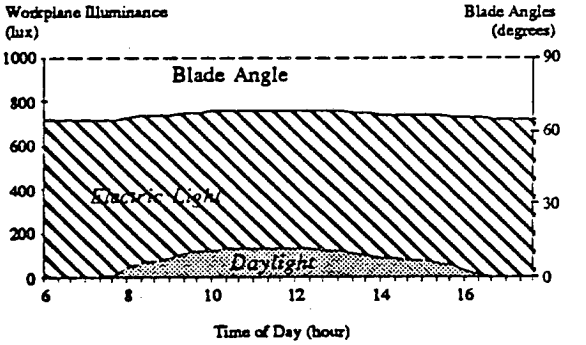

Figure 6-15. Light levels on workplane for integral reset and closed-loop proportional control systems controlled by three photosensors for small office model facing north on clear winter day

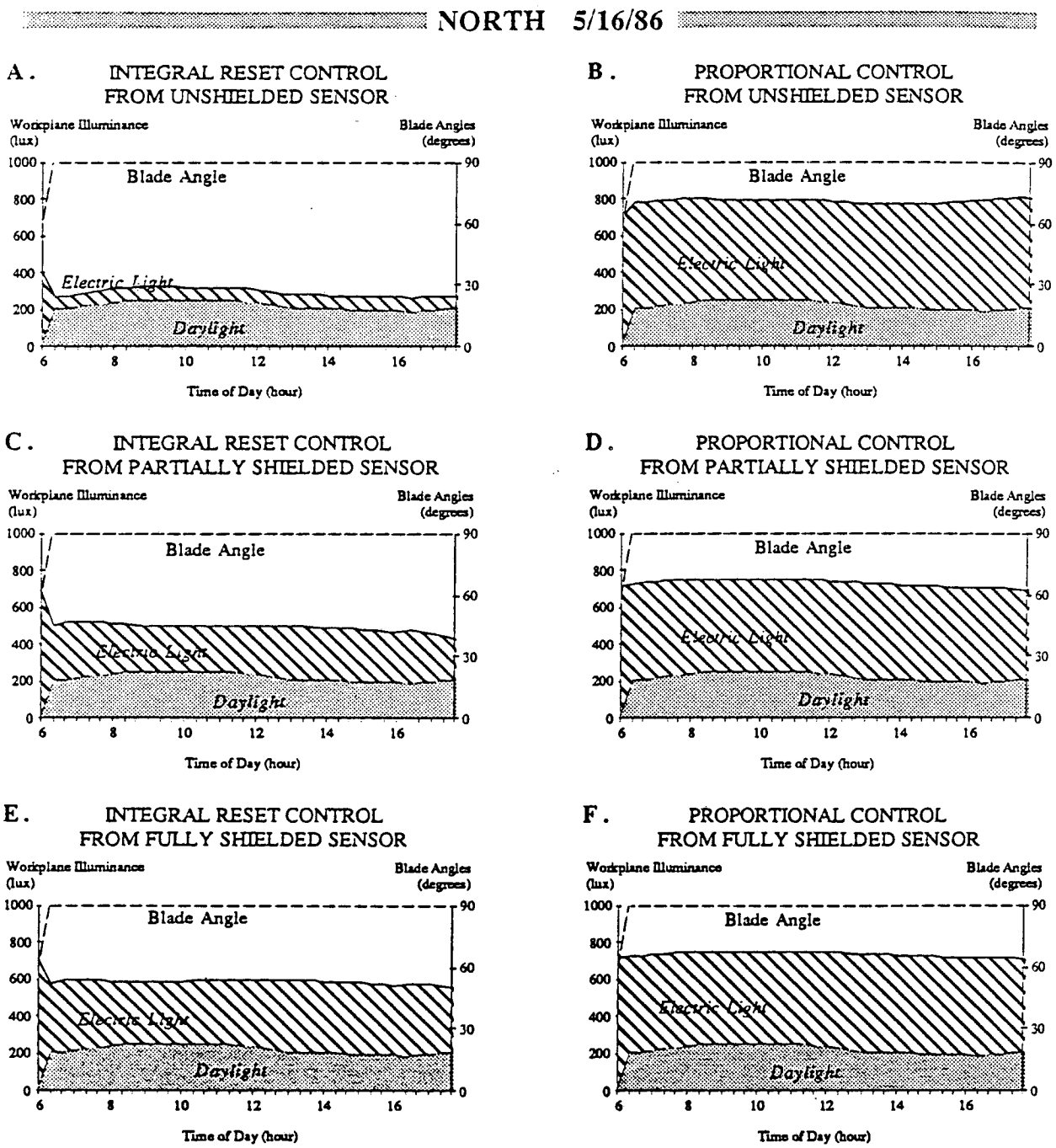

Figure 6-16. Light levels of workplane for integral reset and closed-loop proportional control systems controlled by three photosensors for small office model facing north on clear summer day

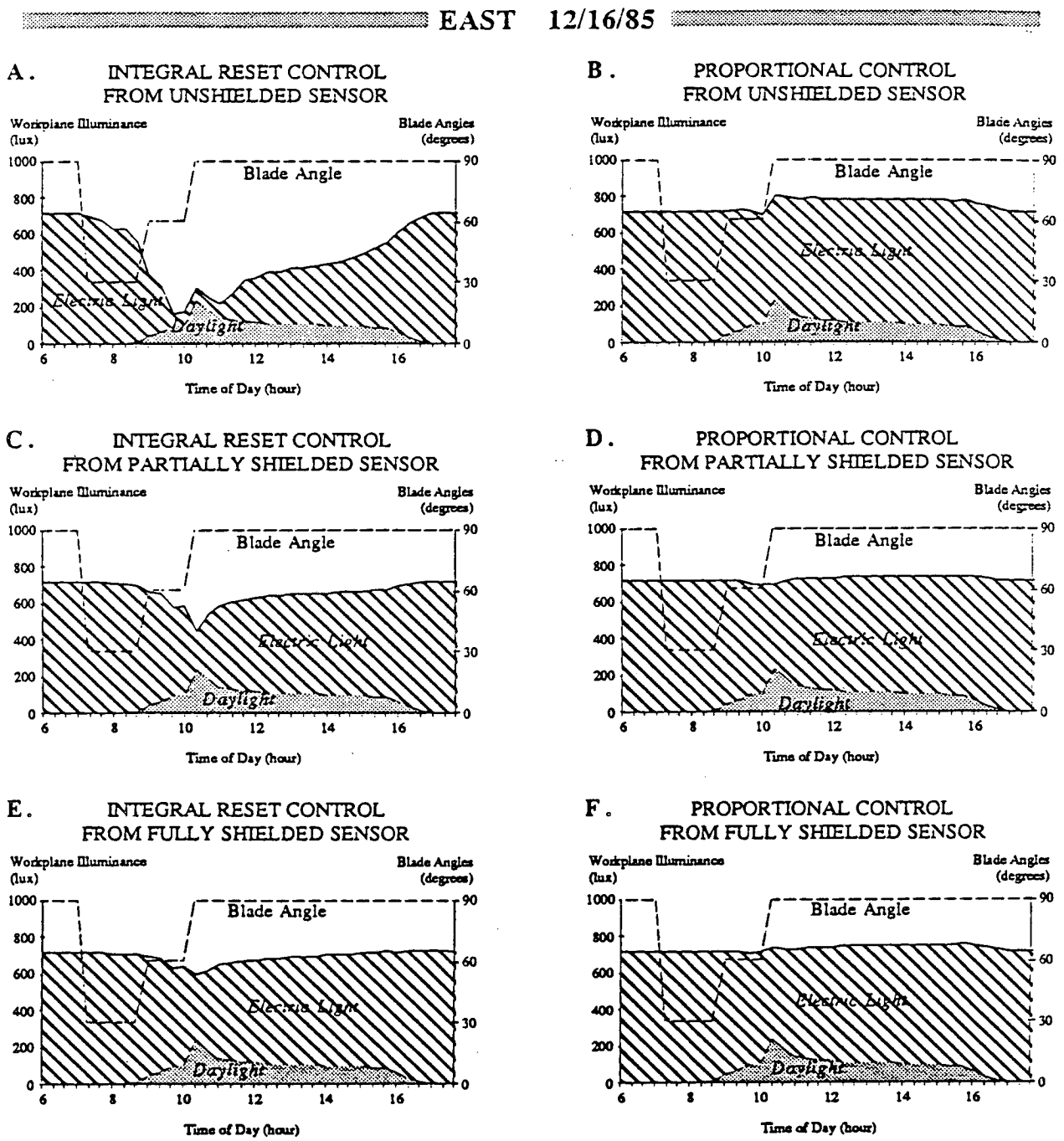

Figure 6-17. Light levels of workplane for integral reset and closed-loop proportional control systems controlled by three photosensors for small office model facing east on clear winter day

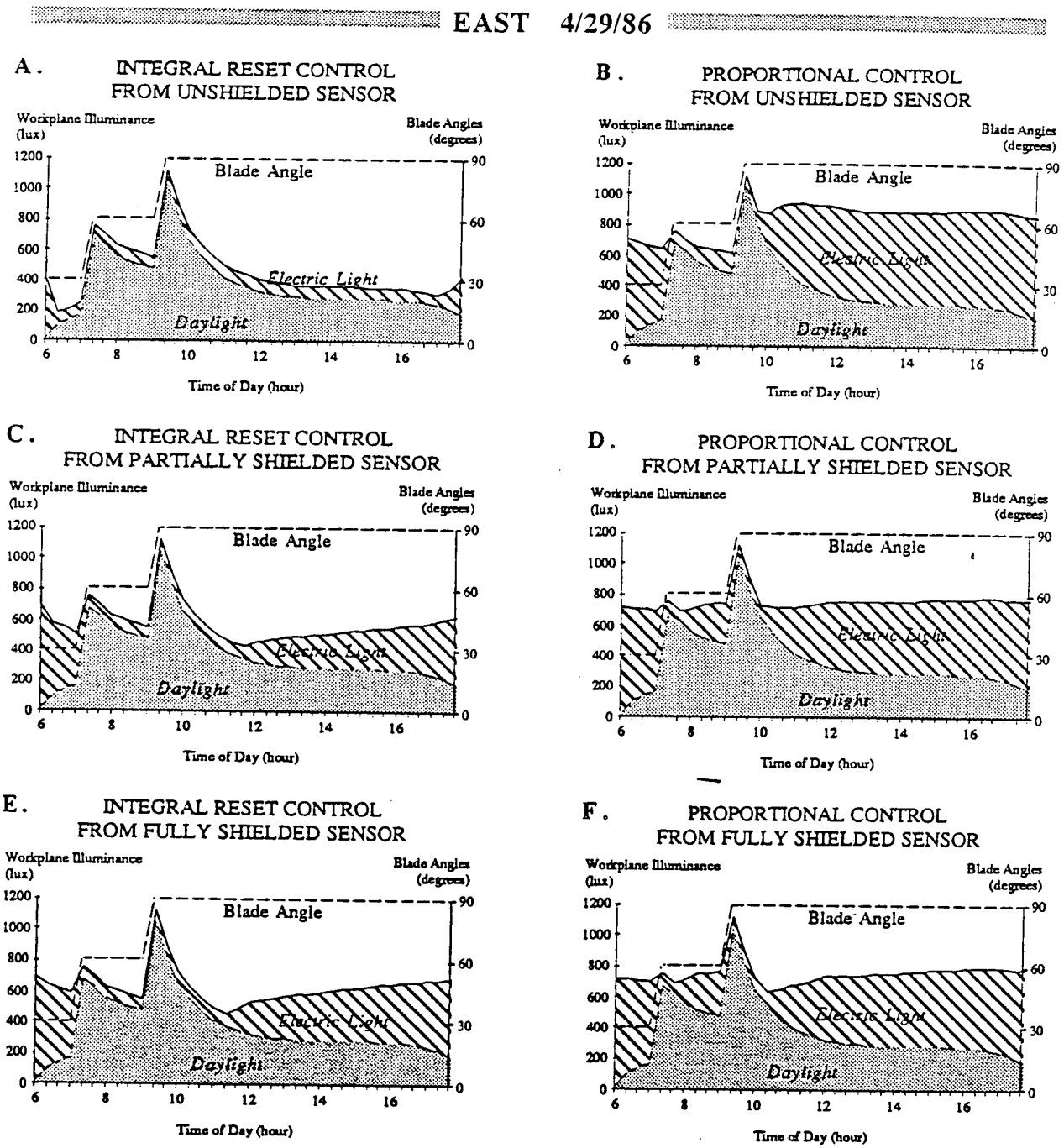

Figure 6-18. Light levels of workplane for integral reset and closed-loop proportional control systems controlled by three photosensors for small office model facing east on clear summer day

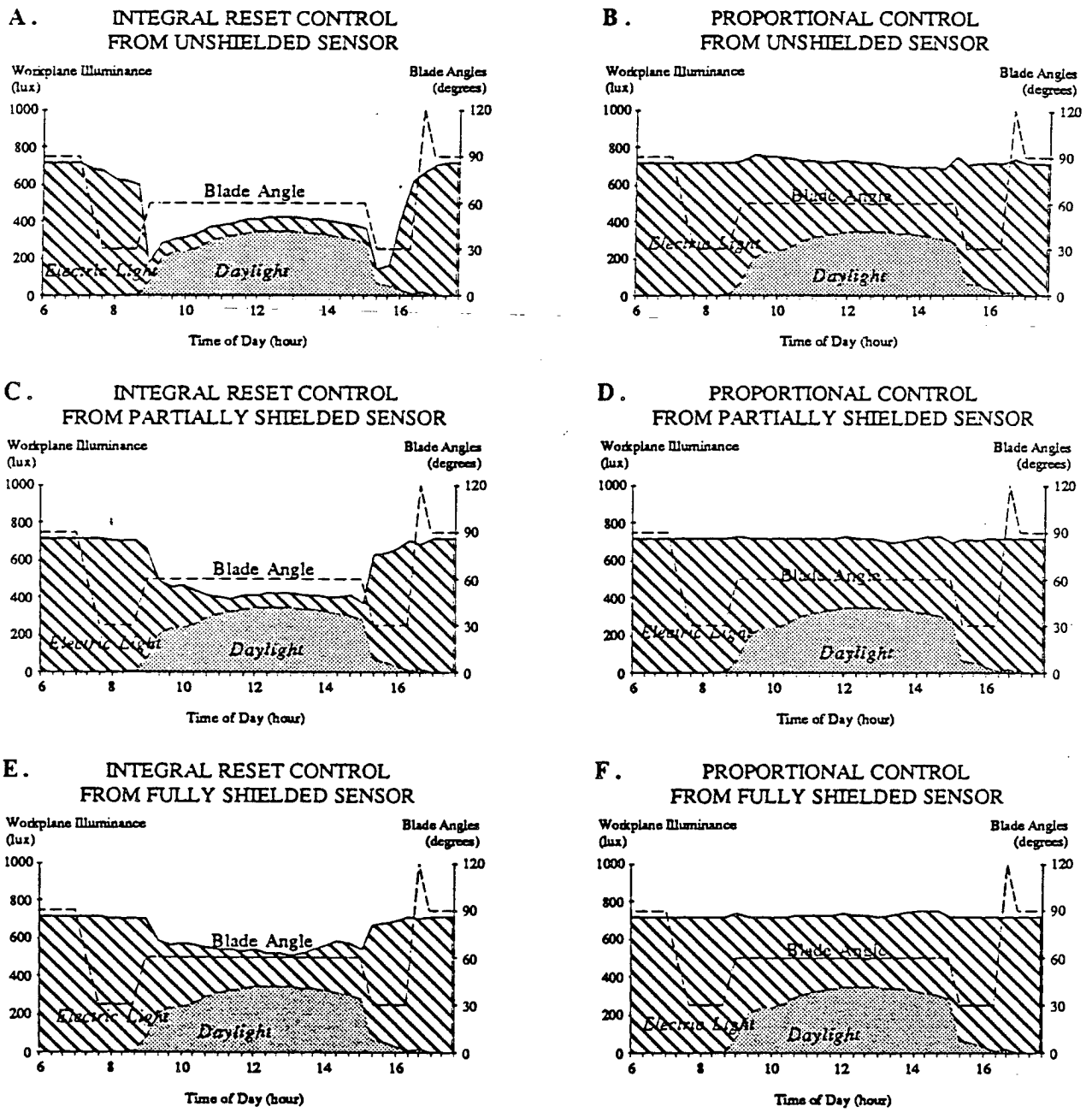

Figure 6-19. Light levels of workplane for integral reset and closed-loop proportional control systems controlled by three photosensors for small office model facing south on clear winter day

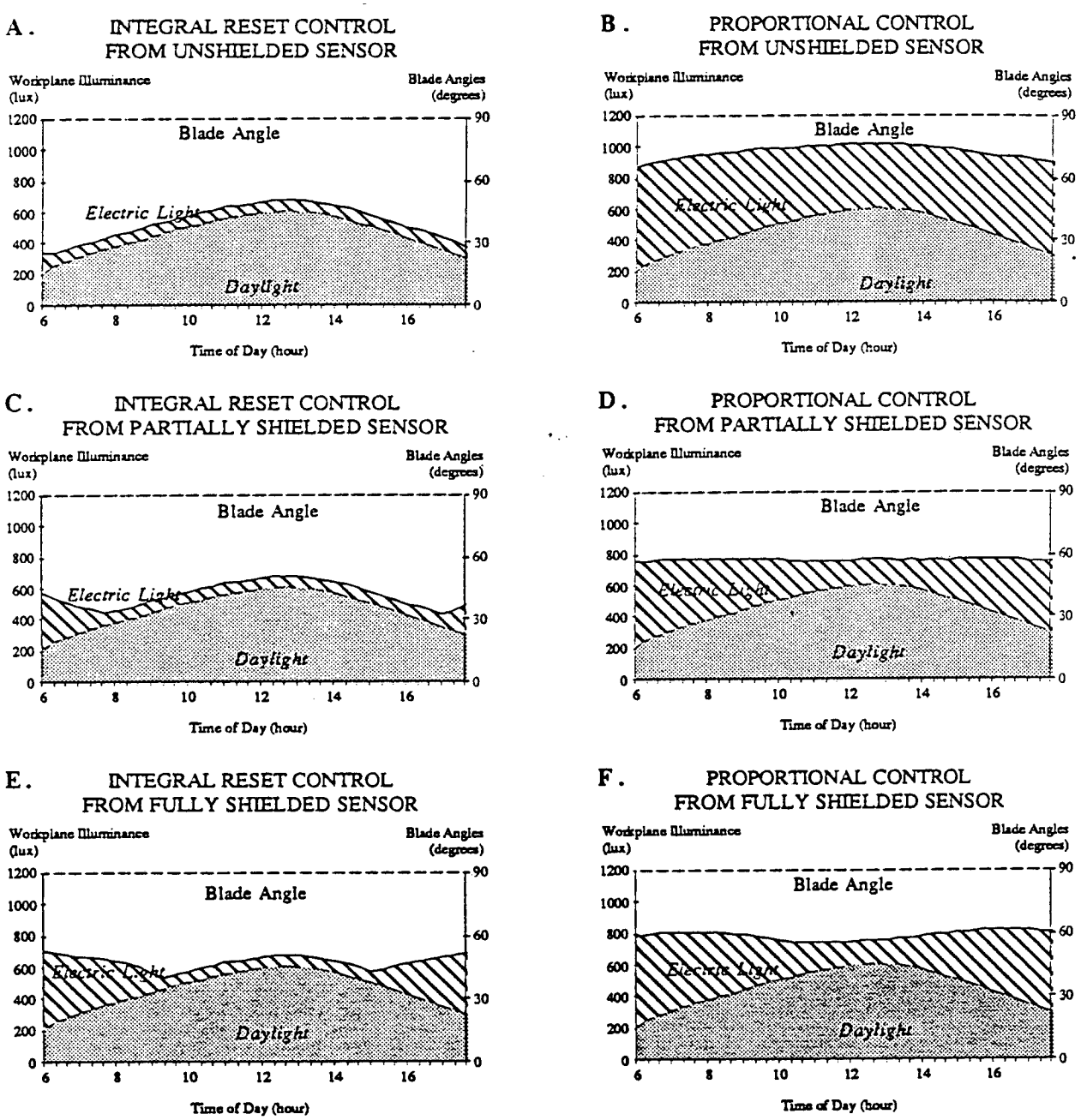

Figure 6-20. Light levels of workplane for integral reset and closed-loop proportional control systems controlled by three photosensors for small office model facing south on clear summer day

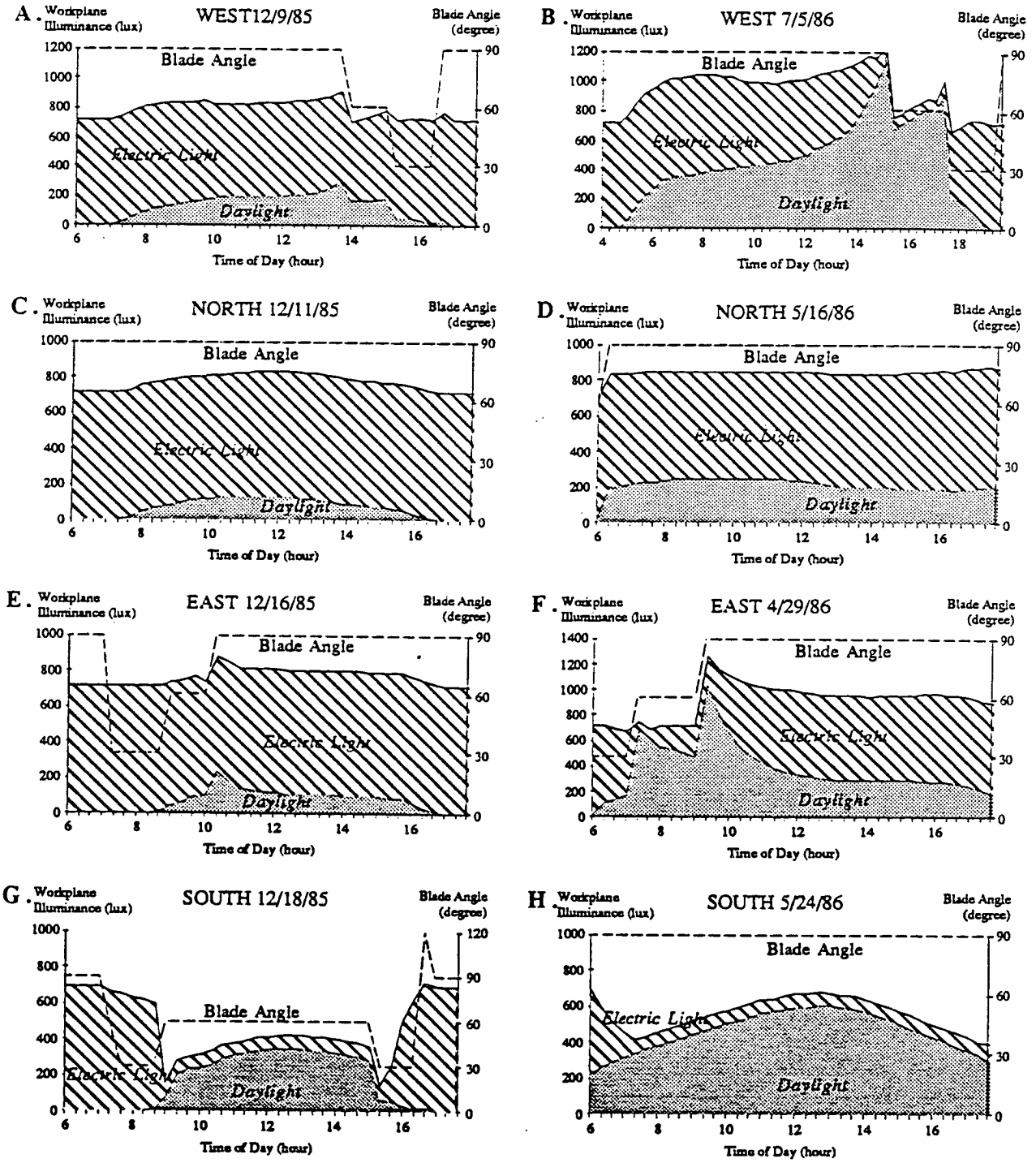

Figure 6-21. Light levels of workplane (front and rear portions of room) for open-loop proportional control systems controlled by window-aimed photosensor for semi-infinite room model facing all directions (clear winter day)

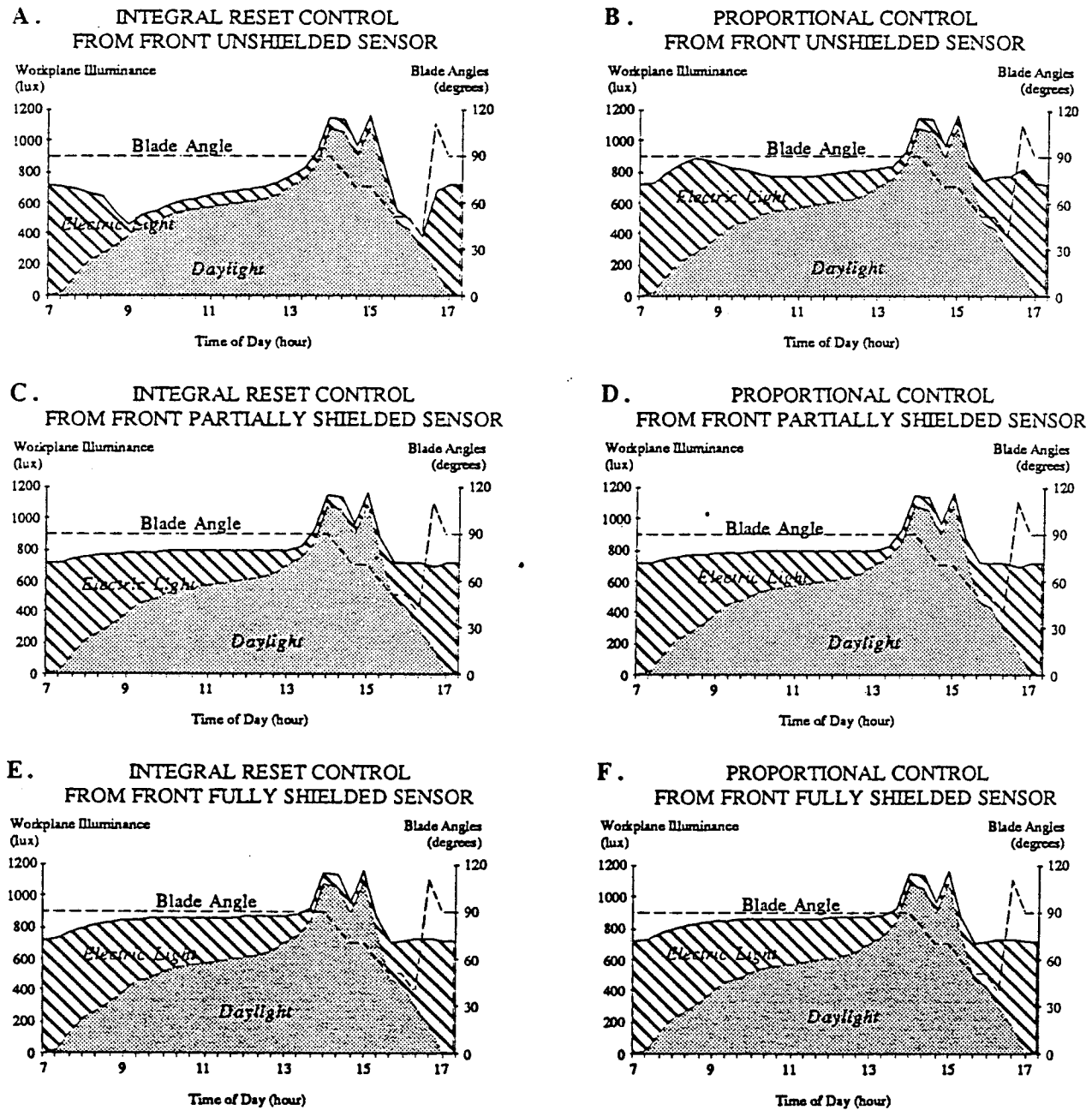

Figure 6-22. Light levels on workplane (front portion of room) for integral reset and closed-loop proportional control systems controlled by three photosensors for semi-infinite room model facing west (clear winter day)

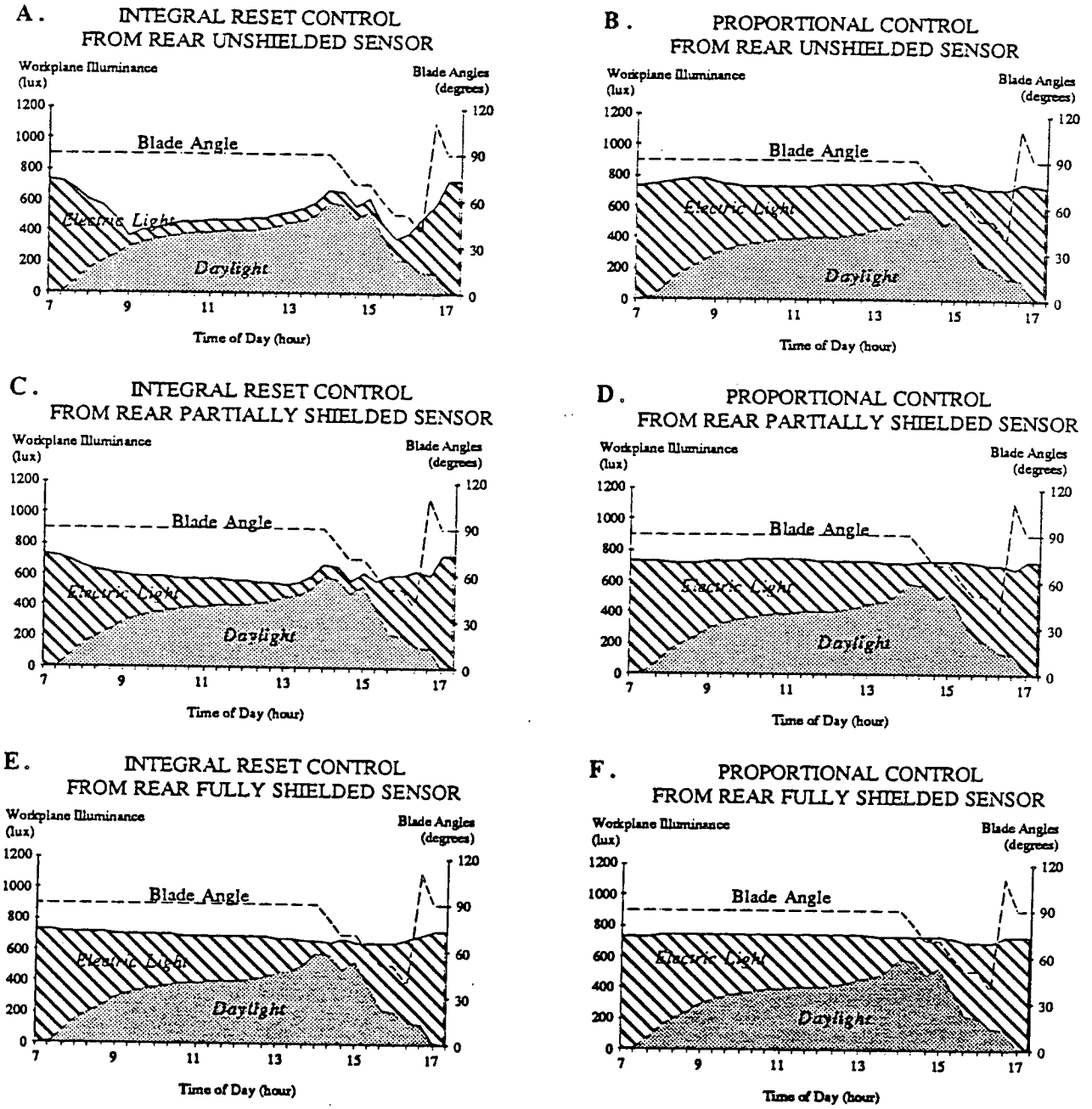

Figure 6-23. Light levels on workplane (rear portion of room) for integral reset and closed-loop proportional control systems controlled by three photosensors for semi-infinite room model facing west (clear winter day)

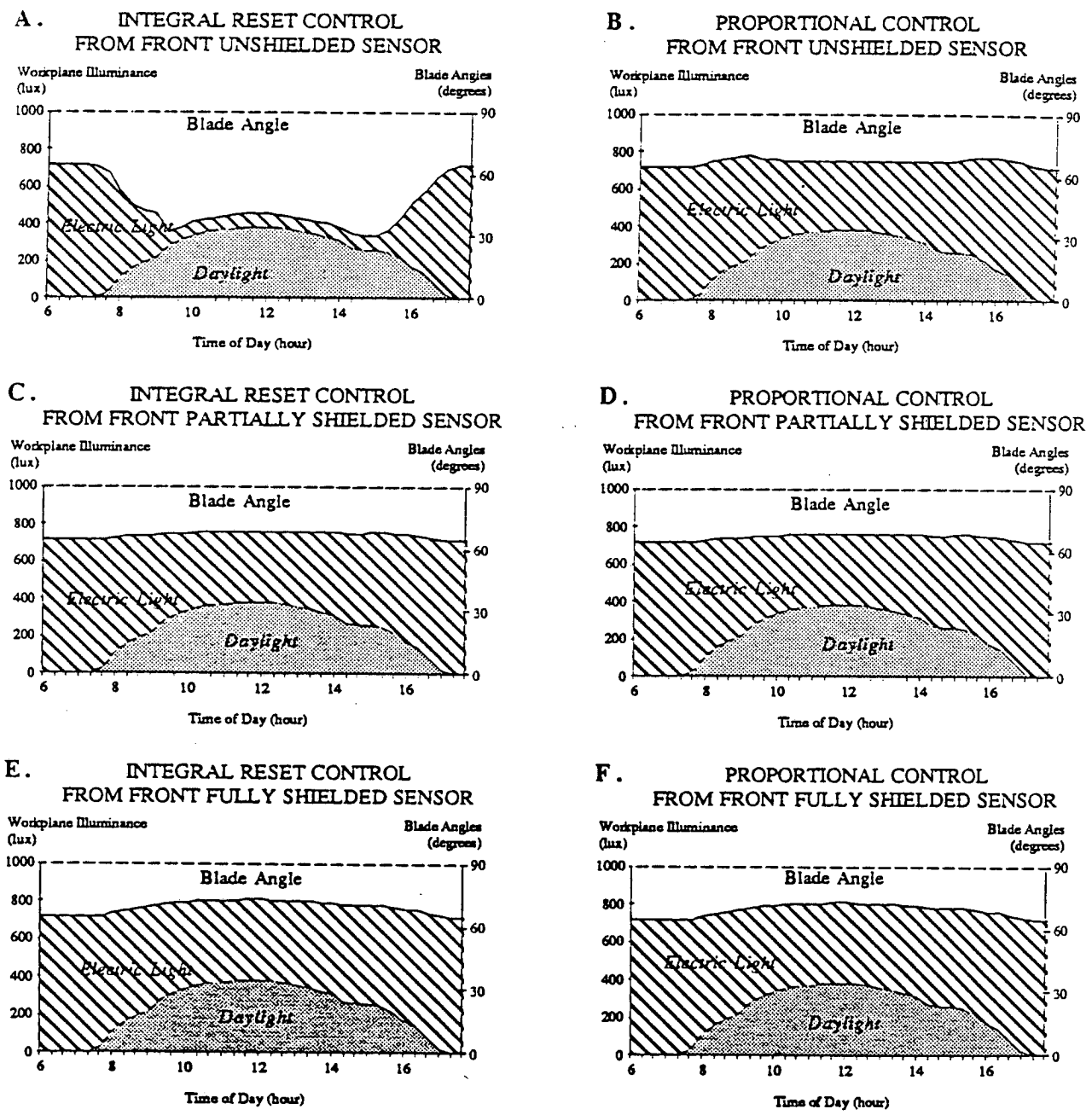

Figure 6-24. Light levels on workplane (front portion of room) for integral reset and closed-loop proportional control systems controlled by three photosensors for semi-infinite room model facing north (clear winter day)

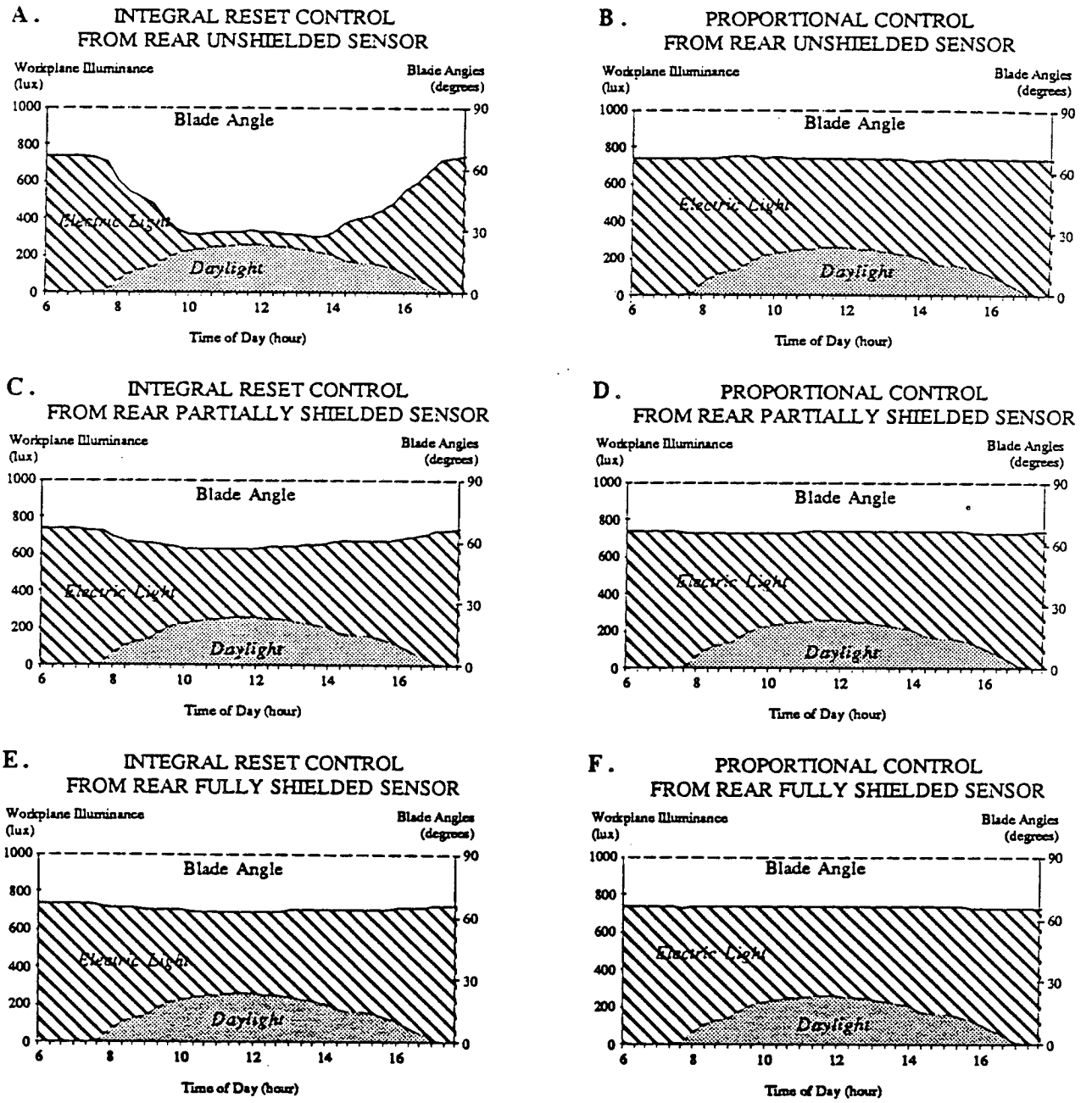

Figure 6-25. Light levels on workplane (rear portion of room) for integral reset and closed-loop proportional control systems controlled by three photosensors for semi-infinite room model facing north (clear winter day)

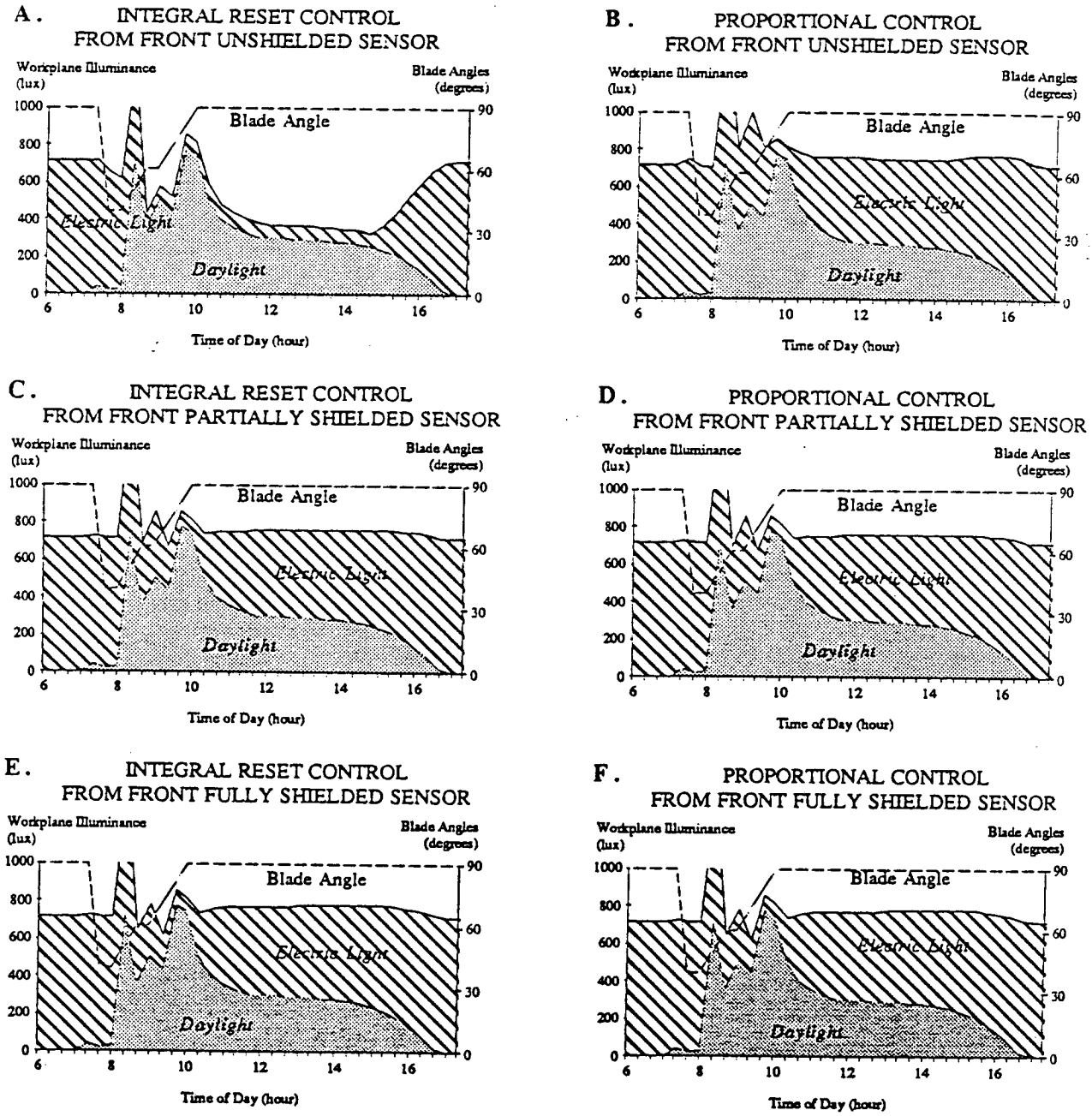

Figure 6-26. Light levels on workplane (front portion of room) for integral reset and closed-loop proportional control systems controlled by three photosensors for semi-infinite room model facing east (clear winter day)

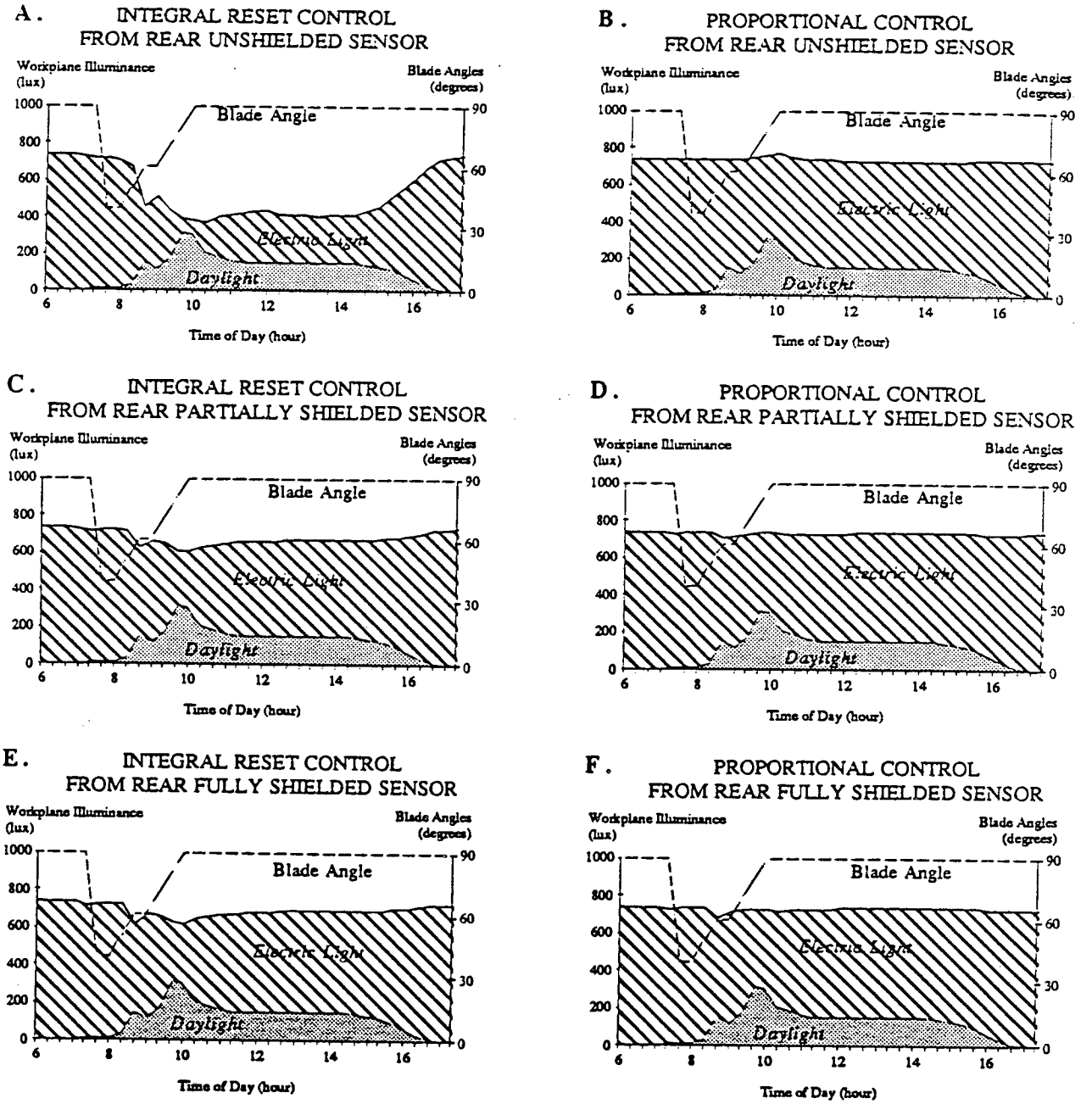

Figure 6-27. Light levels on workplane (rear portion of room) for integral reset and closed-loop proportional control systems controlled by three photosensors for semi-infinite room model facint east

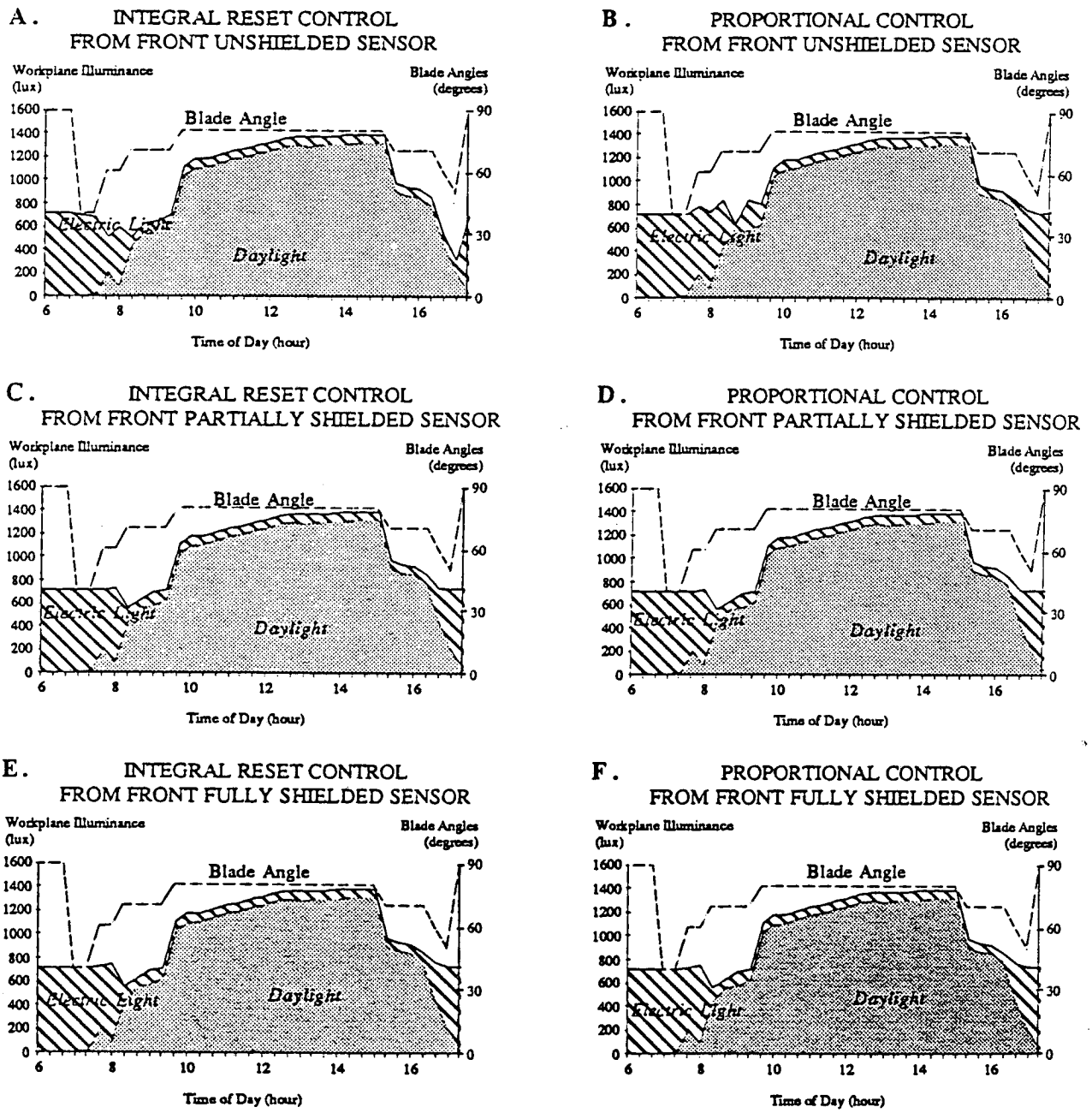

Figure 6-28. Light levels on workplane (front portion of room) for integral reset and closed-loop proportional control systems controlled by three photosensors for semi-infinite room model facing south (clear winter day)

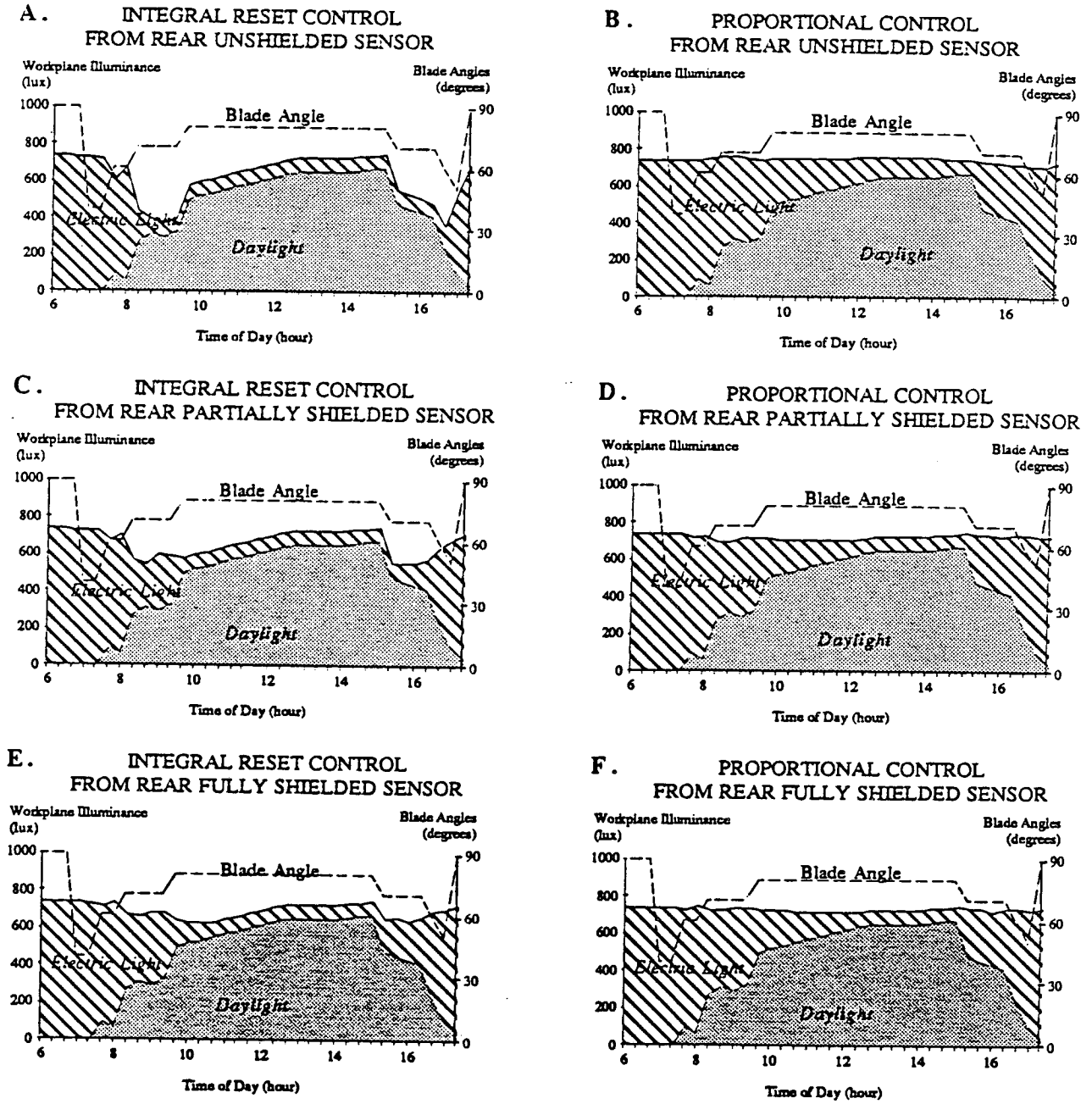

Figure 6-29. Light levels on workplkane (rear portion of room) for integral reset and closed-loop proportional control systems controlled by three photosensors for semi-infinite room model facing south (clear winter day)

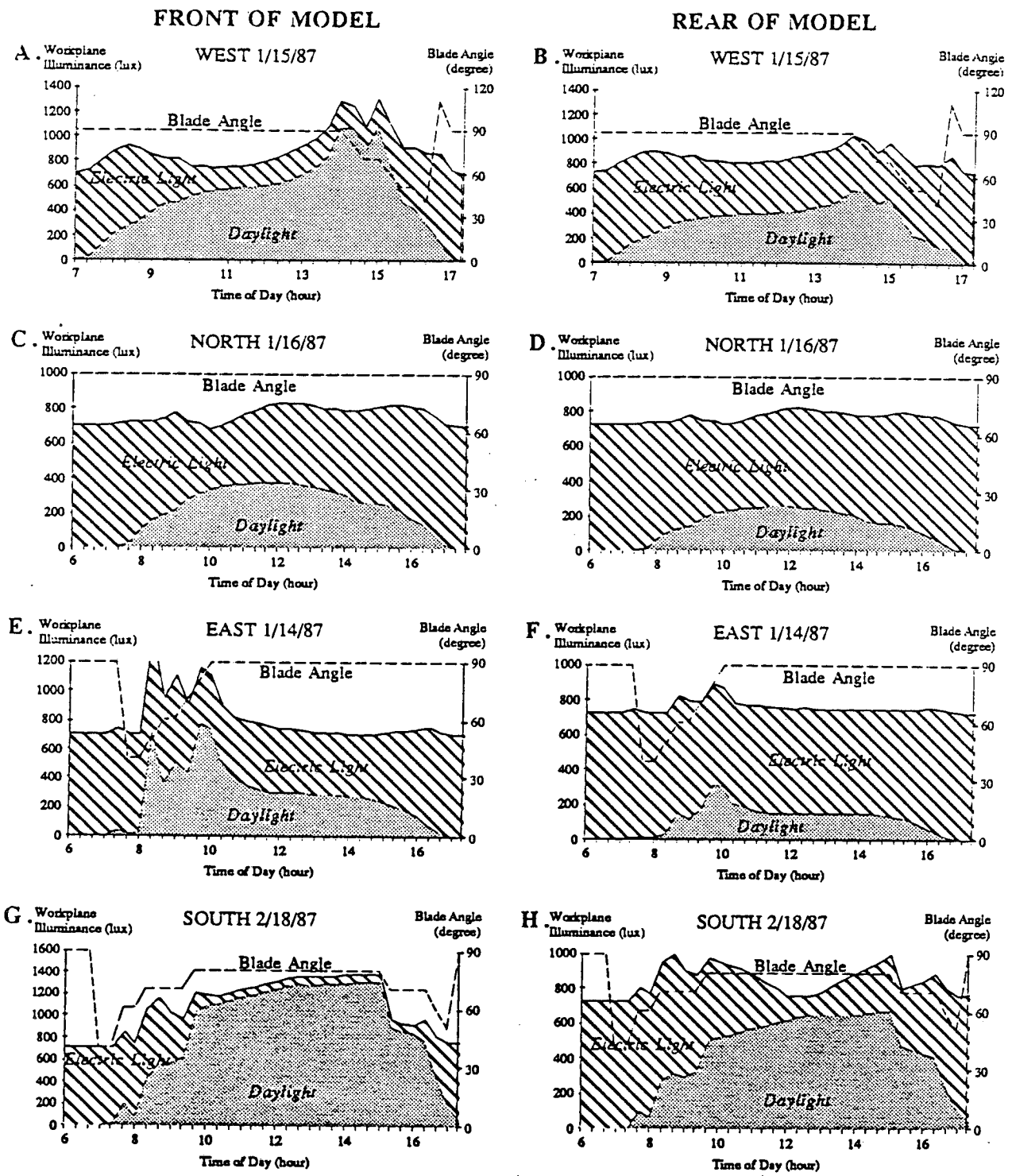

Figure 6-30. Light levels on workplane for open-loop proportional control systems controlled by window-aimed sensor for small office model facing all directions on clear winter and summer days

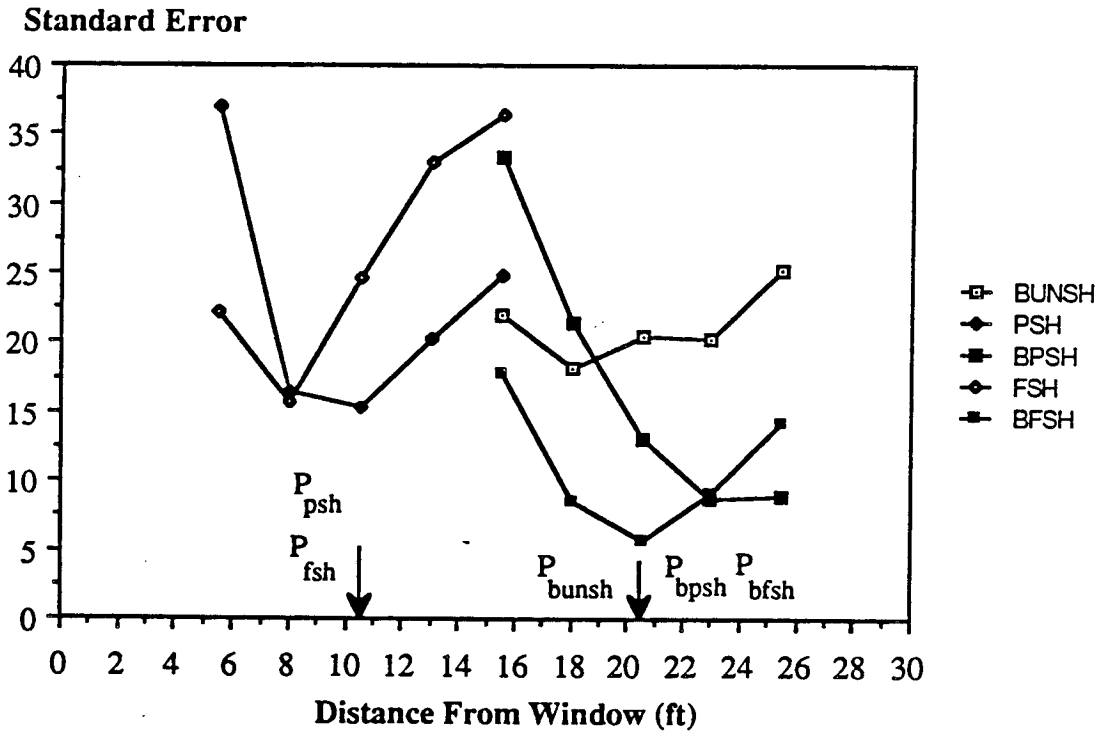

Figure 6-31. Goodness of fit expressed in terms of standard error of workplane illuminance vs. photosensor signal for workplane points at varying room depth. Data are for semi-infinite room model facing west at 11:00 am on clear winter morning without shading device installed

A.

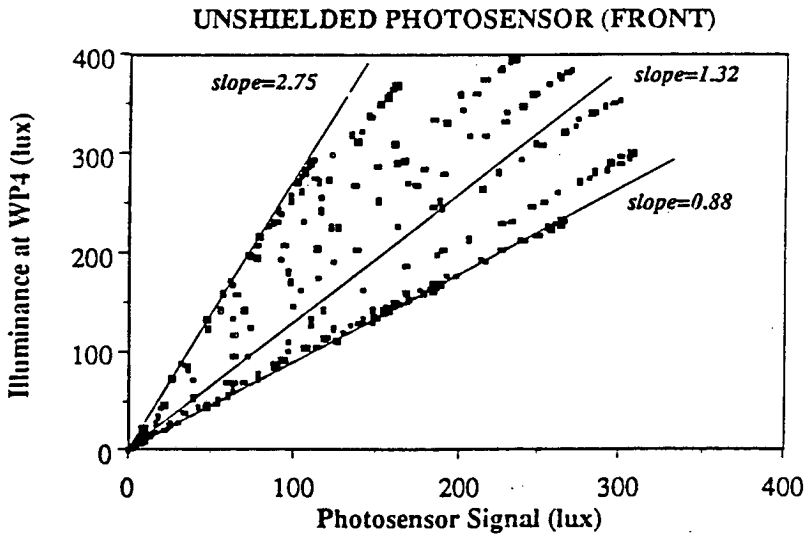

B.

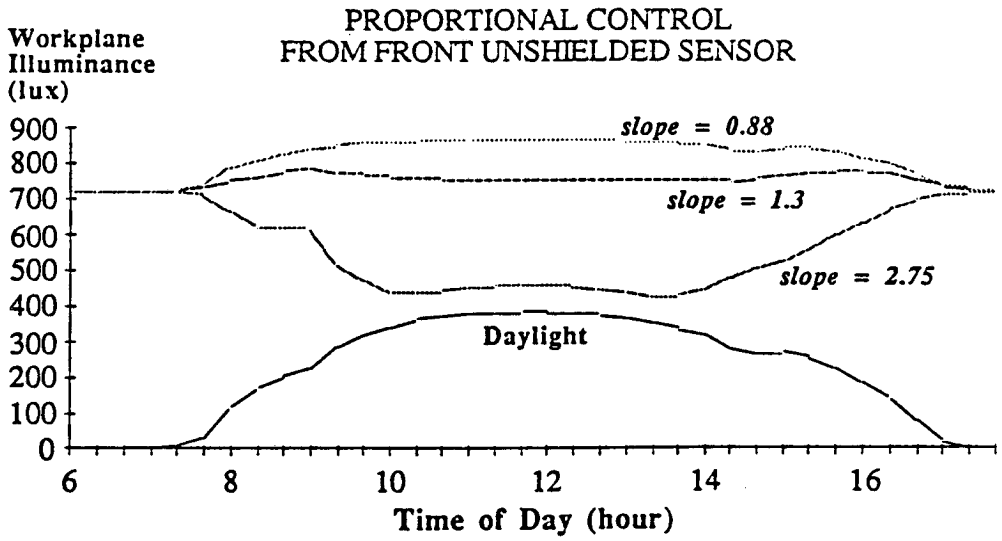

Figure 6-32. Effect of different scale factor calibration settings on total maintained light levels at front of semi-infinite room model pointing north. Three possible values for a line fitting the day-light only data for the front unshielded photosensor are shown in A. Figure B shows the daylight level at the workplane point WP4 as a function of time of day, and three total light level curves corresponding to each of the slopes shown in A

Section 7

DISCUSSION

EFFECT OF PHOTOSENSOR SHIELDING ON DAYLIGHT TRACKING CAPABILITY

The scatter plots of workplane vs. photosensor signal indicate that the control sensor's precision in tracking the illuminance at the task is affected by the sensor's location, orientation, and susceptibility to direct light from the window. It is also affected by the geometry of the room. For all directions, sensors that were shielded from the window or from both the window and walls (the P_{psh} and P_{fsh} photosensors, respectively) most closely followed the changing daylight levels at the workplane. The similarity of the daylight response plots for these two sensors indicates that shielding a ceiling-mounted control photosensor from walls other than the window-wall does not improve tracking capability. In fact, the standard errors and correlation coefficients indicate that the partially-shielded photosensor slightly outperformed the fully-shielded photosensor for all situations. In general these differences were not large; however ,they were consistent over the many cases examined. The daylight response plots for the unshielded ceiling-mounted photosensor, P_{unsh}, on the other hand, were clearly less well correlated than either the partially- or fully-shielded photosensors except in the rear of the semi-infinite room model when all three sensors performed about equally well. Because the principal difference between the unshielded and partialy shielded sensors is the former's susceptibility to direct light from the window, simply shielding the sensor from direct light from the window is sufficient to markedly improve the sensor's ability to track changes in the workplane illuminance.

The results show that shielding the ceiling-mounted control photosensor from direct window light improves the performance of integral-reset systems; however, in all cases, total light levels at the workplane dropped below the design level for portions of the day. With closed- and open-loop proportional control algorithms (especially closed-loop) satisfactory results could be obtained even with the unshielded photosensor. Thus the results indicate that with the existing technologies tested, the proper choice of control algorithm is more important than either the placement of the photosensor or its spatial responsivity.

WHY PROPORTIONAL CONTROL OUTPERFORMS INTEGRAL CONTROL

The reason the integral-reset system performs less well than the closed- or open-loop proportional control systems is implied in the expressions for the response of the different systems to changes in daylight on the control photosensor (Eqs. 3-6, -11, and -17). The

response of an integral reset system to a given change in the daylight component of the photosensor signal is fixed not according to the daylight conditions prevailing in the room, but by the electric light distribution in the room and the geometric relationship between the task and photosensor. Since daylight in a side-daylit room enters the space from the side window while electric light comes from the ceiling, the relationship of daylight at the task photosensor output is clearly quite different from that of electric light (compare **bold face** columns in Tables 6-1 and 6-2). Given the inherent asymmetries in a side-daylighted room, an integral-reset system driven by a ceiling-mounted photosensor would generally be expected to provide inadequate illumination except at night or when the task surface is very close to the window. Using a photosensor shielded from direct light from the window prevents the integral control system from reacting quite as extremely to a given change in daylight, but even a fully-shielded ceiling-mounted photosensor will usually over-respond.

Stated another way, an integral reset system operates by lowering the amount of electric light provided as daylight increases in such a way as to maintain a constant total amount of light on the control photosensor. It simply turns out that for most daylighting applications, maintaining a constant amount of light on the ceiling results in progressively lower total light levels at the workplane as daylight increases. A properly calibrated closed-loop proportional control system gets around this difficulty by allowing the total amount of light on the photosensor to increase as the amount of daylight increases.

The operational difference between proportional control and integral control can also be seen by inspection of the block diagram shown in Figure 4-9. With integral control, the controller requires that the feedback signal from the photosensor exactly track the setpoint (for low frequency changes). If there is *no daylight* and the ratio between the two gain constants $K_{F\text{-}W}$ and $K_{F\text{-}S}$ remains constant, an integral controller will maintain constant illuminance at the workplane even if there are unwanted fluctuations in *electric* light level due to temperature changes, voltage fluctuations, etc. Even long-term changes in wall surface reflectance will be properly compensated for with integral control as long as the $K_{F\text{-}W}/K_{F\text{-}S}$ ratio does not change significantly. This is strong evidence that integral control is the appropriate control algorithm to use for the lumen maintenance control strategy, provided that there are no other sources of illumination.

However, once daylight enters the space, a given increase in daylight at the workplane causes a large increase in the photosensor signal (relative to the electric light case) because the $K_{W\text{-}W}/K_{W\text{-}S}$ ratio for daylight is typically lower than the $K_{F\text{-}W}/K_{F\text{-}S}$ ratio for electric light.† Effectively, this means that the gain of the feedback loop is larger for daylight than

† The $K_{W\text{-}W}/K_{W\text{-}S}$ ratio is identical to the task-sensor ratio for daylight listed in column 8 of Tables 6-1 and 6-2. Similarly the $K_{F\text{-}W}/K_{F\text{-}S}$ ratio is identical to the electric light task-sensor ratio listed in column 3 of the same tables.

it is for electric light. With integral control, this "gain change" must be answered by reducing the electric light component of the photosensor (by reducing the output of the electric lights) so that S_T once again equals the setpoint. But because $K_{F\text{-}W}/K_{F\text{-}S}$ is higher than $K_{W\text{-}W}/K_{W\text{-}S}$, the electric light level will be reduced too far, causing the total light level at the workplane to drop below the design level. With proportional control, the photosensor output S_T is not required to equal the setpoint level and, in fact, increases as the daylight level goes up. This effectively reduces the sensitivity of the proportional control system to the difference in gain between daylight and electric light. With proper calibration, the system sensitivity is reduced just enough to properly compensate for these gain differences.

EFFECT OF REDUCED SYSTEM SENSITIVITY ON ELECTRIC LIGHT VARIANCES

However, reducing the sensitivity of the system with proportional control has some unwanted side effects. In particular, because the gain of the proportional control system is reduced relative to integral control, the proportional control will now only partly compensate for variances in electric light output (such as those caused by lamp lumen depreciation, or voltage and temperature fluctuations). The more the system sensitivity must be decreased to obtain good daylighting performance from a particular photosensor, the less accurate the control will be for electric light changes. Since the sensitivity for shielded photosensors did not have to be reduced nearly as much as that for unshielded photosensors to obtain satisfactory daylighting performance, this would tend to argue for shielded photosensors. A proportional control system driven by a shielded ceiling-mounted photosensor will provide good daylighting control with only minor compromises in lumen maintenance performance.

It is interesting to ask whether a photoelectric control system can achieve both good daylighting performance and uncompromised lumen maintenance control. Conceptually, this requires the system to "know the difference" between electric light and daylight. Differentiating daylight from electric light is clearly achievable by various techniques. One scheme is to use a separate photocell placed directly facing the controlled electric light fixtures to give the control system a "handle" on the instantaneous electric light output. Coupled with a sensor that detects input power (or current), a control system could be devised to optimally exploit both daylighting and lumen maintenance control strategies. Other approaches are possible as well, but any such scheme requires relaxing some of the criteria imposed in Section 3. Also, the savings associated with lumen maintenance is generally much lower than that associated with daylighting. It is therefore arguable whether the advantages of optimal daylighting and lumen maintenance control are worth the disadvantages of greater control complexity and cost.

IMPLICATIONS FOR CALIBRATION

The responses of both closed- and open-loop proportional control systems are set according to prevailing daylight conditions in the room and thus can better provide reasonably constant illuminance for most daylight conditions. This is shown in the equations for the open-loop and proportional control scale factors (M) given in Eqs. 3-13 and 3-19. The scale factors of these systems are explicit functions of the daylight conditions at the time of calibration. It is not surprising that systems that respond to changes in daylight in a way that explicitly takes into account the daylight conditions in the space respond more appropriately than integral reset systems, which do not account for the daylight conditions.

If calibration is performed under typical daylight conditions (as we have done in the simulations shown previously), one is assured of good results under most conditions. Of course, in any realistic situation, the end-user will not have access to the type of data shown in Figures 6-1 through 6-8 and thus will have no way of knowing when it is a good time to calibrate. For this reason, it is important that manufacturers of daylight-following controls produce control photosensors that properly track illuminance changes at the work-plane. If the spatial response characteristics and location of the control photosensor are such that its daylight scatter plot is close to proportional and shows minimal data scatter relative to changing daylight conditions, the user is more likely to calibrate the response properly. Thus the system will generally supply the design light level with greater precision and more efficiency than it would with a less well-designed photosensor. In this regard, we can identify the window-aimed photosensor as being a poor choice because, for a given level of daylight at the workplane, this sensor can produce a signal varying by as much as 10 to 1 depending on the blind blade angle, season, or sun angle. With such a large degree of variance, it would be virtually impossible to obtain reasonable performance because the control photosensor does not measure a quantity that is indicative of workplane illuminance.

In Tables 6-1 and 6-2, it was shown that the ratio of daylight on the unshielded photosensor to daylight on the workplane was very different from the equivalent ratio for electric light. The fact that the proportional control systems performed well, even when driven by such a photosensor, is significant since it implies that even photosensors that are relatively more sensitive to daylight than electric light can be accommodated by proper setting of system gain. If an unshielded photosensor is used, then the system gain will be set low so that a relatively large change in photosensor output will be required to effect a relatively small change in electric light output. Conversely, system gain would be set higher if a sensor shielded from direct window light were used.

From Tables 6-1 and 6-2, it is seen that the single parameter fits of the daylight scatter plots vary somewhat between different room orientations and particularly according to the room shape. The fits for partially-shielded sensors generally show the best correlation the least variability with respect to these variables, providing an additional reason for using this type of sensor. However, it is apparent from the variations of the fits that it is probably not reasonable for manufacturers to provide a factory-set gain value; for proper system operation, calibration must be performed on-site in each controlled zone. It is certainly possible, however, that with some added circuitry, a self-calibrating system could be devised. This would require a more intelligent system than that considered in this report. However, it would alleviate the need for trained personnel to calibrate the system and thus might improve user acceptability.

COMPARISON OF OPEN-LOOP AND CLOSED-LOOP PROPORTIONAL CONTROL

It is clear that the open- and closed-loop proportional control systems perform significantly better than comparable integral-reset systems, by allowing adjustment of system gain. It is tempting to assume that these systems are equivalent, but some important differences between the two algorithms may favor the closed-loop control approach. The root of these differences is in the absence of a balancing (voltage divider) network to the non-inverting input on the OLC system circuit diagram (compare Figs. 3-3 and 3-4). (In reality, some OLC circuits do allow adjustment of the voltage offset at the non-inverting input. In these cases, though, the function of the adjustment is to permit the end-user to reduce the maximum electric light level supplied at night to below the full light level the system is capable of delivering). Because there is no means of adjusting the voltage at this input, the OLC circuit designer must configure the circuit so that full light output occurs when there is zero (or negligible) photosensor signal. To ensure that the photosensor will read nearly zero when the electric lights are on full at night, the manufacturer of an OLC system must use a control photosensor that is much more sensitive to daylight than to the electric light that it controls. On a practical level, this means that to use a ceiling-mounted control photosensor with an OLC system, the sensor's field of view should be restricted primarily to daylight coming through the window. A sensor designed in this way (such as P_{wdw}) will tend to be sensitive to the brightness of the ground plane (i.e., the area of ground outside the controlled building space), a parameter that we have shown is not well correlated with interior workplane illuminance. Further work on the effects of varying ground plane reflectances under real sky conditions is required before we can predict the most appropriate spatial response for an OLC photosensor.

Section 8

PRELIMINARY DESIGN GUIDELINES

A major purpose of this research was to develop data and methods that can form the basis of guidelines for designing, installing, and operating effective daylight-following systems. From the results described in this report, some preliminary guidelines emerge.

SYSTEM IDENTIFICATION AND SELECTION

Proportional control systems were found to be far superior to integral-reset systems for daylighting applications using one photocell sensor and existing technologies on the market. Specifiers of daylight-following systems need to be aware that various products are available and should ascertain from the manufacturers the details of the control systems offered. Unfortunately some of the terms used in this report, such as "integral-reset" and "proportional control," are borrowed from classical controls theory and are not commonly used by distributors, contractors, or even manufacturers.[1] This makes the task of identifying the capabilities of a given system more difficult. Systems can be identified, however, by examining their calibration procedures using the following "tests" as a guideline.

1. If the calibration procedure calls only for a nighttime calibration, then the system uses integral reset control and should typically be avoided for daylighting applications. It may, however, be quite appropriate for lumen maintenance control as discussed in Section 7.

2. If the calibration procedure calls for calibration only during the day, the system probably uses open-loop proportional control. This type of control is reasonably well suited to daylighting applications. However because open-loop proportional control results in unwanted additional constraints in the spatial response and placement of the photosensor, workplane illuminance levels may vary more than with closed-loop proportional control

3. If the calibration procedure requires calibration both during the day and at night, the system uses closed-loop proportional control. This type of control is the best suited for daylighting applications.

Regardless of whether an open- or closed-loop proportional control system is used, the specifier should require that the calibration controls be accessible from the controlled building space. This permits easy system calibration and adjustment.

---

[1] The lighting controls industry is sufficiently immature that there are no commonly used terms for characterizing the different types of control algorithms. It is unfortunate that most of the dimming photoelectric control systems sold today in the U.S. for daylighting applications are of the integral reset type.

PHOTOCELL SPATIAL RESPONSE

If the control system selected uses closed-loop proportional control, the ceiling-mounted photocell should have a large field of view but be blocked from direct light from the window. This combination of sensor placement and control algorithm is recommended for most daylighting applications. If the photocell provided by the manufacturer is not adequately shielded from the window, the photocell should be placed sufficiently far away from the window so that is does not "see" a large area of the ground outside the building.

With an open-loop proportional control system, an unshielded ceiling-mounted photosensor should be used. The photosensor should not be aimed pointing out the window.

PHOTOSENSOR PLACEMENT

In a room where there is only one task area of interest, the ceiling-mounted control photosensor should be located above the task. If there are several task areas separated by some distance, the photocell should be located above a task area that receives a representative amount of daylight. If the daylight levels at a given time are very different between different task areas, separate control zones may be required for each area.

CALIBRATION

After a photoelectric control system is installed and interior furnishings are in place, the system response must be calibrated to the particular space conditions. As previously noted, open- and closed-loop proportional control systems must be calibrated during the day.

In selecting the time at which to perform the daytime calibration, the following guidelines generally apply:

- The calibration should be done when the sun is shining and not blocked by clouds. If the local climate rarely has sunny days, the calibration may be performed under bright overcast conditions.
- There should be no direct sun shining into the space at the time of calibration. Direct sun on the task is especially to be avoided.
- The contribution of daylight to the required illuminance at the task surface at the time of calibration should be sufficiently large to cause significant but not full dimming of the electric lights. For example, if the electric lights can supply 70 footcandles (700 lux) at full light output and dim maximally to 10 footcandles (100 lux), and the total light level desired is 70 ftc, the system should be calibrated when the daylight level at the task is slightly under 60 ftc (70 - 10 = 60).

- If the space contains an operable shading device (such as a venetian blind) that can be controlled by the occupant, the occupant should set the venetian blind to a comfortable position before calibrating.

Calibration Procedure

The specific procedure for calibrating the response of the photoelectric control system is system-dependent. Most proportional systems, though, will follow a calibration procedure similar to that given below.

Nightt ime calibration. If the system uses closed-loop proportional control, the nighttime setpoint level should be established before the daytime calibration. The nighttime calibration should be done at night or with all sources of daylight blocked off. (The latter approach is less desirable). The night setpoint level adjustment should initially be set so that the lights are substantially dimmed. Then, if the electric lighting system is intended to provide full electric light output at night, the setpoint level should be raised until the lights *just* reach full intensity. If the electric lighting system at full light output provides more light than is necessary at night (e.g., if the lamps are new or the lighting system was overdesigned), the setpoint level can be backed off until the desired light level is reached. This completes the nighttime calibration.

Daytime calibration. Once the appropriate daytime condition has been selected using the guidelines given above, the daytime calibration may be performed. A photometer is placed at the task surface, and the adjustment knob that controls the gain of the system response is adjusted until the total light level indicated by the photometer (daylight plus electric light) equals the desired level (generally the light level supplied by full electric lighting at night). If this light level appears too low compared to the brightness outside, it is permissible to adjust the electric light level slightly higher. Some caution is required here since if the electric light level is set too high, energy savings may be minimal.

If the light level from daylight alone is sufficient to exceed the design level, it will be necessary to calibrate later in the day when the daylight levels have dropped below the design level. The calibration procedure described above need only be performed once in each individually controlled space. If done correctly, adjustments should be necessary only if the furnishings change significantly.

Recommendations with respect to the zoning or grouping of luminaires into separate control zones is beyond the scope of this report. This topic is covered in References 3 and 8.

Section 9

CONCLUSION

This study has shown that the ability of daylight-following lighting systems to provide a minimum specified light level at the task surface is influenced by 1) the control algorithm used, 2) the spatial response of the ceiling-mounted control photosensor, and 3) the location of the photosensor relative to task and window. Best performance was obtained with a closed-loop proportional control system controlled by a photosensor with a large field of view but shielded from direct light from the window. A minimum specified illuminance level could be maintained at specific points on the task surface regardless of daylight condition or room geometry provided that the system gain was properly calibrated to account for the local luminous environment. The study found that daylight conditions varied sufficiently due to room orientation, geometry, and window shading system to preclude the use of factory-preset gain. This implies that proper calibration is prerequisite to the successful operation of daylight-following systems and that, in the building commissioning process, calibration be viewed with the same importance as, for example, balancing the heating, ventilating, and air-conditioning (HVAC) system.

The research showed that open-loop proportional control also performed adequately but offered less precise control than closed-loop systems due to the necessity of using a photosensor that was not shielded from direct window light. Integral-reset systems performed poorly, although performance could be improved slightly by completely shielding the photocell from direct window light. The data suggest that integral-reset control for daylighting applications should only be used for daylighting applications after careful evaluation.

The control photosensor should be located, aimed, and shielded in such a way that the signal generated by the sensor is linearly related to the illuminance at the workplane. A ceiling-mounted photosensor that viewed a large angle but was shielded from the direct window luminance produced an output most closely correlated with illuminance at the workplane. A ceiling-mounted photocell aimed at the window did not produce a signal that was well correlated with workplane illuminance, indicating that such a configuration should be avoided.

Finally, these studies indicated that daylight-following systems, if properly designed and calibrated, have significant potential for reducing peak power needs in daylit spaces and for reducing overall lighting energy requirements in buildings.

Section 10

REFERENCES

1. V. Crisp. "Energy Conservation in Buildings: A Preliminary Study of the Use of Automatic Daylight Control of Artificial Lighting." *Lighting Research and Technology, 9 (1),* 1977, pp. 31-41.

2. F. Rubinstein. "Photoelectric Control of Equi-Illumination Lighting Systems." *Energy and Buildings, 6,* 1984, pp. 141-150.

3. J.E. Kaufman, ed. *IES Lighting Handbook, Applications Volume* 7th Edition, New York, Illuminating Engineering Society, 1987.

4. D.K. Anand. *Introduction to Control Systems*. New York: Pergamon Press Inc., 1974.

5. W. Oldham and S. Schwartz. *An Introduction to Electronics*. New York: Holt, Rinehart and Winston, Inc., 1972, pp. 500-506.

6. F. Winkelmann and S. Selkowitz. "Daylighting Simulation in the DOE-2 Building Energy Analysis Program" *Energy and Buildings, 8,* 1985, pp. 271-286.

7. K. Papamichael and S. Selkowitz. "The Luminous Performance of Vertical and Horizontal Slat-Type Shading Devices." In *Proceedings of the Illuminating Engineering Society Conference,* Boston, August 1986.

8. U.S. Department of the Navy. Naval Civil Engineering Laboratory. *Lighting Controls Systems Handbook.* Port Hueneme, California: Report Number CR 85.010, 1985, pp. 2-12.

LAWRENCE BERKELEY LABORATORY
TECHNICAL INFORMATION DEPARTMENT
1 CYCLOTRON ROAD
BERKELEY, CALIFORNIA 94720